INL/EXT-19-55395
Revision 1

Evaluation of Hydrogen Production Feasibility for a Light Water Reactor in the Midwest

Konor Frick, Paul Talbot, Daniel Wendt, Richard Boardman, Cristian Rabiti, Shannon Bragg-Sitton (INL)

Daniel Levie, Bethany Frew, Mark Ruth (NREL)

Amgad Elgowainy, Troy Hawkins (ANL)

September 2019

The INL is a U.S. Department of Energy National Laboratory
operated by Battelle Energy Alliance

Idaho National Laboratory

INL/LTD-19-55395
Revision 1

Evaluation of Hydrogen Production Feasibility for a Light Water Reactor in the Midwest

Konor Frick, Paul Talbot, Daniel Wendt, Richard Boardman, Cristian Rabiti, Shannon Bragg-Sitton (INL)
Daniel Levie, Bethany Frew, Mark Ruth (NREL)
Amgad Elgowainy, Troy Hawkins (ANL)

September 2019

Idaho National Laboratory
Idaho Falls, Idaho 83415

http://www.inl.gov

Prepared for
U.S. Department of Energy
Office of Nuclear Energy
Under DOE Idaho Operations Office
Contract DE-AC07-05ID14517

EXECUTIVE SUMMARY

Increased electricity production from renewable energy resources coupled with low natural gas prices has caused existing light-water reactors (LWRs) to experience ever-diminishing returns from the electricity market. Via a partnership among Idaho National Laboratory (INL), The National Renewable Energy Laboratory (NREL), Argonne National Laboratory (ANL), Exelon, and Fuel Cell Energy, a techno-economic analysis of the viability of retrofitting existing pressurized water reactors (PWRs) to produce hydrogen (H_2) via high-temperature steam electrolysis (HTSE) has been conducted. Such integration would allow nuclear facilities to expand into additional markets that may be more profitable in the long term.

To accommodate such an integration, a detailed analysis of HTSE process operation, requirements, and flexibility was conducted. The technical analysis includes proposed nuclear system control scheme modifications to allow dynamic operation of the HTSE via both thermal and electrical connection to the nuclear plant. High-fidelity Modelica simulations showcase the viability of such control schemes. However, due to limited knowledge of solid oxide fuel cell (SOFC) stack degradation due to thermal gradients, thermal cycling of the HTSE was not included. Therefore, the control schemes proposed are only utilized to re-distribute steam at startup, and only the portion of electricity utilized in the electrolyzers is cycled.

From the detailed analysis of the nuclear integration and the HTSE process design, a comprehensive cost estimation was conducted in the APEA and H2A models to elucidate capital and operational costs associated with the production, compression, and distribution of hydrogen from a nuclear facility. Alongside this costing analysis, market analyses were conducted by NREL and ANL on the electric and hydrogen markets, respectively, in the PJM interconnect.

Utilizing the electricity data market projections in the PJM interconnect from NREL and hydrogen demand/pricing projections from ANL, a five-variable sweep over component capacities, discount rates, and hydrogen pricing was completed using the stochastic framework RAVEN (Risk Analysis Virtual ENvironment) through its resource dispatch plugin HERON (Heuristic Energy Resource Optimization Network). Each combination of variables was evaluated over a seventeen-year timespan, from 2026–2042 (inclusive), to determine the most economically advantageous solution. Following the five-variable sweep, an optimization was conducted to establish the best sweep point to determine optimal component sizing and setpoints.

Results suggest positive gain is achievable at all projected hydrogen market pricing levels and at all discount rates. However, exact component sizing and net returns vary based on these values, and if incorrect sizing is selected, major net losses can occur. The optimal result occurred with set points as follows: high hydrogen prices, the largest possible HTSE unit in the sweep set at 7.47 kg/sec (645.4 tpd), a contractual hydrogen market agreement 7.29 kg/sec (629.8 tpd), and a hydrogen storage size of 115,188 kg. The analysis suggested that with a discount rate of 8%, a ΔNPV = 1.2 billion over the seventeen-year span can be achieved. The results illuminate that by operating in multiple markets the nuclear facility can avoid the sale of electricity during times of low electricity market pricing, while maintaining the ability to capitalize on the high electricity market pricing.

It should be noted that the analysis conducted in this report is a differential cash flow analysis and, as such, does not present profit levels. Instead, it highlights the net benefit between building and competing in the hydrogen market, utilizing nuclear facilities and conducting business as usual in the electricity markets. Additionally, results presented in this report exhibit conservatism due to five key assumptions:

1. Given the limited knowledge on SOFC stack degradation due to thermal gradients, the high-temperature steam electrolysis plant is not allowed to thermally cycle. This limitation decreases

electricity generation capacity in the nuclear plant, reducing capacity payments and the maximum output to the electrical grid.

2. This analysis considers building a separate hydrogen pipeline for use in the nuclear facility. Research is currently being conducted to determine if existing natural gas pipelines can accommodate direct hydrogen injection. If hydrogen can be integrated into existing natural gas pipelines, then a capital savings of ~$19,000,000 per kg/sec (1 kg/sec = 86.4 tpd) of installed HTSE capacity could be realized.
3. Fast transients in the electric grid are typically served by flywheels and electric batteries. With electrolysis-only operation, the nuclear plant can flex its electricity just as quickly. However, for this analysis, the ancillary services market has been neglected. Should the nuclear plant have the ability to operate in the ancillary services market during periods when it is producing hydrogen, an additional substantial income stream that would increase overall system profitability could be considered.
4. Subsidies for non-emitting generation technologies are not introduced in the cash flow analysis, but instead are completed assuming zero subsidies. Profitability is based solely on electricity pricing.
5. Electric pricing is assumed to never go negative. Instead, it is assumed overall system curtailment by the Independent System Operator (ISO) will occur in such a manner that pricing remains at or above zero. This assumption inflates the "business as usual" scenario, thus decreasing the ΔNPV calculated. If negative pricing scenarios continue to occur as they do today, one would expect a further increase in ΔNPV.

Overall, results advocate that, through market diversification, nuclear power plants have the potential to substantially increase current profit margins, increase market penetration, and ultimately solidify their place as a mainstay in energy production.

ACKNOWLEDGEMENTS

This work was completed with funding from the U.S. Department of Energy's Hydrogen and Fuel Cell Technologies Office within the Office of Energy Efficiency and Renewable Energy, through an H2@Scale CRADA, in collaboration with the U.S. Department of Energy’s Crosscutting Technology Development Integrated Energy Systems program within the Office of Nuclear Energy.

Funding and technical expertise was provided by Exelon Corporation and its subsidiaries. Particular thanks are extended to Uuganbayar Otgonbaatar of Exelon Corporation for the oversight and direction provided throughout this project.

Additional thanks are extended to Fuel Cell Energy for its technical contributions to this report regarding high-temperature steam electrolysis design.

CONTENTS

FIGURES

TABLES

ACRONYMS

AE	alkaline electrolysis
AEO	annual energy outlook
ANL	Argonne National Laboratory
APEA	Aspen Process Economic Analyzer
ARMA	Auto-Regressive Moving Average
BOP	balance of plant
BWR	boiling water reactor
CAPEX	capital expenditures
CO_2	carbon dioxide
CRADA	Cooperative Research and Development Agreement
DCC	direct capital cost
DOE	Department of Energy
EFORd	equivalent forced outage rate demand
EIA	Energy Information Agency
FCTO	Fuel Cell Technology Office
H_2	hydrogen
HERON	Heuristic Energy Resource Optimization Network
HHV	higher heating value
HPC	high-performance computing
HTSE	high-temperature steam electrolysis
INL	Idaho National Laboratory
LHV	lower heating value
LMP	locational marginal price
LTE	low-temperature electrolysis
LWR	light-water reactor
LWRS	Light Water Reactor Sustainability
MACRS	modified accelerated cost recovery system
MWe	megawatt electric
MWh-e	megawatt hour electric
MWt	megawatt thermal
NG	natural gas
ΔNPV	differential net present value

NPV	net present value
NRC	Nuclear Regulatory Commission
NREL	National Renewable Energy Laboratory
O_2	oxygen
O&M	operating and maintenance
OPEX	operating expenses
OTSG	once-through steam generator
PEM	polymer-electrolyte membrane
PJM	PJM Interconnection
PPA	power purchase agreement
PWR	pressurized water reactor
RAVEN	Risk Analysis Virtual ENvironment
ReEDS	Regional Energy Deployment Systems
RPM	rotations per minute
RTO	Regional Transmission Organization
SMR	steam-methane reforming
SOEC	solid oxide electrolysis cell
TCI	total capital investment
TCV	turbine control valve
TEA	techno-economic analysis
tpd	tonnes per day
UCAP	unforced capacity
UTSG	U-tube steam generator
VARMA	vector auto-regressive moving average

1. INTRODUCTION

Light-water reactors (LWRs) are increasingly challenged to compete with natural gas (NG) combined-cycle power plants in wholesale electricity markets due to the historically low cost of natural gas. In addition, in areas where wind and solar power generation are being deployed, the minute-by-minute selling price of electricity is often less than the marginal cost of operation. Such pricing structures make it unsustainable for nuclear power plants to remain solely in electricity markets. Expansion into additional energy markets is required to maintain profitability. Chief among them is the hydrogen market.

Hydrogen markets are growing ubiquitously in the United States and globally. Hydrogen is being recognized as an important energy carrier for energy storage and production of steel, fertilizers, and synthetic fuels. It is needed to refine petroleum crude and for direct use in fuel cells for electricity generation and for small- and heavy-duty transportation. As markets for clean hydrogen are built up, water-splitting electrolysis processes supported by LWRs provide a tremendous opportunity to change air pollutant emissions.

Via partnership among Idaho National Laboratory (INL), The National Renewable Energy Laboratory (NREL), Argonne National Laboratory (ANL), Exelon, and Fuel Cell Energy, a techno-economic analysis (TEA) has been conducted on the viability of retrofitting existing pressurized water reactors (PWRs) to produce hydrogen via high-temperature steam electrolysis (HTSE). This TEA is primarily focused on hydrogen generation for markets in the Midwest as a possible starting point for conversion of LWRs into poly-generation hybrid facilities. LWRs operating in this region can support growth in the industrial manufacturing sector due to future hydrogen needs, which provides a good opportunity to assess the value proposition of direct use of nuclear-generated heat by industry.

This assessment did not consider steam arbitrage to an energy complex, although a wide variety of industrial users could take advantage of the low-cost steam produced by an LWR [1]. Such an energy park is possible and could be explored later. This report focuses instead on the hybrid operation of a nuclear power plant that encompasses both thermal and electrical integration for hydrogen generation via HTSE. A 640tpd HTSE unit requires less than 9% of the total thermal energy produced by a typical 1100MWe LWR. With electricity being the main source of energy provided to the electrolysis plant, the LWR power generation system will not be significantly impacted, as operations at >90% steam flow are well characterized via standard plant operations.

1.1 Light-Water Reactor Energy Costs Comparison

Hydrogen is traditionally produced by steam methane reforming (SMR). The cost of producing hydrogen using SMR is highly dependent on the cost of natural gas. Through electrolysis the cost of producing hydrogen is directly linked to the cost of electricity. Through thermal integration and behind the meter connections, existing nuclear plants can provide a reliable and cost-competitive supply of steam and electricity for hydrogen production for decades to come [2,3]. A comparison of the cost of producing high-pressure steam using a natural-gas-fired package boiler versus the cost of producing the same quality and quantity of steam using an LWR is shown in Figure 1 [4,5,6]. Existing LWR plants produce high-pressure steam for $4.00–5.25/1000-lb ($8.80-11.55/1000-kg) depending on the size of the nuclear plant and capital recovery for upgrades to the plant. This is currently 15–45% lower than the cost of producing steam using an NG package boiler even before any cost for CO_2 emissions is levied against SMR. The data suggests the cost of steam production by the existing U.S. fleet of LWRs will remain competitive, even with plant upgrades for future license extensions.

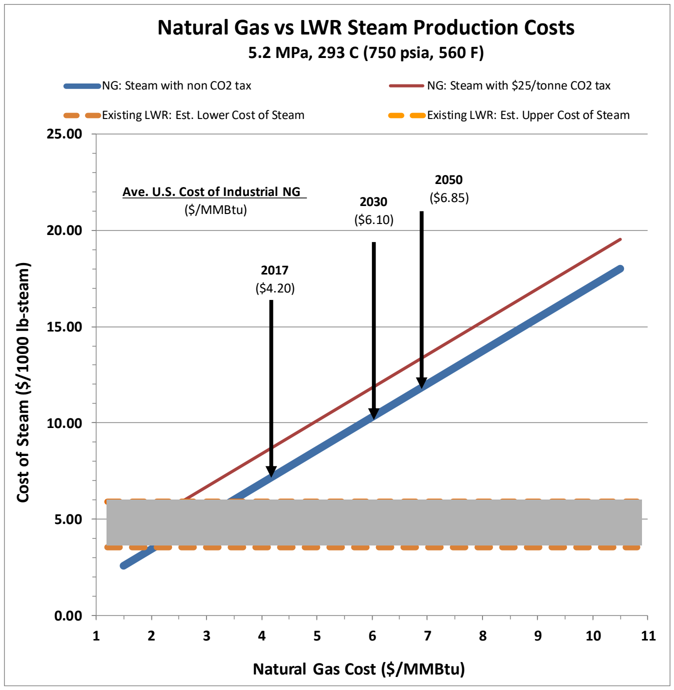

Figure 1. Cost of high-pressure steam production using natural gas and nuclear energy. Arrows indicate U.S. DOE Energy Information Agency (EIA) cost projections for natural gas.

In 2018, the marginal cost of producing electricity with an LWR ranged between $25 and $40/MWh for multi- and single-unit plants, respectively. These costs are trending down, following capital and operating costs that were required to meet Nuclear Regulatory Commission (NRC) guidance following the Fukushima accident. Electricity produced by single-unit nuclear plants is naturally more expensive than electricity produced by multi-unit plants.

1.2 Future Paradigms for LWRs

There are five potential business cases for LWR operation:

1. *Traditional baseload*. The nuclear plant operating as a baseload power station at full capacity, except during regular outages to refuel and perform maintenance or plant upgrades. This mode of operation is not sustainable for many nuclear plants as average electricity pricing drops due to low natural gas prices and increased renewable generation.

2. *Flexible operation*. A nuclear power station dispatches power by ramping down and up to meet net generation demands[1]. This mode of operation impacts revenues and increases costs due to the potential for increased maintenance and decreased fuel utilization factors, although these increases are small.

3. *Dedicated energy park*. Nuclear arbitrages power and thermal energy (steam or a secondary heat-delivery loop) to one or more energy users according to the energy demands of the users. This paradigm requires a coordinated buildup of energy users near the power plant where thermal energy is used in the industrial processes. A wide variety of industrial users could take advantage of the low-cost steam produced by an LWR [1].

[1] Net demand = Total electric demand – renewable energy contributions.

4. *Hybrid operations*. The nuclear plant both participates on the electricity grid and apportions power or thermal energy to one or more energy users according to market signals in order to maximize revenue to the nuclear plant. Hybrid operations will usually require energy or product storage to ensure continuity of the industrial product supplier. The business case for hybrid options depends on efficient use of the energy and the capital required for the overall system.

5. *Power revenue optimization*. The nuclear plant produces and stores energy during periods of over-generation in order to dispatch additional electricity to the grid during periods when demand exceeds generation. Power revenue optimization is a form of hybrid operations when the secondary, non-electrical product is sold to the market in a manner that optimizes the profit for the overall integrated energy system.

In the analyses described in this report, a hybrid operations approach was taken, where the nuclear plant can select whether to produce hydrogen or to sell electricity to the power grid based on economics.

1.3 LWR Hybrid Operations

Under hybrid operations, a nuclear plant can shift energy to a secondary process that productively utilizes excess generation capacity. A hybrid system can also provide an offtake for energy when the local marginal price of electricity on the grid is less than the value of directing energy to a secondary user. This requires a tightly coupled connection to the power generation operations of the nuclear plant. The LWR hybrid plant may apportion energy between the industrial user and the electricity grid to optimize the revenue of the nuclear plant, depending on specific day-ahead electricity grid capacity commitments and reserve capacity agreement requirements. One benefit of LWR hybrids may be the opportunity to regulate reactive power, as well as frequency, if the response time constants of the hybrid are sufficiently agile. Such ancillary grid services may someday be valorized by the regional reliability office or grid balancing authorities.

Figure 2 depicts a hybrid system implemented into an integrated energy system. Electricity is provided to the grid when the electrical selling price is high and to a hydrogen production facility when pricing is low. The illustration also illuminates the thermal integration of the industrial process with the nuclear facility. In the case of high-temperature steam electrolysis, the ratio of thermal energy delivered to the electrolysis plant is less than 9% of the total thermal energy produced by the nuclear plant. This steam energy is used to maintain the HTSE in a hot-standby mode. This allows the HTSE unit to immediately respond to pricing fluctuations on the grid, thus giving the nuclear power plant the agility to avoid sale of electricity during low electric pricing scenarios. The remainder of the steam produced by the LWR produces electricity that can be sold to the electric grid or utilized to produce hydrogen in the HTSE facility. The integrated system additionally includes storage containers for the products produced via HTSE, namely H_2 and O_2. Product storage is necessitated by system requirements for operational flexibility and operational down time.

In the petrochemical world, it is commonplace to sign yearly to multi-year contracts with companies for production of a product rather than to have a daily market bid on commodities. This is similar to a Power Purchase Agreement (PPA) in the power world. Such agreements create a baseline economic value for the provider but also create an additional challenge in terms of flexibly for maximizing profitability. To allow for flexible operations outside of contractual agreements, storage capabilities are required. The exact sizing of storage appropriate to maximize flexibility for profitability is an objective function of integrated energy systems that is area and unit dependent. This report will seek to determine the proper storage size for the specific markets and systems presented henceforth.

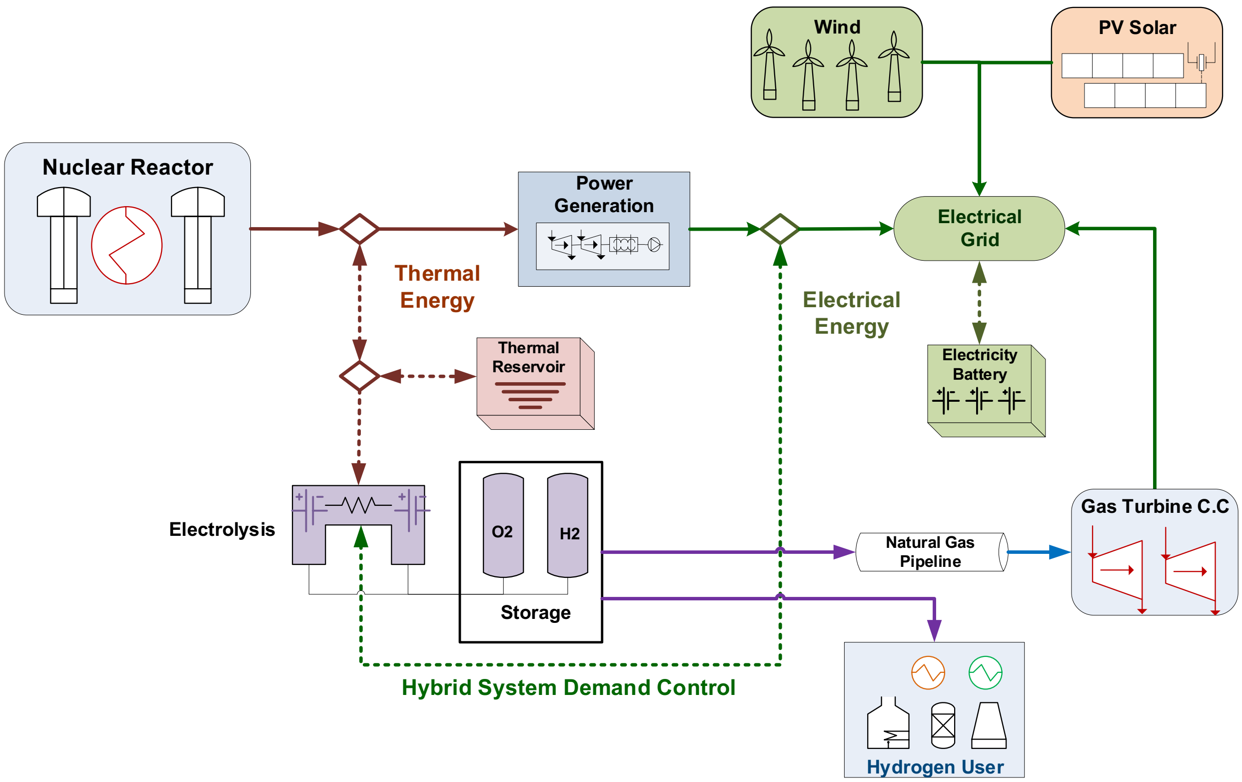

Figure 2. LWR co-generation plant for hydrogen production.

This TEA focuses on H_2 generation industries located primarily in the Midwest region of the country. The Midwest has a high concentration of nuclear power plants operating in a deregulated market and has near-term hydrogen market potential from its agricultural and industrial sectors.

1.4 Hydrogen as an Energy Network

Hydrogen can be used for production of iron pellets, nitrogenous fertilizers, polymers, synthetic fuels, forest products, food products, and for fuel-cell vehicles. Hydrogen generation is also being considered for large-scale and long-term energy storage when power-generation capacity exceeds the demand of the grid. It can also be injected into NG pipelines and burned as fuel for heating and power generation with a fuel cell or gas turbine. If hydrogen is produced from clean, low-emissions energy sources, its utilization in multiple energy sectors will have a significant impact on air quality and can help to significantly reduce greenhouse gas emissions in the United States and throughout the world. A U.S. DOE concept referred to as H_2@Scale (meaning hydrogen at scale; see Figure 3) explores the potential for wide-scale hydrogen production and utilization in the U.S. to enable resiliency of the power-generation and transmission sectors while also aligning diverse multibillion-dollar domestic industries, domestic competitiveness, and job creation [7].

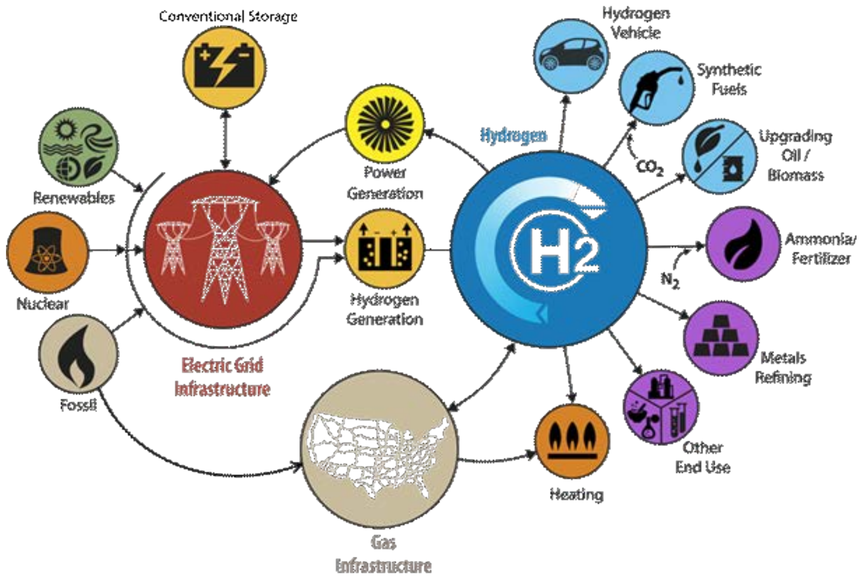

Figure 3. Visualization of U.S. DOE concept for H2@Scale. Image extracted from [8].

As previously described, SMR is the conventional process for producing hydrogen. SMR uses steam and high-temperature heat to convert natural gas into H_2 and CO_2. SMR is mature, and plants have been built by gas product supply companies such as Air Products, Praxair, Air Liquide, and Linde (among others). Alternatively, electrolysis can be used to split water into hydrogen and oxygen using electricity or pure thermal energy. Low-temperature alkaline electrolysis (AE) technology is fully commercial, but is more expensive than SMR, except on a small scale where pure hydrogen is needed or in regions where the cost of natural gas is high (unlike the U.S.). With assistance from DOE [9], advanced water-splitting materials and technologies are rapidly being advanced by electrolysis technology development companies. This includes the use of polymer-electrolyte membrane (PEM) electrolysis and HTSE. These two processes improve the overall efficiency of water splitting and, when nuclear or renewable electricity and heat are used, environmental emissions are near zero.

$$H_2O \text{ (steam)} + CH_4 \text{ (natural gas)} + (O_2) \xrightarrow{\textit{Combustion Process}} H_2 + CO_2 \quad \text{[SMR Reaction]}$$

$$H_2O \text{ (alkaline solution)} + \text{electricity} \xrightarrow{\textit{Electrochemical Cell}} H_2 + O_2 \quad \text{[AE]}$$

$$H_2O \text{ (distilled water)} + \text{electricity} \xrightarrow{\textit{Polymer Electrolyte Membrane Cell}} H_2 + O_2 \quad \text{[PEM Electrolysis]}$$

$$H_2O \text{ (steam)} + \text{electricity} \xrightarrow{\textit{Solid Oxide Electrolyte Cell}} H_2 + O_2 \quad \text{[HTSE]}$$

The focus of this TEA to determine the cost benefit and technical requirements associated with retrofitting an existing nuclear power plant to support hydrogen generation via HTSE in a “smart way.” Such a system would ideally be able to compete in both the electricity and hydrogen markets in a way that drastically increases profitability and reduces risk to the nuclear owner/operator.

1.5 References

[1] C. McMillan, R. Boardman, et al., *Generation and Use of Thermal Energy in the United States Industrial Sector and Opportunities to Reduce its Carbon Emissions*, NREL/TP-6A50-66763, INL/EXT-16-39689, October 2016. https://www.nrel.gov/docs/fy17osti/66763.pdf

[2] L. Davis and C. Hausman, "Market Impact of a Nuclear Power Plant Closure," American Economic Journal: Applied Economics 2016, 8(2): 92-122

[3] U.S. Energy Information Agency, 2016 Outlook for Natural Gas Prices—U.S. Average.

[4] Nuclear Energy Institute, *Nuclear Costs in Context*, August 2017.

[5] Contingency (or risk) is calculated as 10% of total costs plus $4/MWh.

[6] Based on 6/4/2018 NYMEX forward energy prices for relevant hub less 2015-2017 average basis differential to nuclear plants.

[7] https://www.energy.gov/eere/fuelcells/h2-scale

[8] H2@Scale figure produced by National Renewable Energy Laboratory. Bryan Pivovar, Lead of national laboratory team responsible for initiative and championing H2@Scale.

[9] Hydrogen production technology development falls under the DOE Energy Efficiency/Renewable Energy Fuel Cell Technology Office (or FCTO).

2. HYDROGEN PRODUCTION

Hydrogen can be produced using a number of different technology pathways and resources. Today, 95% of the hydrogen produced in the United States is made by reforming natural gas – SMR – in large centralized plants [1]. SMR is the most economic technology available in most cases, primarily owing to an abundance of low-cost NG. The cost of producing H_2 using SMR is highly dependent on the cost of natural gas. For this report, the cost of hydrogen production via SMR process was based on three NG price scenarios, which utilized pricing data from the U.S. Energy Information Administration's Annual Energy Outlook (AEO) 2018 report [2]: low oil and gas resources and technology (high NG prices), high oil and gas resources and technology (low NG prices), and reference NG price scenarios. The reference NG price scenario provided SMR baseline cases throughout this assessment. Figure 4 shows NG prices for industrial users in the PJM region as projected by the AEO for 2018.

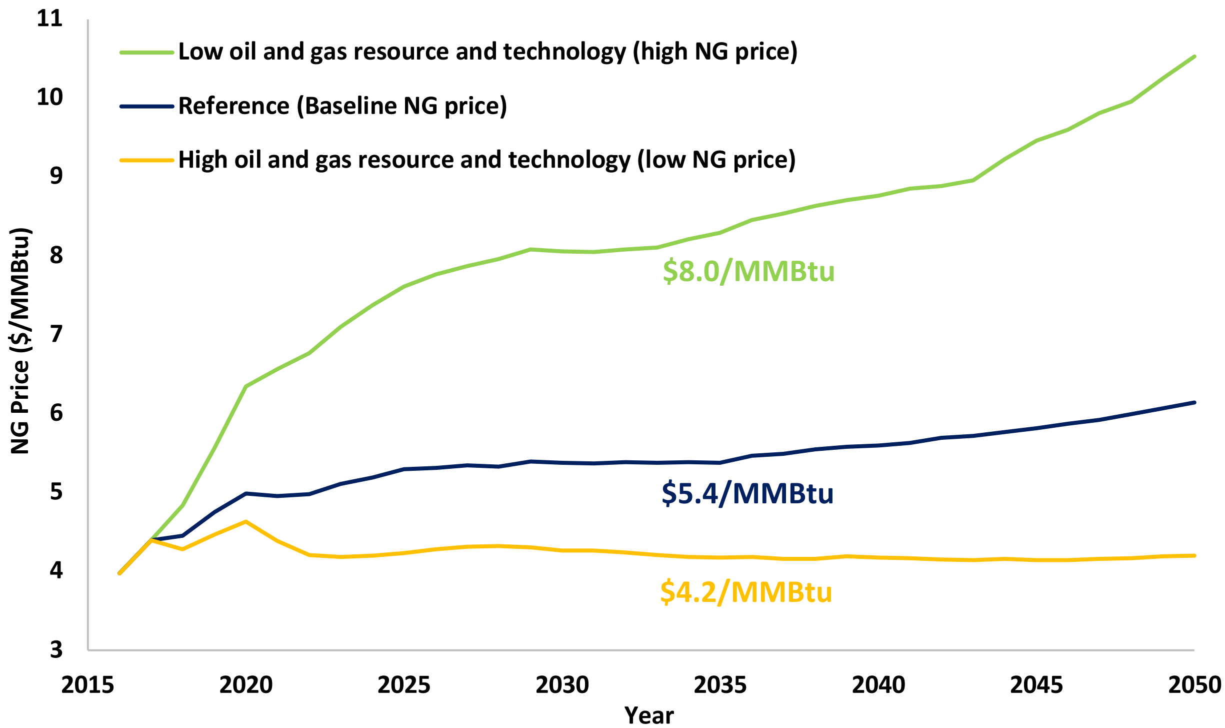

Figure 4. NG prices (2017$) projected by the AEO for 2018 [2]. Mean NG prices are $8.0/MMBtu (million British thermal units), $5.4/MMBtu, and $4.2/MMBtu for high, baseline, and low NG price scenarios, respectively.

Alternative hydrogen production technologies with differing costs and maturity levels are available or under development. For example, interest in electrolysis—the splitting of water into H_2 and O_2 using electricity—has grown in recent years. Electrolysis offers distinct advantages over SMR, and although current electrolytic production costs are high, further research and development are expected to reduce costs. This includes the use of low-temperature PEM electrolysis, which uses only electric power for H_2 production, and high-temperature solid-oxide electrolysis (HTSE), which uses electricity and heat. These two processes could generate H_2 without carbon emissions when nuclear or renewable electricity and heat are used for electrolysis. This section gives an overview of HTSE technology and describes the benefits of utilizing HTSE via thermal integration with a nuclear reactor.

2.1 High-Temperature Electrolysis

This section details the process of hydrogen generation via high-temperature steam electrolysis. It first gives a brief background on the technology itself and how it can be commercialized in an industrial process. Then, a detailed discussion on current operational modes is presented.

2.1.1 Background

High-temperature steam electrolysis is an updated version of low-temperature electrolysis (LTE) with higher efficiencies. While LTE uses only electrical energy, HTSE boosts overall efficiencies by utilizing both heat and electricity to split water into hydrogen (H_2) and oxygen (O_2) in solid oxide electrolyzer cells (SOECs). SOECs are effectively solid oxide fuel cells (SOFCs) operating in reverse. Figure 5 shows a cross-section of a representative planar "SOEC stack."

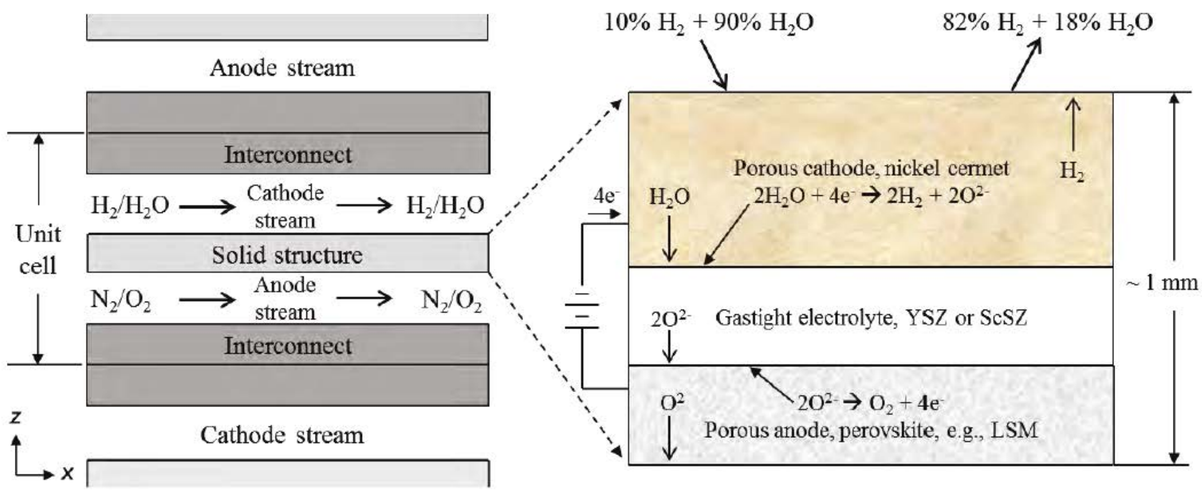

Figure 5. Cross-section of a cathode-supported planar SOEC stack. The case of co-flow is depicted. [3, 4]

The cathode-supported cell consists of a three-layer solid structure (composed of porous cathode, electrolyte, and porous anode) and an interconnected (separator) plate [5]. An oxygen-ion-conducting electrolyte (e.g., yttria-stabilized zirconia [YSZ] or scandia-stabilized zirconia [ScSZ]) is generally used in SOECs [6]. For electrically conductive electrodes, a nickel cermet cathode and a perovskite anode, such as strontium-doped lanthanum manganite (LSM), are typically used. The interconnect plate separates the process gas streams; it must also be electrically conducting and is usually a metallic material, such as a ferritic stainless steel. Stack operation typically occurs at the "thermoneutral point." At the thermoneutral point, thermal energy consumed by the electrolysis reaction precisely matches heat generation via irreversible losses [4]. In practical terms, this means that all of the energy input into the stack is absorbed by the electrolysis reaction, meaning zero heat consumption or loss from the environment.

HTSE has an operating range of 600–850°C and uses electricity and heat to produce hydrogen. Electrolysis efficiency increases at higher operating temperatures, requiring less electrical energy. This increased efficiency can lower production costs because the thermal energy required is generally less expensive than electrical energy. This assessment focuses on (oxygen-conducting) SOEC-based HTSE, which is driven by steam and electricity from the pressurized LWR.

Thermal energy from a generator is utilized to preheat feedstocks for the HTSE unit via intermediate heat exchangers as depicted in Figure 6. Then, depending on the pre-heating capability of the generator, and HTSE design parameters, additional topping heat is added via electrical resistance heating to boost feedstock temperatures. Once feed stock temperature and pressure is sufficient it is then run through the electrolyzer stacks. In the stacks, electricity is supplied, and the electrolysis process begins to take place, splitting the steam into oxygen and hydrogen. During normal operation, a portion of the hydrogen produced is recycled back into the stacks to reduce corrosion and pitting.

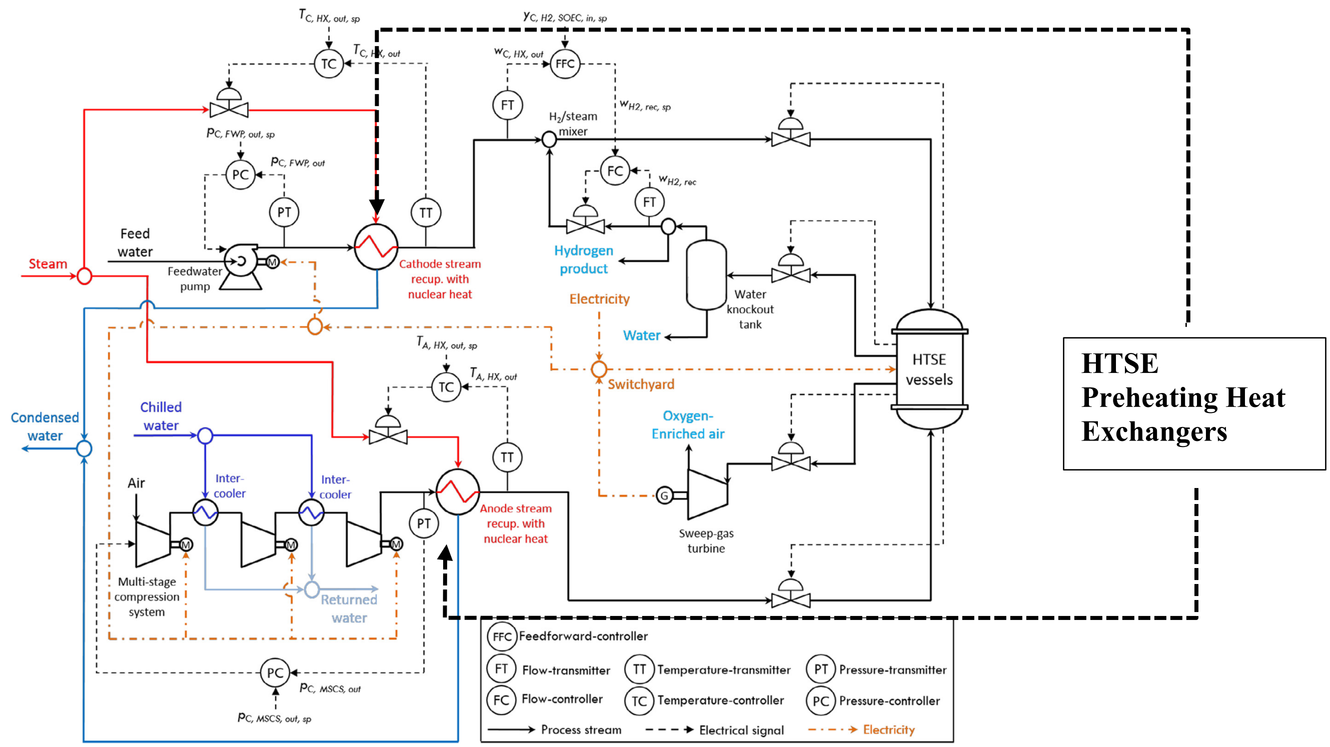

Figure 6. Representative connection of generator with HTSE pre-heat train [4].

The overall energy split of thermal energy vs. electrical topping energy vs. electrical energy for electrolysis is generator and HTSE specific. As a general rule when working with LWRs, the split of the total energy input into the HTSE is about 3–10% thermal energy, with electrical breakdowns ranging from 5–20% electrical topping energy and the remainder of the electricity utilized for electrolysis.

2.1.2 Modes of Operation

HTSE units are a new technology, and since integration with large-scale generators has yet to be experimentally validated on a commercial scale, the community is undecided on how proper thermal ramping would be accomplished.

During system startup and shutdown, the rule of thumb manufacturers recommend is a temperature gradient of no more than 2°C per minute to avoid SOEC cell cracking. Assuming a standard operating temperature of 800°C, 6.5 hours would be required. Such ramp rates are impractical in a large-scale system attempting to operate flexibly between markets. To compensate for the long startup time, vendors have introduced a “hot standby mode.”

Hot standby mode operation takes advantage of the relative breakdown of energy input into the system. In hot standby mode, the electrolysis portion of the energy provided to the system is cycled off, while the thermal energy and topping heat remain. Assuming the cell operates at the thermoneutral point, as is typical of most SOEC cells, this will ensure proper preheating and recuperation takes place, thermal gradients are not induced, and hydrogen generation can continue at any moment.

This mode of operation is particularly beneficial because seventy percent of the energy provided to the system has little to nothing to do with thermal gradients and thus can be considered thermally agnostic. In a 2012 paper published by Petipas et al., it was shown that the electrolysis portion of the energy provided to the cell can be cycled on and off at will with little to no effect on stack performance [7]. This capability allows the HTSE unit to operate as a flexible generator on a significant portion of its operating capability. In the future, as cells continue to advance the ability to thermally flex on shorter timescales, additional flexibility options will arise.

2.2 HTSE Models

INL has spent several years developing detailed simulations of the HTSE process, in particular for nuclear-integrated cases. These simulations have been developed using two code packages: Aspen HYSYS, a state-of-the-art, steady-state chemical process simulator [8]; and Modelica [9, 10], a nonproprietary, object-oriented, equation-based programming language used to conveniently model complex transient physical and cyberphysical systems (e.g., systems containing mechanical, electrical, electronic, hydraulic, thermal, or control components).

This study makes extensive use of these models and the modeling capability at INL to evaluate integration of a nuclear reactor with a Rankine power cycle and an HTSE plant located in close proximity to the reactor site. This report assumes a basic familiarity with code packages like Modelica and Aspen HYSYS; hence, a detailed explanation of the software capabilities, thermodynamic packages, unit operation models, and solver routines is beyond the scope of this work.

2.2.1 Modelica Models

A high-fidelity transient HTSE model in Modelica has been completed at INL with associated control algorithms as depicted in Figure 7 and Figure 8 based on design parameters from a Dominion Engineering design report [4, 11]. A summary of these system parameters is described in

Table 1. Included in the model are custom heat recuperation systems, a multi-stage compression unit, a sweep gas turbine, and numerous feedback/feedforward controllers to maintain the desired process conditions, such as temperatures, pressures, mass flow rates, and mole fractions at various locations in the considered HTSE plant.

Table 1. Single 53.3 MWe HTSE train parameters.

Parameter	*Value*
Nominal H_2 Production	0.4015 kg/sec [12,700 tonne/yr]
Nominal Electricity Consumption	53.3 MWe
Nuclear Process Heat	14.6 MWt [4.63 MWe]
Nominal Electric to total energy utilization rate ($\eta_{electric\_to\_total}$)	0.92
Operating Pressure	1.96 MPa
Stack Inlet Temperature	850°C
Stack Exit Temperature	750°C
Stack Operating Voltage	1.185V
Steam Utilization Rate	80%

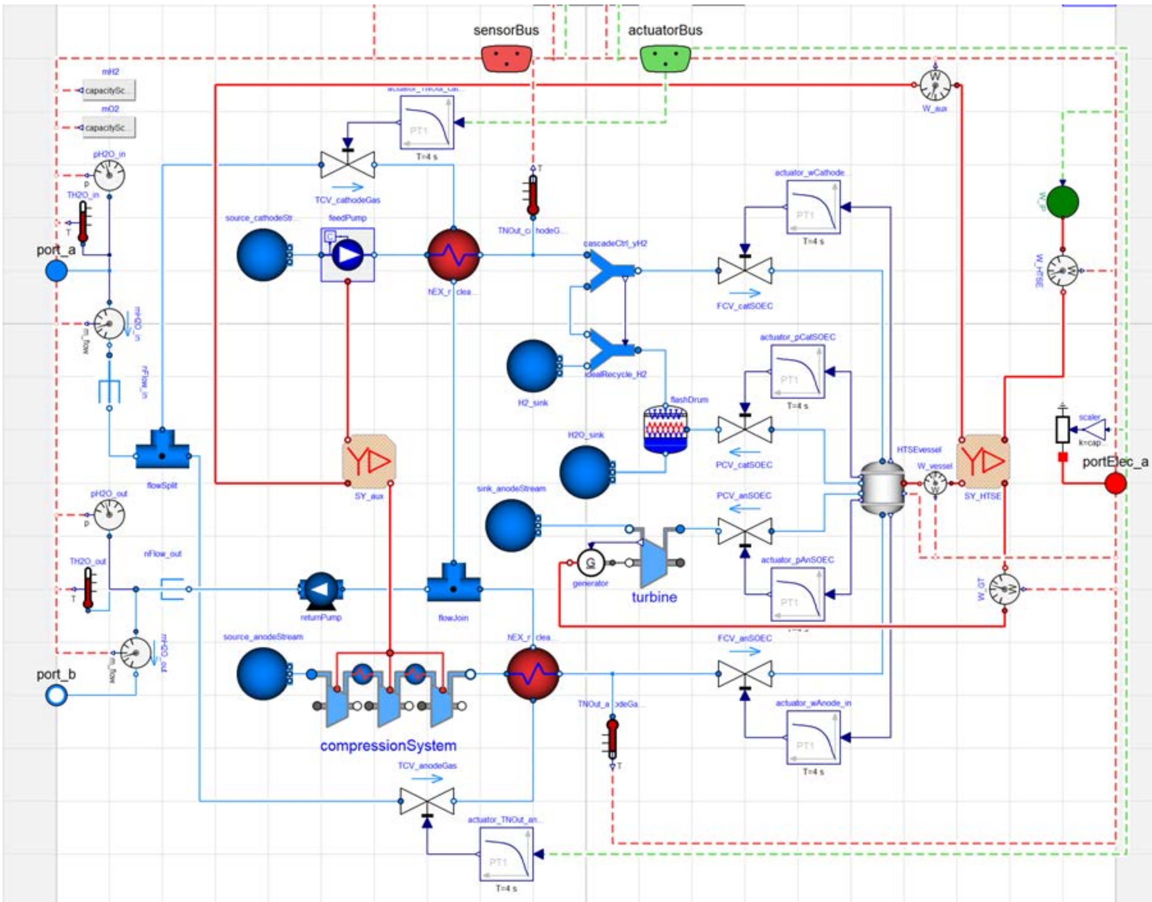

Figure 7. Preheating section with integration to steam generator (Modelica).

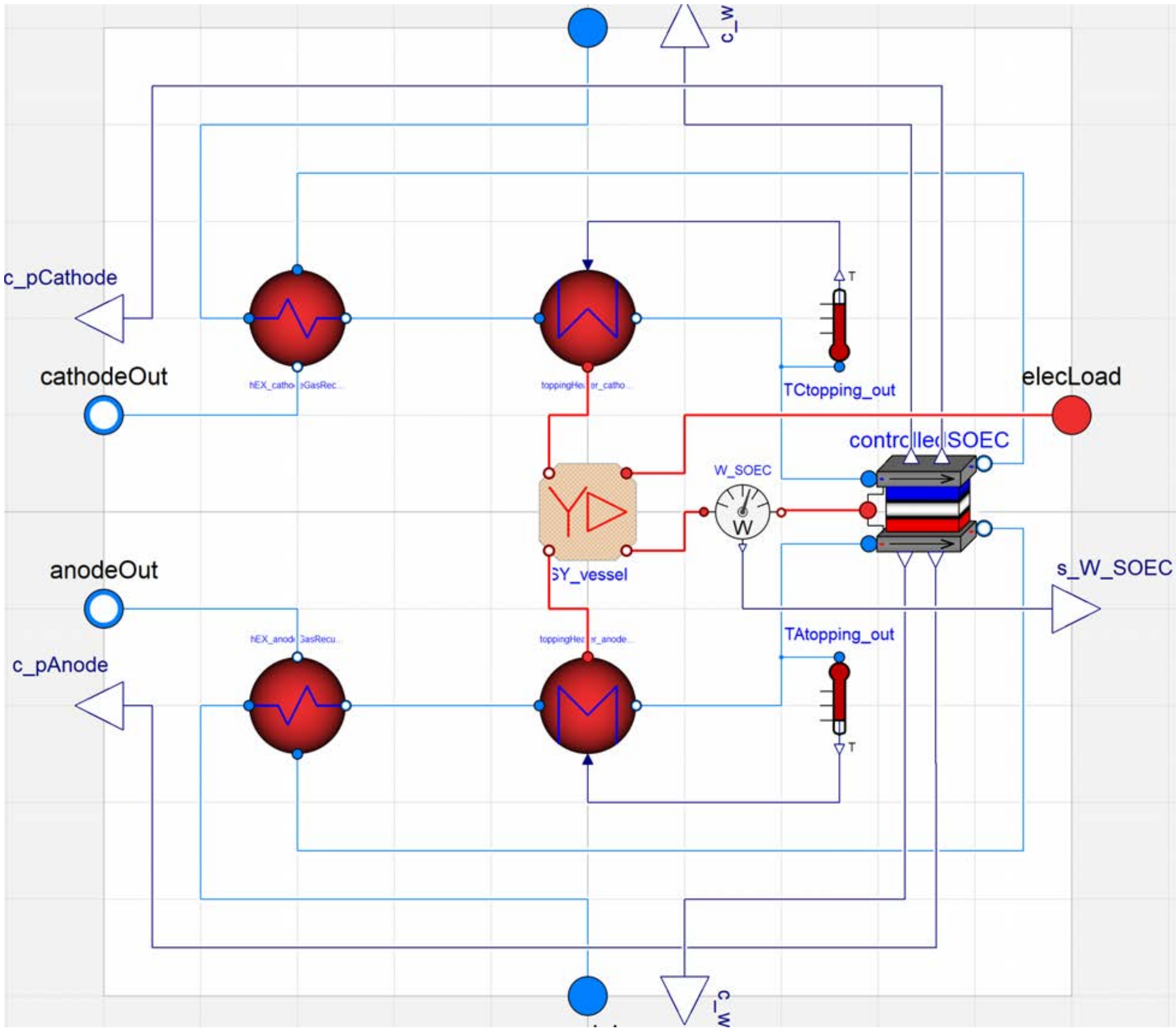

Figure 8. HTSE vessel with electrical topping heaters and recuperation (Modelica).

For the process modeled here, the energy duty of the HTSE process at nominal conditions when integrated with a standard light-water reactor is 92% electricity input with a floating range (90–94%) depending on flexible operation of the system. Thermal energy from the LWR is utilized to preheat feed stocks in the HTSE module. Via custom design of the hydrogen and oxygen separation processes, heat recuperation can be used to superheat steam that is supplied to the HTSE process. As much recuperation as possible is utilized, then for the final temperature boosting step to 850°C, electrical topping heaters are engaged as depicted in Figure 8 [4]. The aforementioned thermal loop providing heat integration is a closed loop. Further analysis on the details of integrating with a nuclear power plant (distance, nuclear system controls, feed water system re-entry, etc.) will be discussed in a later chapter.

2.2.2 ASPEN/HYSYS Model Based on FCE

In addition to the models produced in Modelica, separate ASPEN/HYSYS models were developed focusing on another HTSE configuration. The ASPEN model is based on a lower-pressure design, thus decreasing potential capital costs.

The energy duty of the process is approximately 85–90% electricity input. Thermal energy is used to produce and supply superheated steam combined with a gas recycle stream. With custom design of the hydrogen separation process, heat recuperation can be used to superheat steam that is supplied to the HTSE process from intermediate-temperature steam generators.

Hydrogen can be efficiently produced using HTSE with steam temperatures up to approximately 800°C in SOECs. The steam and associated electricity would be produced by the associated reactor and provide the required input to the HTSE unit operations. Heat recuperation from the product streams would be used to amplify the temperature of the steam generated in the steam generator to the temperatures required for HTSE. Electricity is simultaneously directed to the HTSE plant [12].

Figure 9 shows the detail of the overall custom HYSYS process model developed for the thermal and electrical integration of the HTSE plant with the pressurized LWR. The model utilizes the steam generator conditions and electricity produced by the power plant for the integration. Electricity is produced by a subcritical Rankine cycle at a plant net thermal efficiency of 32.75%. The HTSE process draws steam from the steam generator for use in the electrolysis process, which takes place at thermo-neutral conditions, defined as isothermal at 735°C and adiabatic. The SOEC operating pressure is 0.5 MPa.

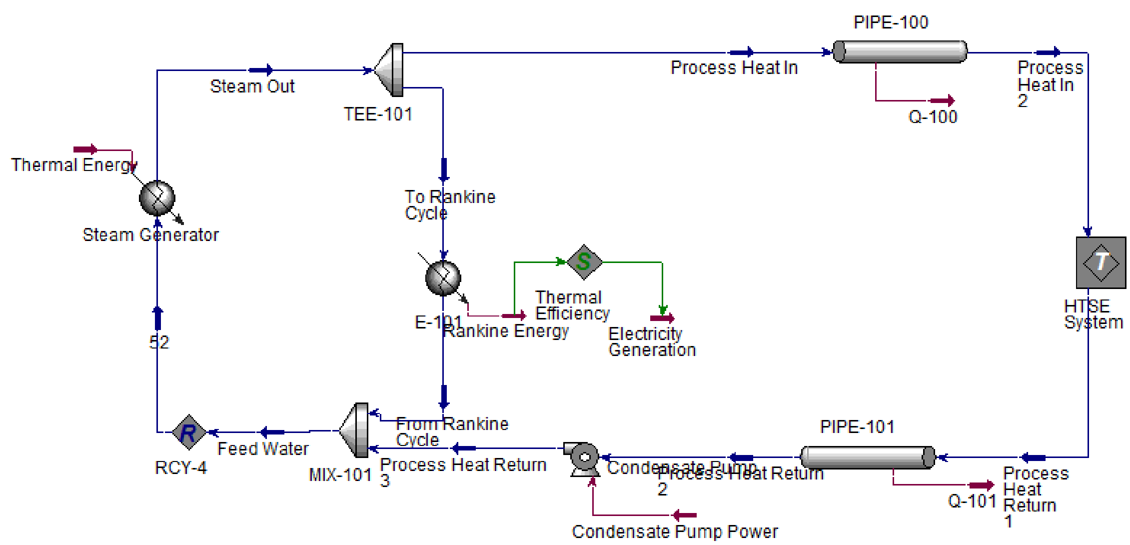

Figure 9. Process flow diagram of the LWR/HTSE integration.

The thermal loop providing heat integration is a closed loop. Steam is used to transfer thermal energy from the nuclear reactor to the HTSE plant 1,000 m away. The condensate is pumped from the HTSE plant back to the steam generator. A separate water source is required for the electrolysis process. This is mostly a safety consideration. Because the steam generator is rated for a specified steam flow, the reactor system would not respond well to a decrease in steam should there be a process disturbance at the HTSE plant, even if it were only a 10% decrease in steam flow.

Figure 10 shows the nuclear heat integration and recuperation for the HTSE process with highlights showing low- and high-temperature heat recuperation, nuclear process heat integration, and electric topping heat. Table 2 summarizes the electrolysis cell conditions applied in the analysis.

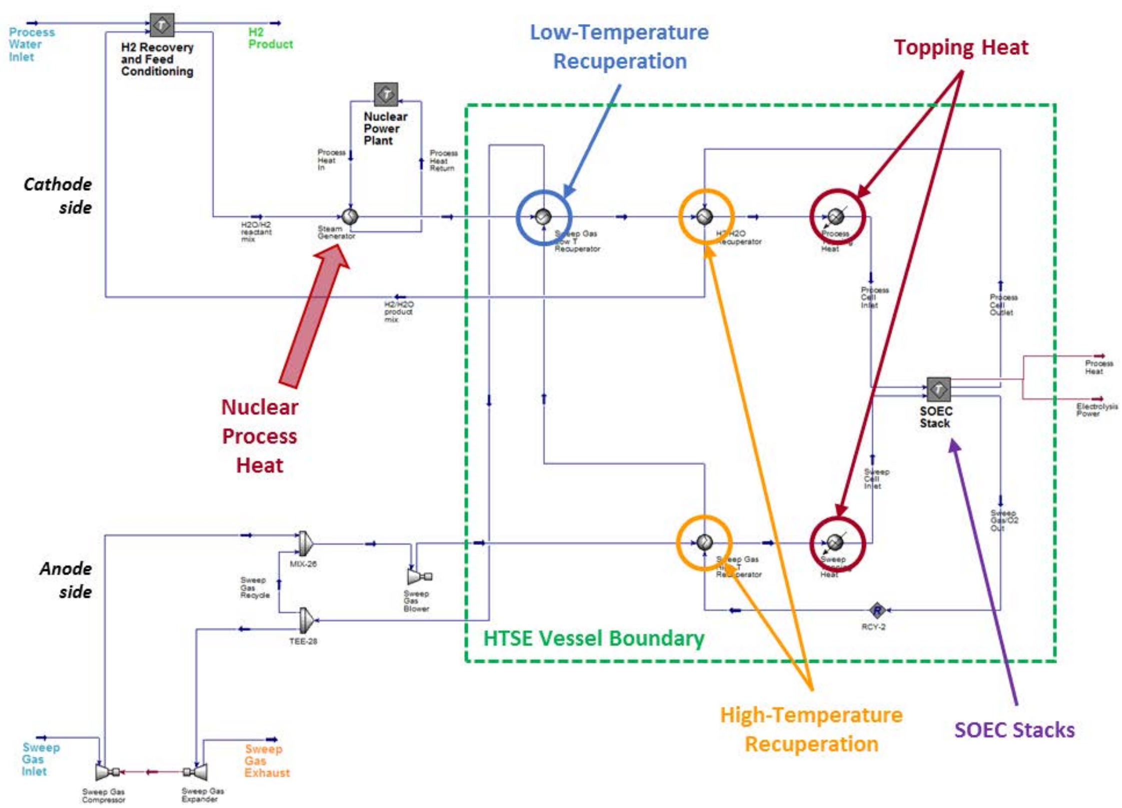

Figure 10. HTSE process flow diagram.

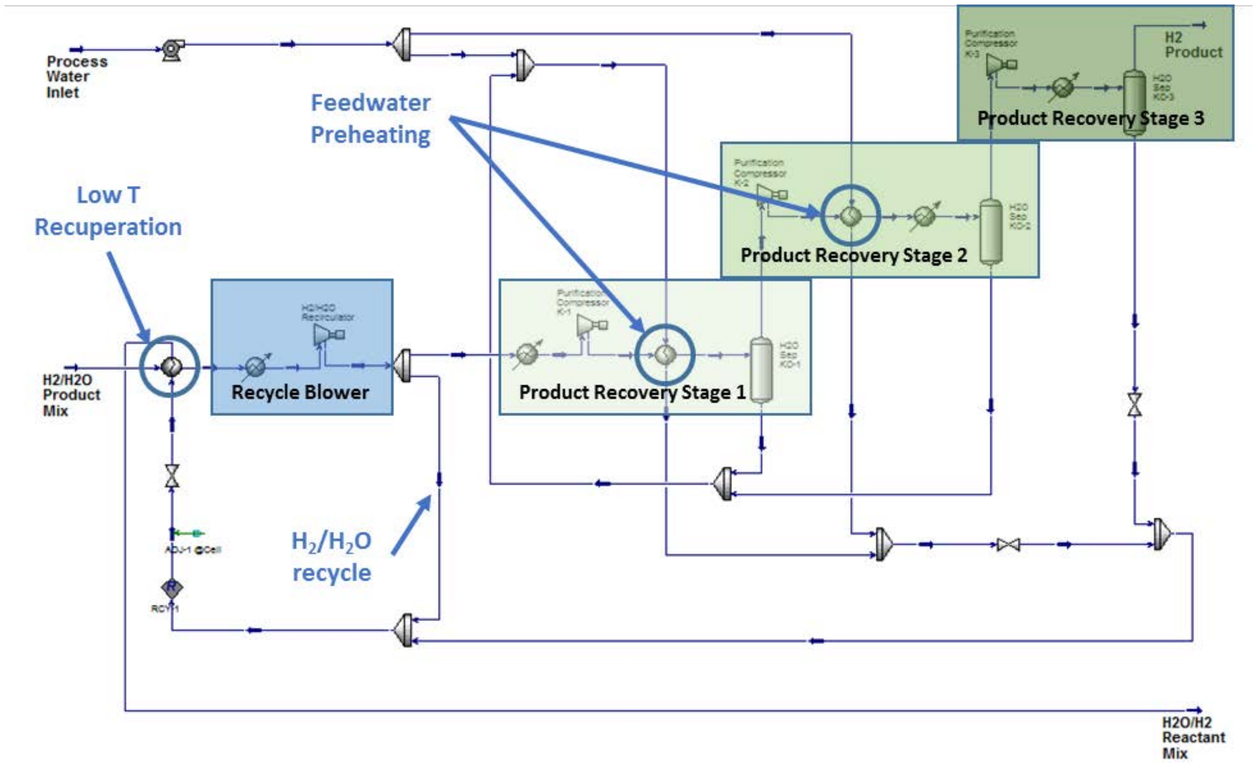

Figure 11. Hydrogen recovery and feed conditioning area process flow diagram.

Table 2. HTSE electrolysis cell parameters.

Parameter	Unit	Value
Number of Cells	–	9,187,596
Cell Area	cm^2	81
Current Density	amperes/cm^2	1.0
Area Specific Resistance	Ohms × cm^2	0.25
Operating Voltage	Volts	1.285
Current (per cell)	Amperes	81
Hydrogen Inlet Mole Fraction	%	50
Operating Temperature	°C	735
Operating Pressure	MPa	0.5

2.2.3 Results of the Process Model

Figure 12 graphically presents a high-level material and energy balance summary for the LWR/HTSE-integration case at nominal operating conditions. The breakdowns of electricity and thermal energy consumptions, as well as cooling water use, are summarized in Table 3. A secondary steam loop transfers ~285°C steam from the LWR to the HTSE facility, where feedwater is converted to low-temperature steam.

High- and low-temperature recuperators are subsequently used to superheat the steam used in the electrolyzers. A total of about 109 MWt of thermal energy is needed for this purpose.

The HTSE process requires both the feed and sweep streams to be heated to 735°C, which necessitates additional topping heat from an auxiliary heat source. This heat source could come from a combustor, electric heating, or waste heat from a neighboring process. In this assessment, this topping heat is provided by electrical heaters at the power rating shown in Table 3.

The hydrogen production efficiency for the HTSE process is defined as the higher heating value (HHV) of the product hydrogen, divided by the HHV of feed gas and other thermal-energy input into the process [4]. As shown in Table 3, the production efficiency of hydrogen (32.9%) is very close to the thermal-to-electrical conversion efficiency (32.7%). Standard electrolysis of water typically is less than 25% efficient.

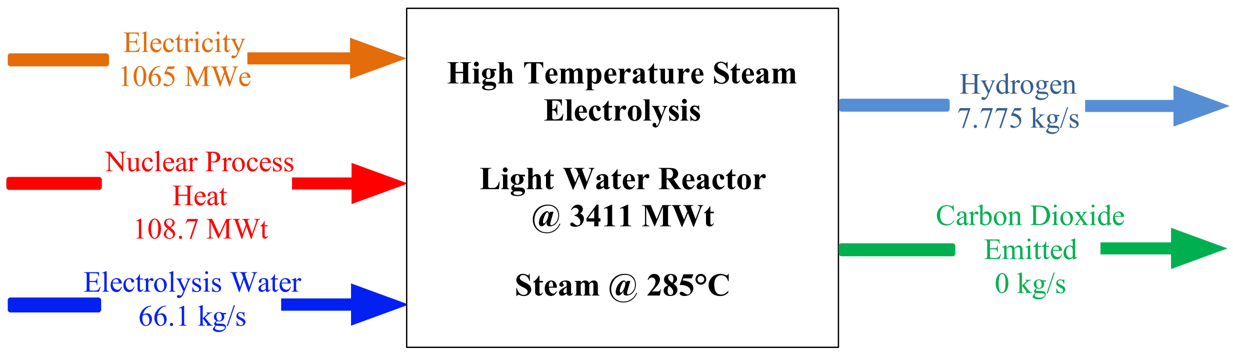

Figure 12. General energy and product flows for the LWR/HTSE integration case.

Table 3. Hydrogen production summary.

Description	Unit	Value
Input		
Reactor Thermal Power	MWt	3411
Outputs		
Hydrogen	kg/s (tpd)	7.775 (671)
Hydrogen Production Efficiency	%	32.9
Power Cycle Thermal Efficiency	%	32.7
Utility Summary		
Total Power Consumed	MWe	1065
Electrolyzer	MWe	956.3
Pumps	MWe	0.1
Compressors	MWe	82.5
Topping Heaters	MWe	26.22
Nuclear Process Heat		
Total Nuclear Process Heat	MWt	108.7
Water Consumption		
Cooling Water for HTSE Process	kg/s	1958
Water Consumed by Electrolysis	kg/s	66.1
Carbon Dioxide (CO_2) Emissions		
Emitted	tpd CO_2	0

Note: The reported values are based on the plant's nominal design capacity—i.e., an OCF of 100%. The actual values depend on the OCF, which in this report is set to 92.4%.

2.3 Economic Modeling Overview

In this section, comprehensive cost estimates were conducted using a combination of the Aspen Process Economic Analyzer, DOE's H2A production tool, and data collected from HTSE vendors. In this report, all costs are presented in 2019 dollars unless otherwise stated. The following sections present the economic results.

2.3.1 Capital Cost Estimation

Depreciable capital costs consist of direct and indirect costs. Direct capital costs (DCCs, or bare-module costs) were estimated based on costs reported by Solid Oxide Electrolyzer Cell vendor FuelCell [13] Energy as well as cost estimates generated by Aspen Process Economic Analyzer. DCC estimates were generated for the HTSE system, feed and utility system, sweep-gas system, hydrogen/steam system, hydrogen-purification system, and nuclear steam delivery system.

FuelCell Energy costs provided the basis for the stack and module cost estimates as well as several minor balance-of-plant equipment items including the DI polisher, water flow meters, and air filters. The 640 tonne H_2 per day process design specifies modular construction in which HTSE modules are installed in 40 separate 16-tpd blocks, with each block comprised of 16 individual 1-tpd modules. Due to use of modular construction, the HTSE module costs do not scale with capacity in the same way as conventional equipment. Instead, it is assumed that HTSE module capital costs will decrease with equipment manufacturing volume as described in the FuelCell Energy technoeconomic analysis final report.

The Aspen Process Economic Analyzer (APEA) [14] was used to estimate the remainder of the balance-of-plant equipment DCCs directly based on the engineering design estimates generated by HYSYS process models; i.e., capital cost scaling methods were not used to estimate baseline process equipment costs. As with the module costs, the balance-of-plant equipment is installed in modular 16 tpd blocks and capital costs will therefore not scale with increased capacity according to conventional cost estimating methods. It is assumed that the installed capital costs for the 16 tpd blocks that include HTSE stacks and modules, as well as the balance-of-plant equipment, will decrease with equipment manufacturing volume according to a power law experience curve relation with an improvement rate of 95% (i.e., installed costs decrease by 5% with each doubling of the total of quantity of blocks produced).

After the DCCs were obtained, the site preparation cost (10%), engineering fee (10%), project contingency (15%), contractor's fee (3%), and legal fee (2%), which make up the indirect costs, were assumed for all cases.

The cost of land is non-depreciable and was taken as 1.5% of the total depreciable capital (TDC) [15]. Finally, the total capital investment (TCI) was calculated by summing the total depreciable and non-depreciable capital costs. Table 4 presents the capital cost breakdown for the baseline HTSE case. Note that the capital costs presented are for inside the battery limits and exclude costs for administrative offices, utilities, storage areas, and other essential and nonessential auxiliary facilities. The results show that the largest single contributor to the TCI is the HTSE vessel (36%), followed by the hydrogen purification system (16.2%).

Figure 13 compares, at different SOEC module (stack, high- and low-temperature recuperators, and topping heaters) costs, the TCIs of the HTSE plant. The results indicate that, as expected, the TCI increases as the module capital cost increases.

Table 4. TCI for the baseline HTSE case: 640 tpd capacity, SOEC module capital cost of $50/kWe.

Depreciable capital costs ($)		
Direct (bare module) costs		
Vessel[a]	196,343,327	[36.0]
Feed and utility system[b,c]	11,626,270	[2.1]
Sweep-gas system[d]	35,703,548	[6.5]
Hydrogen/steam system[d]	47,376,949	[8.7]
Hydrogen-purification system[d]	88,250,872	[16.2]
Nuclear steam-delivery system[d]	4,417,358	[0.8]
Total direct capital cost	383,718,323	[70.4]
Indirect costs		
Site preparation	38,371,832	[7.0]
Engineering and design	38,371,832	[7.0]
Contingencies and contractor's fee	69,069,298	[12.7]
Legal fee	7,674,366	[1.4]
Total indirect capital cost	153,487,329	[28.1]
Non-depreciable capital costs ($)		
Land	8,058,085	[1.5]
TCI ($)	**545,263,737**	**[100]**
Electrolyzer power consumption (MWe)	909.1	
TCI per DC power input to SOEC stacks ($/kWe)	600	

Note: Values in the brackets are the breakdown of TCI expressed in terms of percentage.

[a] Scaled from Tang, E., Wood, T., Brown, C., Casteel, M., Pastula, M., Richards, M. and Petri, R. "Solid Oxide Based Electrolysis and Stack Technology with Ultra-High Electrolysis Current Density (>3A/cm²) and Efficiency" Fuel Cell Technologies Office Award Number DE-EE0006961 Final Report, March 31, 2018. Available: https://www.osti.gov/servlets/purl/1513461

[b] Scaled from P. Krull, J. Roll and R.D. Varrin, HTSE Plant Cost Model for the INL HTSE Optimization Study, Reston (VA): Dominion Engineering, Inc.; 2013 Mar. Report No.: R-6828-00-01.

[c] Excludes a deionized water (DIW) system as it is expected to use the existing DIW facility installed at the Nuclear power plant site.

[d] Estimated by APEA.

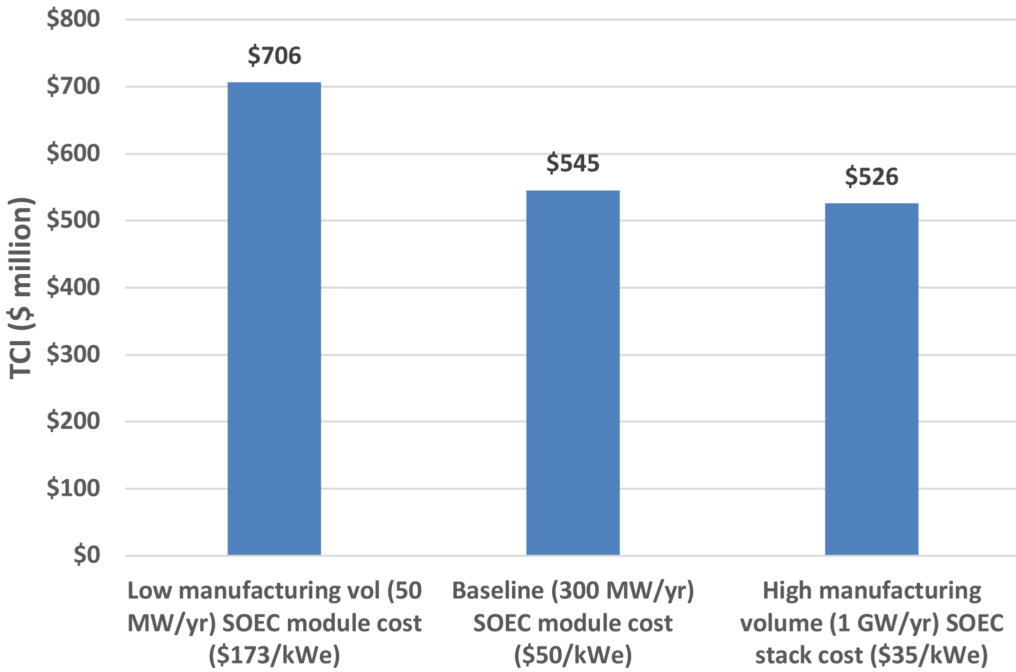

Figure 13. TCIs for HTSE H_2 production process at selected HTSE module annual manufacturing volumes.

2.3.2 Estimation of Maintenance Costs

The stack cell replacement costs were calculated assuming stack replacement every seven years. Royalties were assumed to be 2% of the TDC [14]. Maintenance costs were taken as 2% of the TDC, then multiplied by 2.3 to take into account salaries and benefits for the engineers and supervisory personnel and materials and services for maintenance [14]. An overhead of 26% of the labor and maintenance costs was assumed. Annual property taxes and insurance were estimated at 2% of the TDC, which corresponds to a process of low risk, located away from a heavily populated area [14]. Table 5 provides the manufacturing costs for the baseline HTSE case

Table 5. Annual maintenance costs for the baseline HTSE case: 640 tpd capacity, SOEC module capital cost of $50/kWe.

Direct costs	
SOEC stack replacement costs	11,258,067
Royalties ($)	10,744,113
Labor and maintenance ($)	31,903,165
Indirect costs	
Overhead ($)	5,924,085
Insurance and taxes ($)	10,905,275
Total annual maintenance costs ($)	**70,752,705**

For the remainder of the analysis, it is assumed the maintenance costs scale based on capacity of the HTSE and remain a flat 1.3% of capacity.

2.4 References

[1] U.S. DOE, "Hydrogen Production: Natural Gas Reforming," https://www.energy.gov/eere/fuelcells/hydrogen-production-natural-gas-reforming; 2018 [accessed 18 February 2019].

[2] U.S. EIA, "Annual Energy Outlook 2018," https://www.eia.gov/outlooks/aeo/tables_ref.php; 2019 [accessed 26 January 2019].

[3] Kim JS, McKellar M, Bragg-Sitton SM, Boardman RD. "Status on the Component Models Developed in the Modelica Framework: High-Temperature Steam Electrolysis Plant & Gas Turbine Power Plant." Idaho Falls (ID): Idaho National Laboratory, Nuclear Science and Technology Division; 2016 Oct. Report No. INL/EXT-16-40305. Contract No.DE-AC07-05ID14517. Sponsored by the U.S. Department of Energy.

[4] Kim JS, Boardman R, Bragg-Sitton S. "Dynamic performance analysis of a high temperature steam electrolysis plant integrated within nuclear-renewable hybrid energy systems". Applied Energy. 2018.; 228: 2090-2110.

[5] Udagawa J, Aguiar P, Brandon NP. "Hydrogen production through steam electrolysis: Model-based steady state performance of a cathode-supported intermediate temperature solid oxide electrolysis cell." J Power Sour 2007; 166(1):127–36. https://doi.org/10.1016/j.jpowsour.2006.12.081.

[6] O'Brien J. "Thermodynamic considerations for thermal water splitting processes and high-temperature electrolysis." In: Proceedings of IMECE2008, 2008 ASME international mechanical engineering congress and exposition; 2008 Mar 31-Nov 6; Boston, MA, USA; IMECE2008-68880.

[7] Petipas F, Fu Q, Brisse A, Bouallou C. "Transient Operation of a solid oxide electrolysis cell". International Journal of Hydrogen Energy. Vol. 38. Pgs. 2957-2964. (2013).

[8] Aspentech, "Aspen HYSYS," https://www.aspentech.com/en/products/engineering/aspen-hysys; 2018

[9] MODELICA ASSOCIATION, "Modelica and the Modelica Association;" https://www.modelica.org/; (current as of Aug. 16, 2017).

[10] MODELICA ASSOCIATION, "Modelica Language Specification Version 3.4," Modelica Association (2017).

[11] Krull P, Roll J, Varrin RD. HTSE plant cost model for the INL HTSE optimization study. Reston (VA): Dominion Engineering, Inc.; 2013 Mar. Report No. R-6828- 00-01.

[12] M. Bragg-Sitton, R.D. Boardman, R.S. Cherry W.R. Deason and M.G. McKellar, *An Analysis of Methanol and Hydrogen Production via High-Temperature Electrolysis Using the Sodium Cooled Advanced Fast Reactor*, Idaho Falls (ID): Idaho National Laboratory; 2014 Mar. Report No.: INL/EXT-14-31642. Contract No.: DE-AC07-05ID14517.

[13] Tang, E., Wood, T., Brown, C., Casteel, M., Pastula, M., Richards, M. and Petri, R. "Solid Oxide Based Electrolysis and Stack Technology with Ultra-High Electrolysis Current Density (>3A/cm²) and Efficiency" Fuel Cell Technologies Office Award Number DE-EE0006961 Final Report, March 31, 2018. Available: https://www.osti.gov/servlets/purl/1513461

[14] Aspentech. "Aspen Process Economic Analyzer," https://www.aspentech.com/en/products/pages/aspen-process-economic-analyzer; 2019 [accessed 12 February 2019].

[15] W.D. Seider, J.D. Seader, D.R. Lewin DR. *Product & Process Design Principles: Synthesis, Analysis and Evaluation*, (With CD): John Wiley & Sons; 2009.

3. NUCLEAR POWER STATION

In the United States, there are two subsets of nuclear reactors: boiling water reactors (BWRs) and pressurized water reactors (PWRs). BWRs were set forth as the main system of choice by General Electric and consist of a single loop whereby the water is brought in from the condenser, pumped through the nuclear reactor, boiled into steam, and used to drive a turbine as shown in Figure 14.

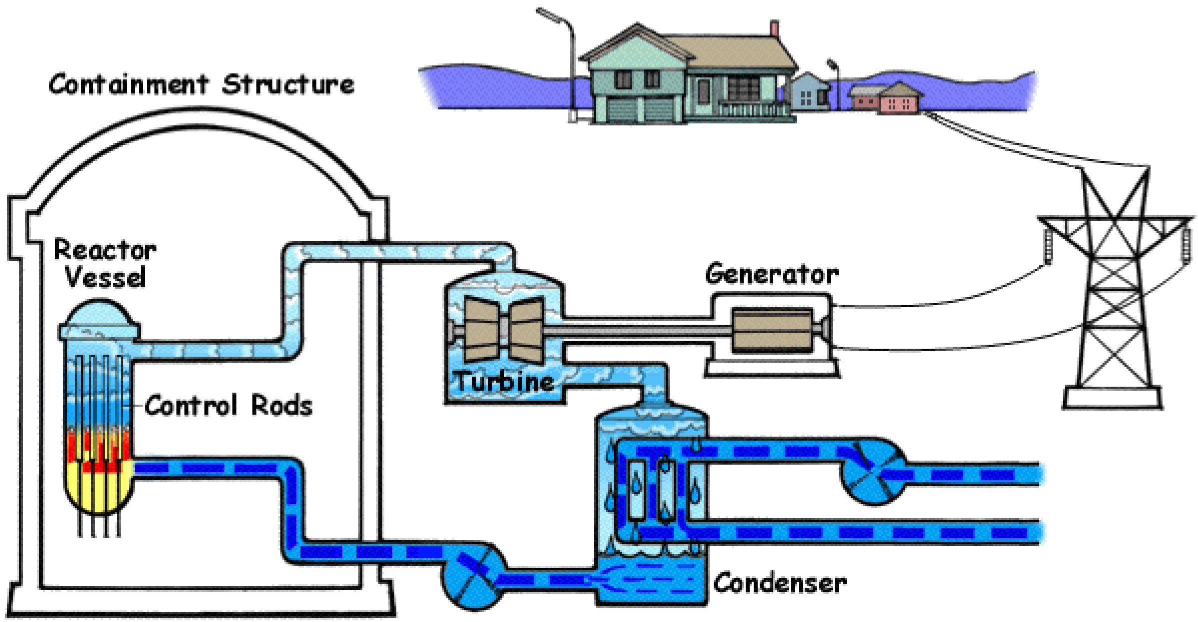

Figure 14. Depiction of a boiling water reactor [1].

PWRs, on the other hand, consist of a secondary and a primary loop as illustrated in Figure 15. In PWRs, the primary and secondary side interact via a steam generator that boils water. The steam generator serves the purpose of keeping the radioactive water in the primary loop contained, as well as allowing the primary side to operate at pressures and temperatures that cannot be achieved in a BWR. Since BWRs do not have a containment loop, the water running through it quickly becomes activated and must be treated as radioactive material. For this reason, BWRs have yet to become the major focus point of integrated energy systems.

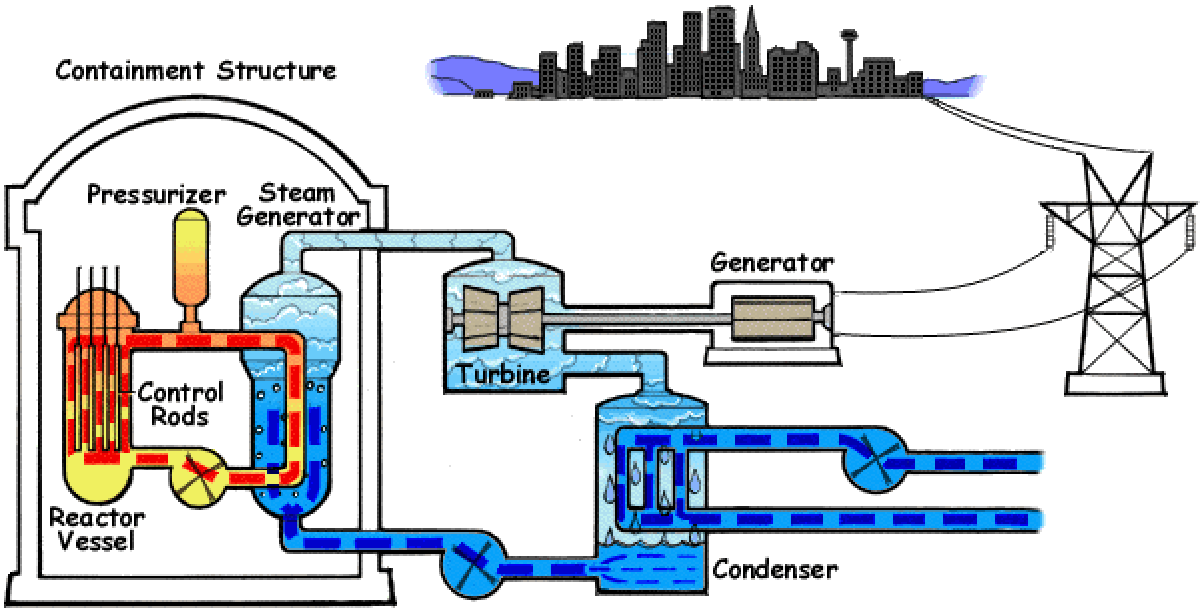

Figure 15. Pressurized water reactor [2].

PWRs are further broken down into two subsets depending on the steam generator design chosen at the plant. The two steam generator designs are U-tube and once-through (OTSGs). U-tube steam generators operate by boiling steam inside the vessel, sending it through dryers at the top, and sending essentially saturated steam to the turbine. OTSGs operate as a single pass where subcooled liquid enters the bottom of the steam generator and begins to boil. By the time it reaches the end of the steam generator, it is superheated. The control algorithms for a U-tube and a once-through are different and must be taken into account when the integration of industrial processes is considered.

Table 6. Representative Westinghouse 4-loop plant specifications [3].

Parameter	*Unit 1*
Thermal Output	3411 MWt
Primary Pressure	2250 psi
Nominal Electric Output	1095 MWe
Steam Generator Type	U-Tube
Steam Generator Pressure	1000-1015 psi
Nominal Steam Flow	15,252,000 lbm/hr

The most common nuclear power plant design in the United States is a Westinghouse PWR, which utilizes a U-tube steam generator. More specifically, a 4-loop Westinghouse configuration is used for approximately 30% of the fleet [4, 5]. Thus, to make this system as applicable as possible, the report considered below is for a Westinghouse 4-loop plant with operating characteristics as depicted in Table 6. Additionally, work has been completed on integrating small modular reactors that utilize OTSGs at the university and national laboratory levels [6,7,8] that can be transferred to the OTSG sector of the United States fleet. Given this and the fact that most of the existing nuclear fleet utilizes U-tube steam generators, the analysis presented here will focus on that subset of the fleet.

Westinghouse designs are standardized on the primary side of the system per a "turn-key" design. The secondary side, or balance of plant, tends to vary according to site-specific needs. However, unlike in other generation stations (coal, natural gas, etc.) balance-of plant transients have a direct impact on nuclear power through reactivity feedback mechanisms.

Nuclear power plants have five main reactivity feedbacks that directly affect reactor power as shown in Equation 1: xenon, boron, control rods, fuel temperature coefficient, and moderator temperature coefficient.

$$\rho = \rho_{Xenon} + \rho_{Boron} + \rho_{Control\ Rods} + \rho_{Moderator} + \rho_{Fuel} + \rho_0 \tag{1}$$

Xenon is a side of effect of the fission process. Fuel reactivity insertion is a byproduct of the fuel temperature and is a negative reactivity source as fuel temperature rises. Control rods are neutron absorbers and can increase or decrease reactivity by being moved in and out of the core to compensate for the effects of the others. The moderator temperature coefficient is designed to be negative such that, as the water in the core heats up, there is a negative reactivity insertion. Finally, boron is inserted via a chemical volume control system to uniformly decrease reactor power. Of these, only boron concentration and control rod insertion length are directly controllable. Both operate on relatively large timescales when compared with the other mechanisms.

Therefore, it is important to have understandable and controllable reactivity insertions. For example, the addition of a large amount "cold" water into the bottom of the steam generator can cause an overcooling event such that moderator temperature in the primary system can fall, causing a reactivity insertion into the reactor and a power excursion.

Nuclear plants expend tremendous resources on characterizing and quantifying all potential impacts that secondary side systems can have on reactor activity. Therefore, when designing a system to interact with the nuclear reactor, it is important to design as few primary side interruptions as possible. To accomplish this, it is essential to understand how a nuclear reactor is controlled during standard operation.

3.1 Standard Four-Loop U-tube PWR Control

As previously mentioned, PWR systems can have one of two options of steam generators, U-tube (UTSG) or once-through steam generators (OTSG). Each has its own control algorithm. UTSGs are provided by Westinghouse, while OTSGs are provided by Babcock and Wilcox. For the analysis presented here, a U-tube steam generator was selected.

A simplified depiction of a U-tube steam generator plant is shown in Figure 16.

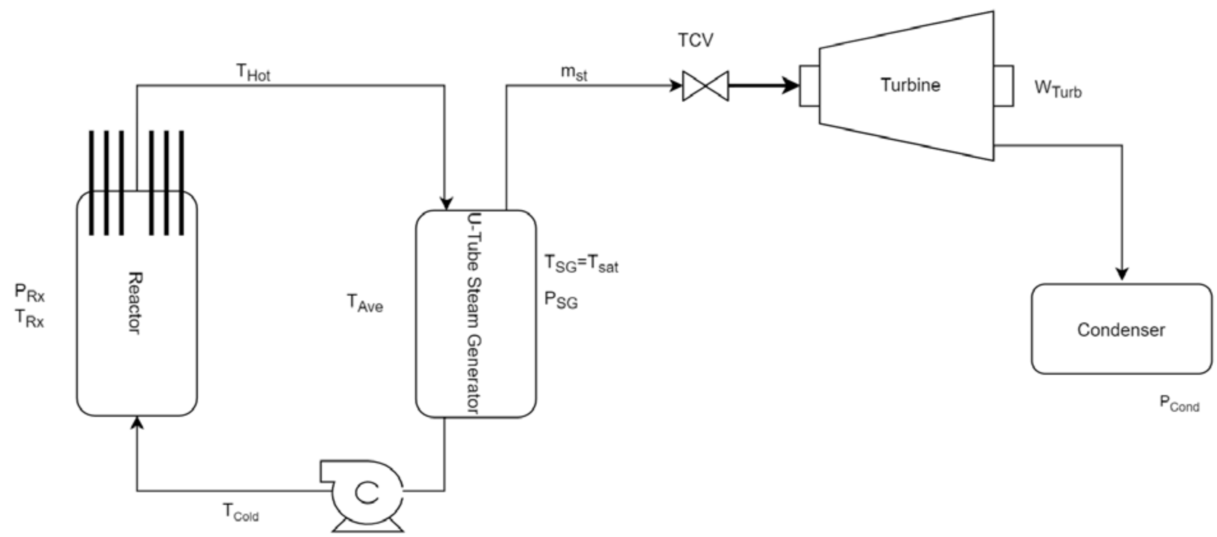

Figure 16. Simplified U-tube steam generator plant.

In UTSG systems, the turbine control valve (TCV) operates to control turbine impulse pressure, which is a surrogate for turbine power and turbine rotations per minute (RPM). As a means of simplifying the control for understanding in this report, one can say the TCV is controlling the turbine output as shown in Equation 2.

$$Error_{TCV} = \frac{\dot{W}_{Turb} - \dot{W}_{Demand}}{\dot{W}_{Demand}} \tag{2}$$

The UTSG can be approximated by Equation 3.

$$\dot{Q}_{SG} \approx UA(T_{ave} - T_{Sat}) \tag{3}$$

where, UA is the effective heat transfer area; T_{ave} is the average temperature of the primary system, and T_{sat} is set by the pressure in the steam generator. In UTSGs, the UA value is approximately constant, since the tube bundles are constantly covered. If one desires the pressure in the steam generator to remain constant for cycle efficiency and material property reasons, then T_{sat} needs to be held constant. At steady state, the amount of heat crossing into the steam generator is equal to the heat produced by reactor (e.g., $\dot{Q}_{Rx} = \dot{Q}_{SG}$). This implies that, at steady state, for the pressure to be held constant and reactor power to change, the average primary temperature T_{ave} needs to change.

This is accomplished via a T_{ave} program based on electric demand, depicted in Figure 17. When electric demand is less than 100%, the heat exchanged across the steam generator is correspondingly reduced, thereby allowing steam generator pressure to remain approximately constant.

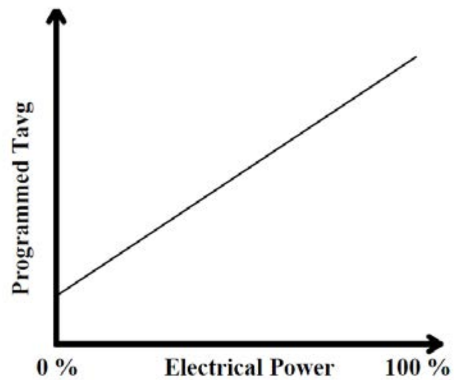

Figure 17. Example T_{ave} program.

To properly model the control algorithms and system level inertia inherent in the system, a transient system model was developed in the physics-based programming language Modelica. A key advantage of Modelica is its separation of physical models and their solvers. This separation enables rapid generation of complex physical systems and control design in a single language without requiring deep knowledge of numeric solvers, code generation, etc.

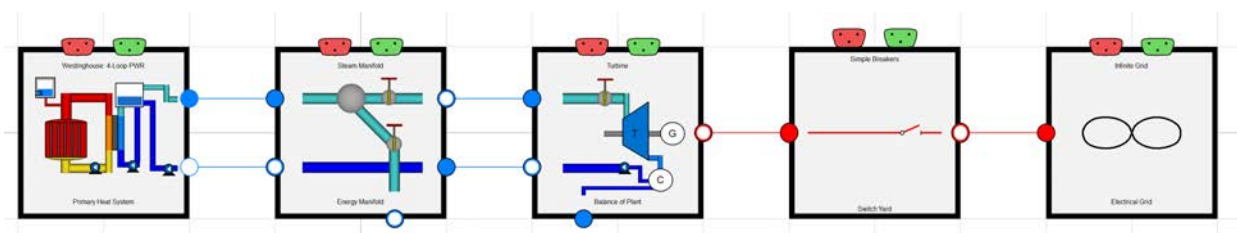

Figure 18. Nuclear power plant depiction in Modelica.

Inside Modelica, each pictorial depiction above corresponds to a section of development. The nuclear reactor depicted in Figure 19 consists of the primary loop with reactivity controllers, fuel bundles, downcomer, reactor coolant pumps, upper and lower plenums, hot leg, cold leg, pressurizer, and associated control systems. A T_{ave} program of the form presented in Equation 4 was utilized.

$$T_{ave} = T_{ave0} + \xi\left(\frac{demand}{demand_0} - 1\right) \tag{4}$$

Where $demand = electric\ power$; $demand_0 = nominal\ output$ and $T_{ave0} = temperature\ at\ full\ power$; $\xi = constant$.

The reactor core model includes traditional point kinetics models, including decay heat groups, fission product behavior, and reactivity feedback. Precursor and decay heat group data are taken from the TRACE manual [11], and fission product data are taken from the *Nuclear Reactor Physics* textbook and the “Chart of the Nuclides” [12,13,14].

Also included is a secondary side system that incorporates a U-tube steam generator broken up into the lower plenum section and the associated steam dome component. (These ensure saturated steam leaves the system.)

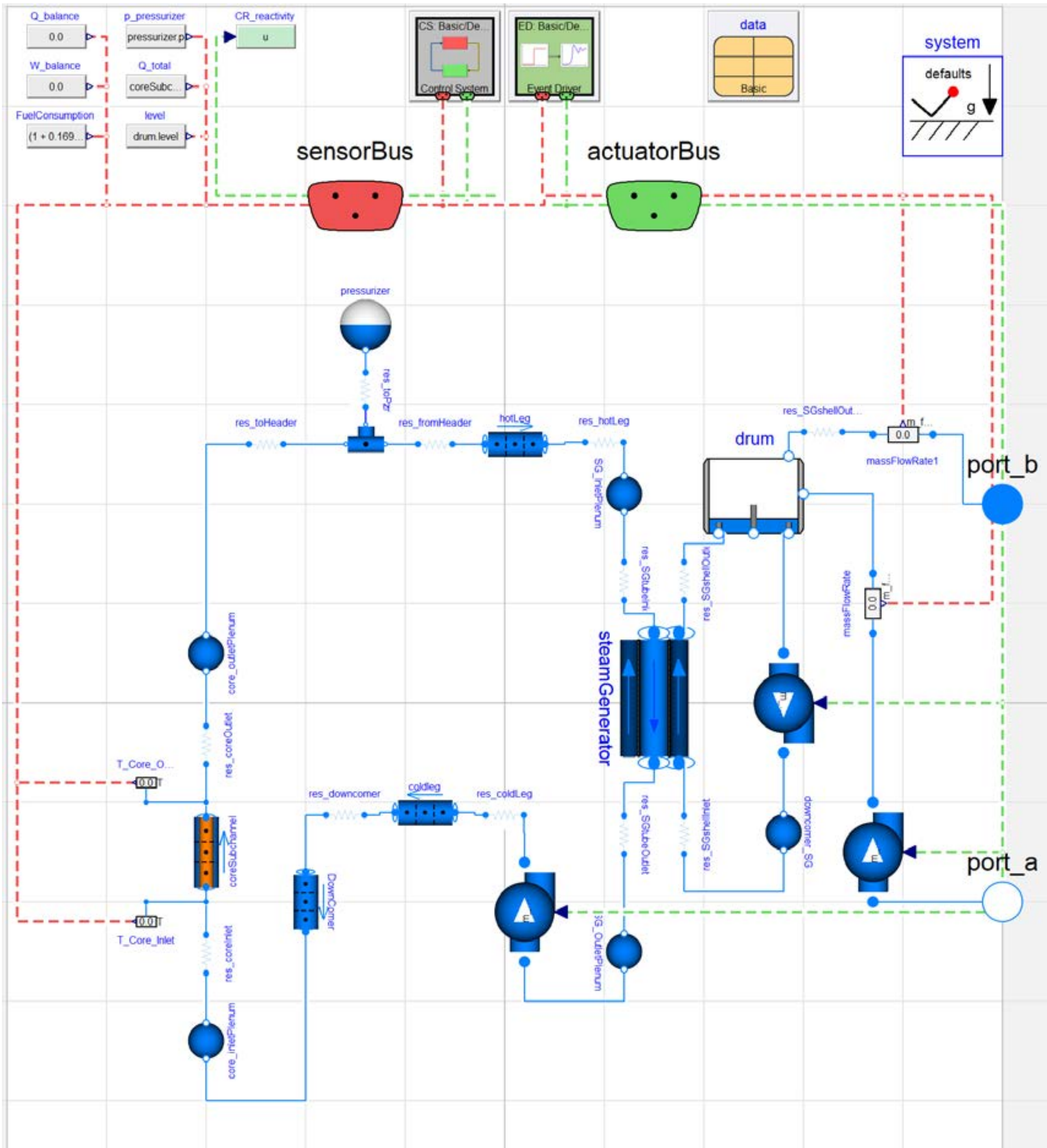

Figure 19. Simplified model of a Westinghouse 4-loop PWR with steam generator.

System conditions and components, shown in Table 7 and Table 8, were sized to be consistent with publicly available data on Westinghouse 4-loop systems [3].

Table 7. Nominal core parameters of the Westinghouse 4-loop PWR.

Parameter	Value	Unit
Core Diameter	3.37	m
Fuel-Type	UO2	-
Cladding-Type	Zircaloy-4	-
Fuel Length	3.66	m
Fuel Radius	3.9	mm
Cladding Thickness	0.57	mm
Gap Thickness	0.079	mm
Fuel Rod Pitch	0.0126	m
Assembly Size	17x17	-
Number of Assemblies	193	-

Table 8. Nominal steam generator operating parameters of the Westinghouse 4-loop PWR.

Parameter	Value	Unit
Number of Steam Generators	4	
Pressure	6.98	MPa
Tube Inner Radius	0.0222	m
Tube Outer Radius	0.197	m
Number of Tubes (per unit)	6500	-
Tube Length	27.6	m
Shell Length	20.6	m
Lower Shell Inner Diameter	3.02	m
Upper Shell Inner Diameter	4.06	m

Following the steam generator is a steam manifold. The steam manifold is modeled simply as piping being directed from the nuclear reactor to the turbine. The manifold is used to direct flow to the turbine and can be used to bypass steam off the main steam line into "n" number of industrial processes, in this case high-temperature steam electrolysis units. The balance-of-plant model is developed to a fidelity level that can include standard 4-loop balance-of-plant control algorithms (e.g., turbine control valves and turbine bypass valves.).

To demonstrate the capabilities of the Modelica model, a small test problem was conducted. For the purposes of the test problem, the reactor only provides electricity to the grid and is operated in load follow mode. A properly tuned control system should maintain steam generator pressure, meet electric demand, follow the prescribed T_{ave} program, and oscillate in power accordingly.

Initially, the reactor is at 100% power (~3411MWt), meeting the nominal turbine demand of 1,095 MWe, and steam generator pressure is maintained at 69.8bar (1012 psi). At hour three, the electric demand begins to drop, causing the turbine control valve to modulate to meet demand. Correspondingly, the programmed T_{ave} program causes the control rods to insert as the programmed T_{ave} begins to decrease. The reactivity insertion caused by the control rods decreases reactor power, and the average primary temperature decreases as illustrated in Figure 20(d). Due to this decrease in the primary system average temperature, the steam generator pressure is maintained approximately constant throughout as desired.

Over the twenty-four-hour test, electric demand drops as low as 72% of nominal demand. Throughout this period, steam generator pressure is maintained constant, reactor power oscillates according to the T_{ave} program, and turbine demand is met throughout. The results presented in Figure 20(a-d) lend credence to the viability of the Modelica models control strategy and overall modeling capability.

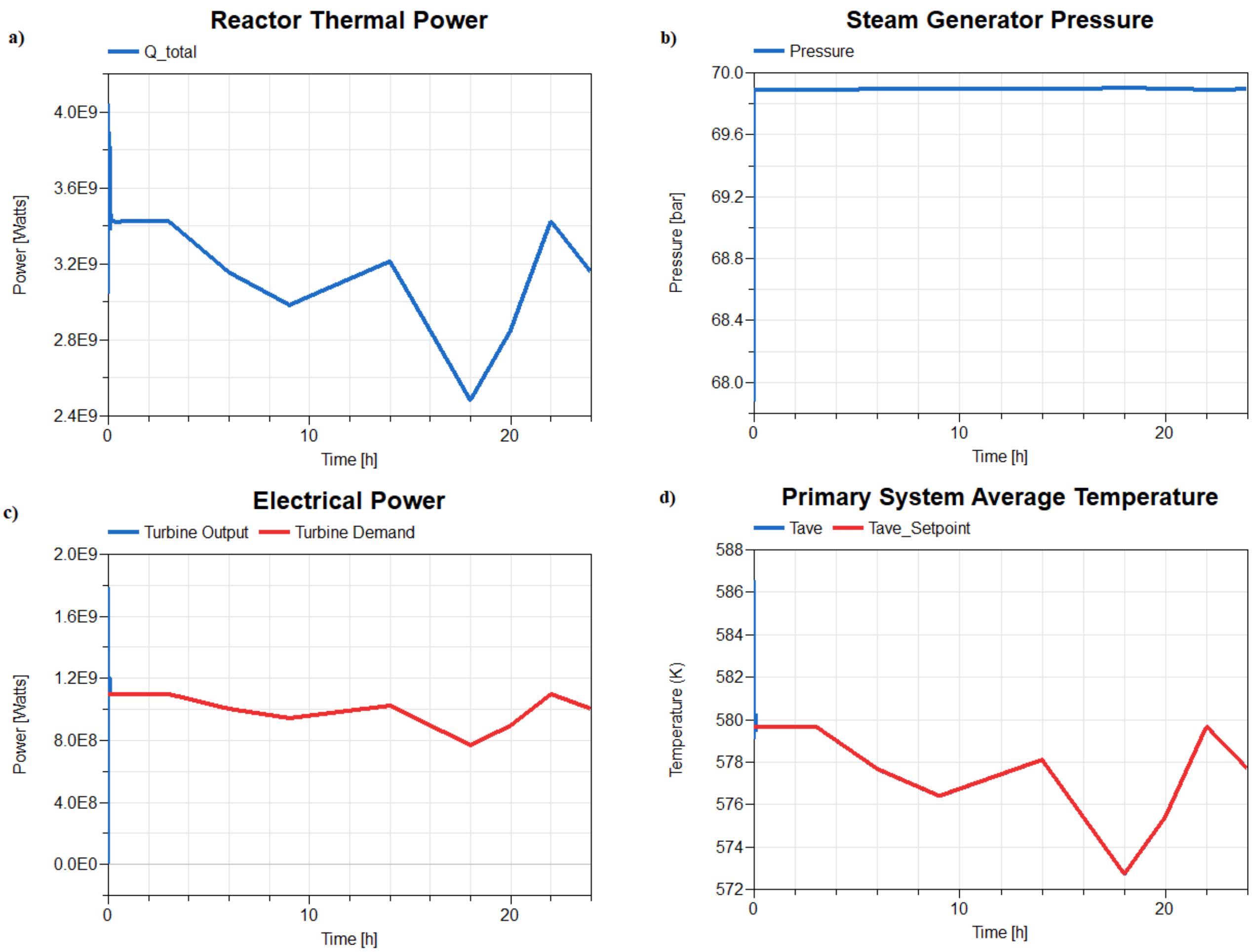

Figure 20. Modelica simulation of U-tube PWR control algorithm. (a) Reactor thermal power. (b) Steam generator pressure. (c) Electrical power. (d) Primary system average temperature.

To properly identify temperature oscillations that occur as bypass steam is bled off the main system turbines, a more in-depth steady-state model of the balance of plant was developed in IPSE pro. IPSE pro is a commercial package used to model complex thermo-dynamic cycles in steady-state operation. From IPSE pro, a number of power levels were simulated, and exit feedwater temperature values were recorded. Feedwater temperature oscillation with respect to turbine power was developed. This temperature oscillation correlation was input as a boundary condition in the transient Modelica models.

3.2 Modification of Four-Loop U-tube PWR Control for Use With HTSE

To increase economic viability of nuclear plants in a changing energy market, there has been discussion on how to thermally integrate current fleet PWRs with HTSE to produce hydrogen. As previously mentioned, the selection of steam generator for the nuclear reactor is the primary factor in how the system is controlled. Therefore, in a retrofit application, it is important to be cognizant of the existing control algorithms.

For the thermal integration depicted in Figure 21, the offtake steam is taken prior to the TCV, as this allows for the highest-grade steam possible. As mentioned in an earlier section, HTSE units operate at ~800°C and, therefore, should utilize the highest-grade steam possible for preheating their feed stocks. By preheating the feedstocks with thermal energy, a large reduction is made in the overall energy requirements for the HTSE, thereby increasing profit margins.

For HTSE integration with light-water reactors, electrical topping heat is provided by the nuclear plant as well as thermal energy. The split can be generally bounded by a 10:1 ratio of electricity to thermal energy, meaning that out of the total energy provided by the nuclear plant to the HTSE, about 10% will be thermal energy and 90% will be electrical energy. The specific ratio is LWR and HTSE design specific, with 10% thermal energy offtake being the bounding scenario. With a 10% steam offtake limit, the bulk of the steam will continue to be sent to the turbine train to produce electricity. However, to accommodate this offtake control scheme, modifications were required.

The steam is used to transfer thermal energy from the nuclear reactor to the HTSE plant 1,000 m away. A separate water source is required for the electrolysis process. This is mostly a safety consideration. Condensate from the HTSE is sent into the main systems condenser, whereby it can be properly processed and reheated through the feed train.

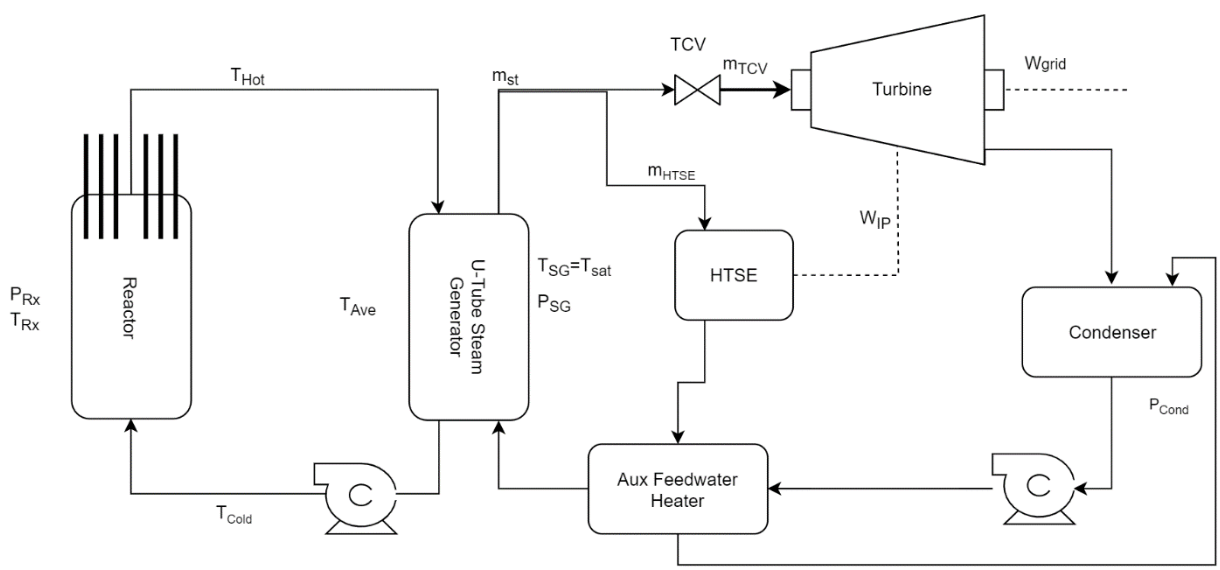

Figure 21. Simplified thermal integration of U-tube PWR plant high-temperature steam electrolysis.

The TCV will operate in the same manner as in standard load follow operation, except now the $\dot{W}_{Demand}$ variable is modified to meet $\dot{W}_{demand} = \dot{W}_{grid} + \dot{W}_{IP}$, where $\dot{W}_{IP}$ is the electricity requirement of the industrial process.

$$Error_{TCV} = \frac{\dot{W}_{Turb} - \dot{W}_{Demand}}{\dot{W}_{Demand}} \tag{5}$$

To ensure steam generator pressure remains constant, a modification to the T_{ave} program's *demand* variable was required. Previously, demand was just electricity demand seen by the turbine. Now, demand is the sum of the steam sent to the HTSE process and the electricity demand as shown in equations 6a and 6b.

$$demand = \dot{W}_{grid} + \dot{W}_{IPeff}$$

$$demand = \dot{W}_{grid} + \frac{\dot{W}_{IP}}{\eta_{electric\_to\_total}} \tag{6a}$$

$$\dot{W}_{IP\_preheating\_effective} = \frac{\dot{W}_{IP}}{\eta_{electric\_to\_total}} \tag{6b}$$

Where $\eta_{electric\_to\_total} = ratio\ of\ electric\ heating\ to\ total\ power\ provided\ to\ HTSE$

In literature and through studies completed at Idaho National Laboratory, it has been determined that 6–10% of the power provided to the HTSE can be provided via steam energy from an LWR. [15, 16]. To show the capability of the modified control scheme, a nominal $\eta_{electric\_to\_total}$ of 0.92 was selected for this report.

To illustrate the modified control scheme in Modelica, an exploratory 10-hour simulation was conducted. The TCV controller and T_{ave} program were both modified to reflect Equations 5 and 6b, respectively. For the test, a collective HTSE size of 266.5MWe was chosen to demonstrate how the reactor/balance-of-plant systems operate when a significant portion of the total system energy is utilized to make hydrogen. The system configuration is shown in Figure 22. In the simulation, approximately 66MWt is sent to the HTSE to preheat feedstocks, effectively reducing turbine output by 21.3MWe. Due to thermal gradient considerations, it is assumed the HTSE will operate in the region between hot standby mode and full hydrogen production. As mentioned in an earlier chapter, hot standby mode means feedstock preheating will continue to take place, and only electricity utilized for electrolysis can be oscillated.

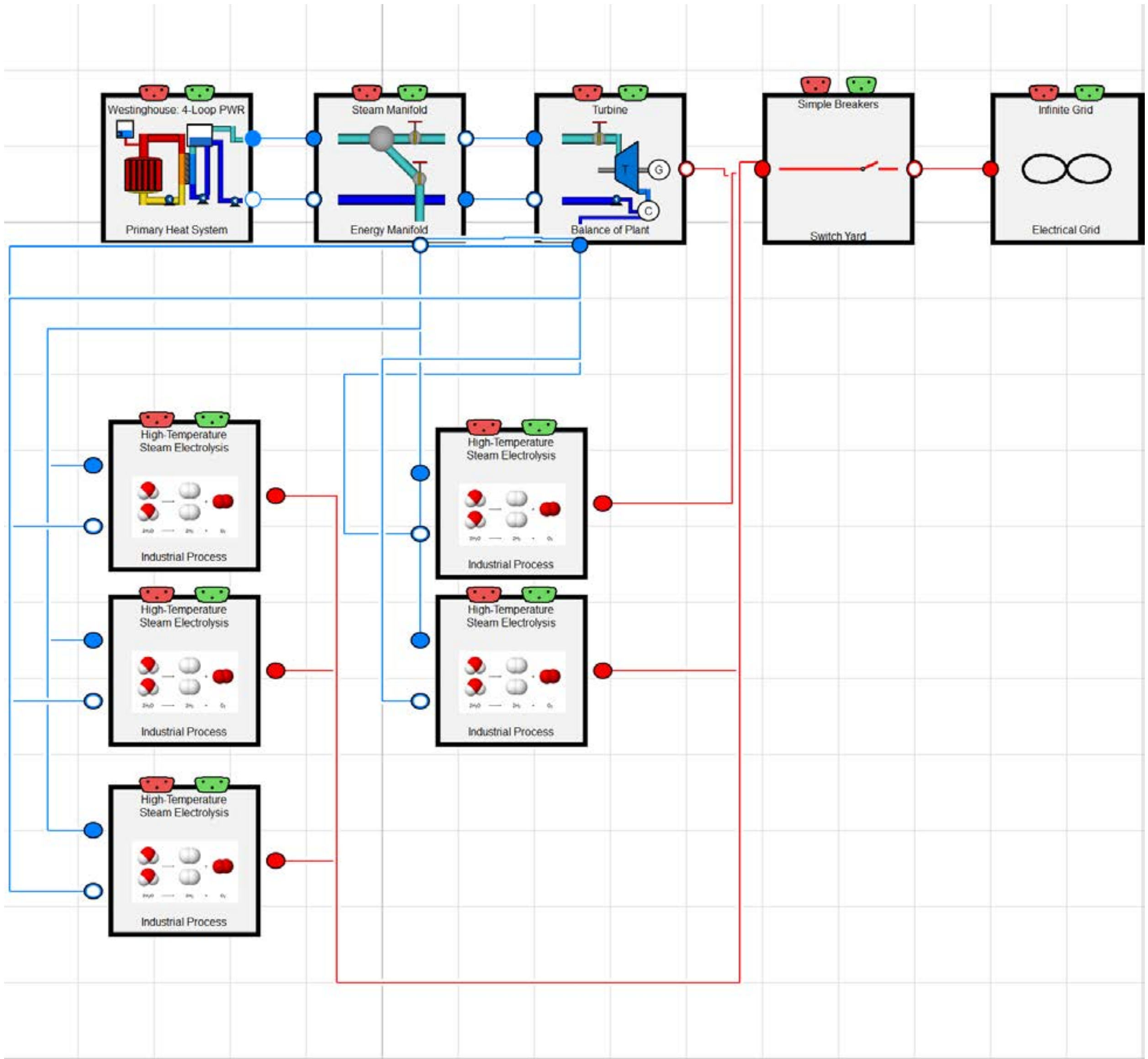

Figure 22. Coupled Westinghouse 4-loop with five parallel HTSE modules, each with a nominal electrical capacity of 53.3MWe.

Initially, power is held constant at nominal conditions for the first two hours of the simulation. At hour two there is a step change in electrolyzer demand to simulate the electrolysis portion of the system being oscillated on and off as electricity demand increases. Since this shift is in electricity consumption alone, there is no oscillation in reactor power or subsequent reactor systems. Results presented in Figure 23(a-d) demonstrate that, through the addition of an HTSE and subsequent control algorithm modifications to the T_{ave} program and turbine control valves, reactor power can be held constant while the end users can oscillate in operation.

Note: While the ratio $\eta_{electric\_to\_thermal}$ may slide a little bit over the operating range, it is assumed that in a deployed system the reactor and HTSE manufacturer would fine tune the T_{ave} program to accommodate any sliding scale of operation.

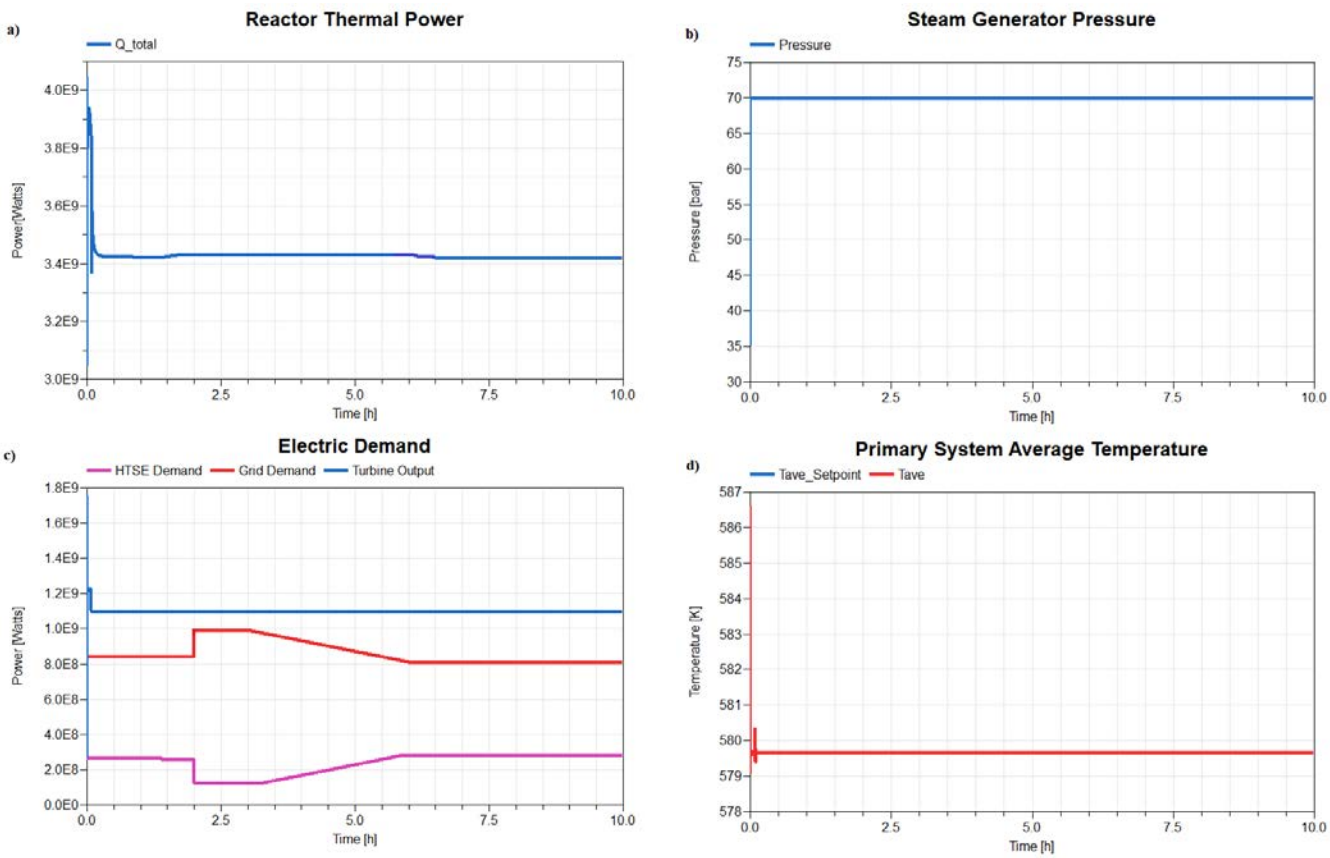

Figure 23. Coupled reactor/HTSE 10-hour simulation. (a) Reactor thermal power. (b) Steam generator pressure. (c) Electrical power. (d) Primary system average temperature. (Note: The first 30 minutes of the simulation is the program initializing and should be disregarded in the results section.)

3.3 References

[1] U.S. NRC, "The Boiling Water Reactor". https://www.nrc.gov/reading-rm/basic-ref/students/animated-bwr.html [accessed 24 June 2019].

[2] U.S. NRC, "The Pressurized Water Reactor". https://www.nrc.gov/reading-rm/basic-ref/students/animated-pwr.html. [accessed 24 June 2019].

[3] Westinghouse Electric Corporation (1984). The Westinghouse Pressurized Water Reactor Nuclear Power Plant

[4] Westinghouse Technology Manual (1990). "Overview and Comparison of U.S. Commercial Nuclear Power Plants". Nuclear Power Plant System Sourcebook.

[5] U.S. NRC, "List of Power Reactor Units". https://www.nrc.gov/reactors/operating/list-power-reactor-units.html. [accessed 25 June 2019].

[6] K. Frick, "Modeling and Design of a Sensible Heat Thermal Energy Storage System for Small Modular Reactors", PhD Dissertation, North Carolina State University, Department of Nuclear Engineering (2018). https://repository.lib.ncsu.edu/bitstream/handle/1840.20/34975/etd.pdf

[7] Konor Frick, J. Michael Doster, Shannon Bragg-Sitton, "Design and Operation of a Sensible Heat Peaking Unit for Small Modular Reactors," *Nuclear Technology*, DOI:10.1080/00295450.2018.1491181

[8] Konor Frick, Corey T. Misenheimer, J. Michael Doster, Stephen Terry & S. Bragg-Sitton (2018): Thermal Energy Storage Configurations for Small Modular Reactor Load Shedding, Nuclear Technology, 202:1, 53-70, DOI:10.1080/00295450. 2017.1420945

[9] MODELICA ASSOCIATION, "Modelica and the Modelica Association;" https://www.modelica.org/; (current as of Aug. 16, 2017).

[10] MODELICA ASSOCIATION, "Modelica Language Specification Version 3.4," Modelica Association (2017).

[11] NUCLEAR REGULATORY COMMISSION, "TRACE V5.0 Theory Manual: Field Equations, Solution Methods, and Physical Models," US NRC.

[12] W. M. STACEY, *Nuclear Reactor Physics*, Wiley-VCH Verlag GmbH & Co. KGaA, Weinheim, Germany (2007); https://doi.org/10.1002/9783527611041.

[13] E. M. BAUM et al., *Chart of the Nuclides: Nuclides and Isotopes 17th Edition*, Seventeenth, Bechtel Marine Propulsion Corporation (2009).

[14] M. Scott Greenwood, Askin, G. Yigitoglu, T. Jay Harrison. "Nuclear Hybrid Energy System Southeast Regional Case Progress Report". Oct. 2018. ORNL/TM-2018/1052

[15] Kim JS, Boardman R, Bragg-Sitton S. "Dynamic performance analysis of a high temperature steam electrolysis plant integrated within nuclear-renewable hybrid energy systems". Applied Energy. 2018.; 228: 2090-2110.

[16] Rabiti C, Epiney A, Talbot P, Kim JS, Bragg-Sitton S, Alfonsi A, et al. Status report on modelling and simulation capabilities for nuclear-renewable hybrid energy systems. Idaho Falls (ID): Idaho national laboratory; 2017 Sep. Report No.: INL/EXT-17-43441. Contract No.: DE-AC07- ID14517.

4. HYDROGEN MARKETS

With the potential of low-cost, carbon free hydrogen via electrolysis becoming more of a possibility in recent years, there has been an increase in hydrogen research via the H2@scale program. As part of the program, research has been conducted into the viability of utilizing hydrogen as an input into existing industries. It has been determined through this work that hydrogen can be used for production of iron pellets, nitrogenous fertilizers, polymers, synthetic fuels, forest products, food products, and for fuel cell vehicles. Hydrogen generation is also being considered for large-scale and long-term energy storage when power-generation capacity exceeds the demand of the grid. Additionally, it can be injected into NG pipelines and burned as fuel for heating and power generation with a fuel cell or gas turbine.

4.1 Demand Curves

In the Midwest, hydrogen demand is expected to increase substantially as the hydrogen economy begins to take off. Demand in the region is anticipated to increase for refineries, ammonia production, natural gas combustion engines, syngas production, and fuel cell vehicles.

Area-specific demand curves were constructed using data provided by Argonne National Laboratory. The demand curves were constructed by assuming the price people are willing to pay for hydrogen is its associated production cost via steam methane reforming (SMR). The assumption is that each customer will build an SMR plant for their individual needs. Credit is not given to joint hydrogen production ventures; instead, each customer is expected to be willing to pay the price of building and operating an SMR facility for their needs. Curves were constructed at each of the three projected natural gas price points.

Using the H2A model for SMR production, the hydrogen production price was generated for each of these customers [1]. The NG price projections for the region were used for low-cost ($4.2/MMBtu), average-cost ($5.4/MMBtu), and high-cost ($8.0/MMBtu) NG [2], in $2017 from Figure 4. The capacity factor used in the H2A model was 90%. Compression and delivery over two miles were estimated using the equations shown in Table 9, which are used to calculate the CAPEX and OPEX associated with the compression and delivery of hydrogen through a pipeline. The future projections for NG prices were also considered when developing the demand curve. Figure 24 contains the demand for the region with the high-, low-, and baseline-NG-price projections. All values for supply and demand are in $2019.

Table 9. Hydrogen pipeline construction costs $2019 [3].

Pipeline		
Pipeline diameter (in.)	$D(V) \propto \sqrt{V}\ ;\ D(50\ tpd) = 4$	(7)
Pipeline material ($/mi):	$76550e^{0.0697D}$	(8)
Labor ($/mi):	$1.136(-51.393D^2 + 43523D + 16171)$	(9)
Right of way (ROW) ($/mi):	$1.04(-9 * 10^{-12}D^2 + 4417.1D + 164241)$	(10)
Miscellaneous ($/mi):	$1.134(303.13D^2 + 12908D + 123245)$	(11)
Compressor		
Power (kW):	$28(V)$	(12)
Compressor Cost ($):	$2.34(1962.2P^{0.8225})$	(13)

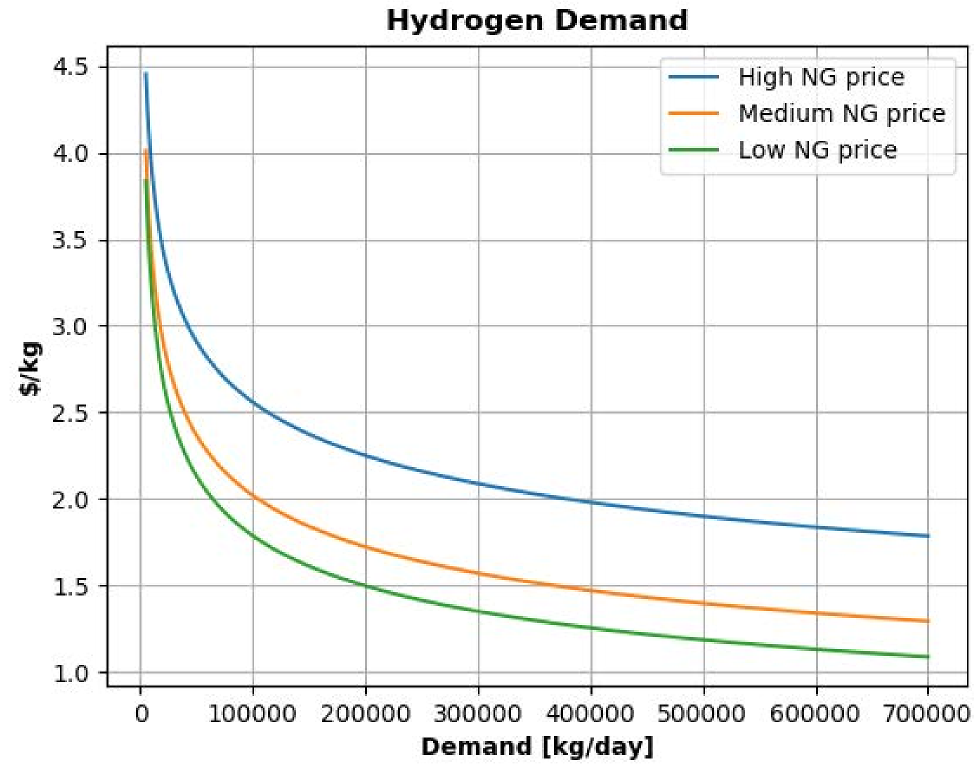

Figure 24. Hydrogen demand in the region when considering high, medium, and low future natural gas prices.

4.2 Hydrogen Pipeline

According to the H2@Scale program run under DOE's Fuel Cell Technologies Office, there are approximately 1,600 miles of hydrogen pipelines in the United Stated [4]. However, hydrogen demand in the Midwest is anticipated to have exponential growth in the coming years. To transport the anticipated demand to end users, a new pipeline needs to be constructed. Using the HDSAM model via Argonne National Laboratory the equations in Table 9 were utilized. All dollars are in 2019 dollars.

To determine the pipeline cost for hydrogen transmission from the nuclear power plant, an assumption of individual pipelines was used. The potential to lower costs via joint pipeline ventures exist but run into legality issues that are beyond the scope of this project. Instead, an individual pipeline network for each end user as depicted in Figure 25 is considered.

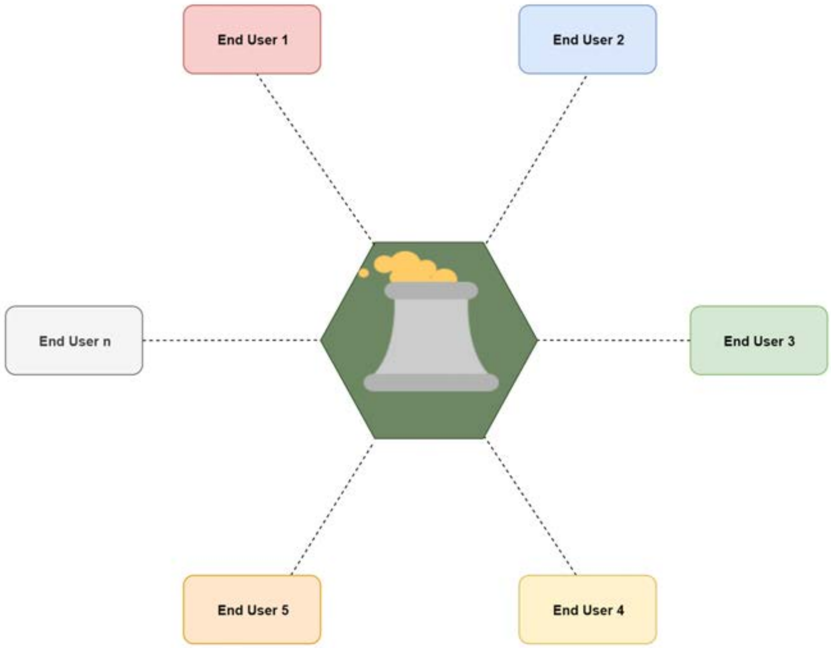

Figure 25. Representation of "n" hydrogen pipelines extended from a nuclear station.

To calculate a proper piping distance, a particular plant was chosen. From this, a geographic region assessment was conducted, and based on plant production capabilities, the piping length required was estimated as a function of production capability. This is depicted in Figure 26.

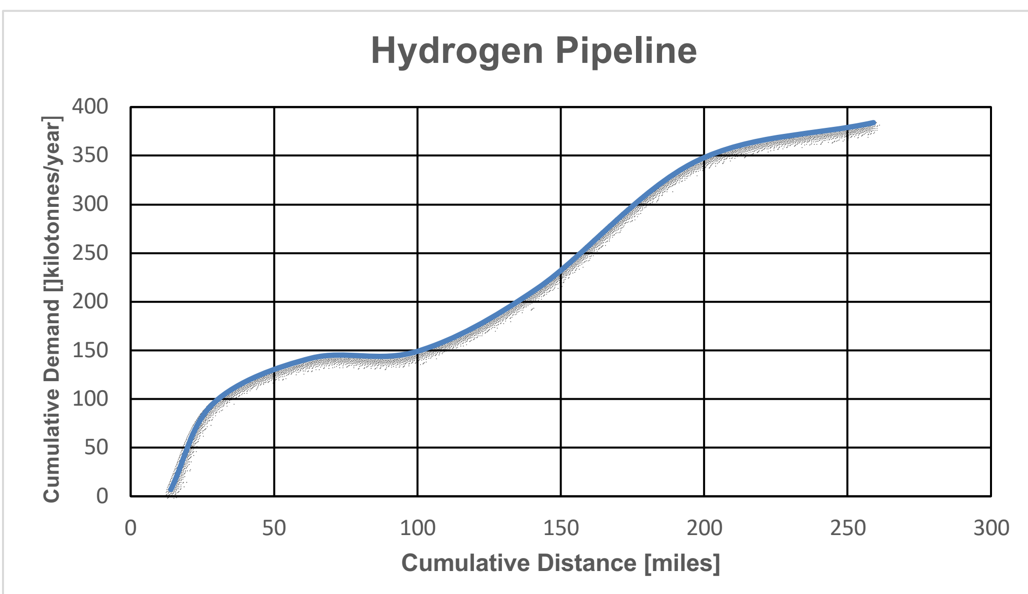

Figure 26. Hydrogen pipeline distance.

For a standard 4-loop PWR, the maximum production rate was determined to be ~240 kilotonnes/year given a power output of ~1,095 MWe. This corresponds to a pipeline distance of approximately 150 miles. For the geographic location selected, there were approximately six end users, and the total pipeline cost came to $861,100/mile of pipeline with a compressor cost of 3.38 million per pipeline. Thus, the total cost of pipeline construction comes to $149,473,900 or $996,492/mile in $2019. This cost can be thought of as an additional capital cost on top of the HTSE cost that would be incurred by the nuclear power station. Another way of thinking about this is as a reduced effective hydrogen selling price as seen by the nuclear power plant. Assuming an end user is a long distance from the nuclear plant, the effective hydrogen selling price as seen by the nuclear plant is reduced proportional to the amount of pipeline that must be installed to deliver it. Assuming a seventeen-year lifespan in the scenario shown above, there is an artificial loss in the hydrogen selling price of 3.6 cents per kg of hydrogen, assuming contractual obligations are set at 240 kilotonnes/year. The artificial loss is 1.6 cents per kg of hydrogen assuming obligations are only 125 kilotonnes/year. In this report, the hydrogen selling prices reported in Figure 24 are used, and hydrogen pipeline costs are captured as an additional capital cost in the cash flow analysis.

4.3 Hydrogen Storage

Throughout the operating lifespan of the plant there will be moments when, from an economic standpoint, it is more beneficial to sell electricity to the grid rather than to produce hydrogen and vice versa. However, hydrogen facilities tend have a very inelastic demand on hydrogen. Therefore, the plant must be able to provide hydrogen to its end users regardless of electricity pricing or face the risk of losing business. In order to fully monetize both the electricity and the hydrogen markets, the nuclear facility needs to build hydrogen storage capabilities that will provide it with "ride through" capability. Hydrogen storage would provide the nuclear facility with the flexibility to operate fully in both markets.

Current hydrogen storage technologies have large variability in capital and operating costs, depending on the storage technique chosen. The Fuel Cell Technologies Office (FCTO) has set an ultimate target for storage costs at $8/kWh on the basis of the lower heating value (LHV), where the LHV of hydrogen is assumed to be 33.3 kWh/kg [5, 6]. This is an equivalent CAPEX of $226/kg of hydrogen stored. Based on industry quotes, the current price is in the range of $500–600/kg for compressed air storage in $2019.

Another option for hydrogen storage is material storage, which involves converting hydrogen to another compound or adding hydrogen to existing compounds to take advantage of the physical storage costs of these materials [5]. Each of these come with additional CAPEX and OPEX for balance of plant and other material costs. The most economically viable option is geological storage, but this relies on a geologic formation in the area capable of storing hydrogen. Additionally, this typically requires larger-scale hydrogen production to justify the investment. For purposes of this report, a nominal cost of $600/kg in $2019 was utilized.

4.4 References

[1] U.S. DOE, "DOE Hydrogen and Fuel Cells Program: DOE H2A Production Analysis," https://www.hydrogen.energy.gov/h2a_production.html; 2013 [accessed 24 June 2019].

[2] U.S. EIA, "Annual Energy Outlook 2018," https://www.eia.gov/outlooks/aeo/tables_ref.php; 2018 [accessed 5 December 2018].

[3] Argonne National Laboratory, "Hydrogen Delivery Scenario Analysis Model (HDSAM)," https://hdsam.es.anl.gov/index.php?content=hdsam; 2019 [accessed 21 June 2019].

[4] Hydrogen Pipelines, "Fuel Cell Technologies Office". Office of Energy Efficiency and Renewable Energy. https://www.energy.gov/eere/fuelcells/hydrogen-pipelines; 2019. [accessed 24 June 2019].

[5] Cassidy Houchins and Brian James, (2017), *Hydrogen Storage System Cost Analysis: Summary of FY 2017 Activities Sponsorship and Acknowledgements*, 10.13140/RG.2.2.34567.85927.

[6] Brian James et al. (2016). *Final Report: Hydrogen Storage System Cost Analysis*.

5. ELECTRICITY MARKETS

In the United States, there are two electricity market configurations: regulated and deregulated. Regulated markets operate in much of the western, central, and southeastern United States, as depicted in Figure 28. For these markets, the grid operator role is carried out by integrated utilities that also act as electricity suppliers. Integrated utilities operate the grid and provide generation, transmission, and distribution services to all retail customers in a specified area. States will oversee utility decisions about the amount of capacity to procure from power plants and other resources, but the utilities propose how to procure those resources. [1]

In a deregulated market, entities known as regional transmission organizations act as electricity suppliers and purchase electricity at independently owned power plants to sell to retail customers. Seven regional transmission organizations (RTOs) operate across the United States: the California Independent System Operator (California ISO), Southwest Power Pool, Electric Reliability Council of Texas (ERCOT), Midcontinent ISO, PJM Interconnection (PJM), New York ISO, and ISO New England, as illustrated by Figure 27. These RTOs cover part or all of 38 states and the District of Columbia. In addition to their grid operator responsibilities, these RTOs operate wholesale electricity markets to buy and sell services needed to maintain a reliable grid, such as capacity, energy, and ancillary services. It should be noted that not all RTOs operate in deregulated markets; in other parts of the United States, RTOs act only as grid operators based on fixed purchase and selling prices.

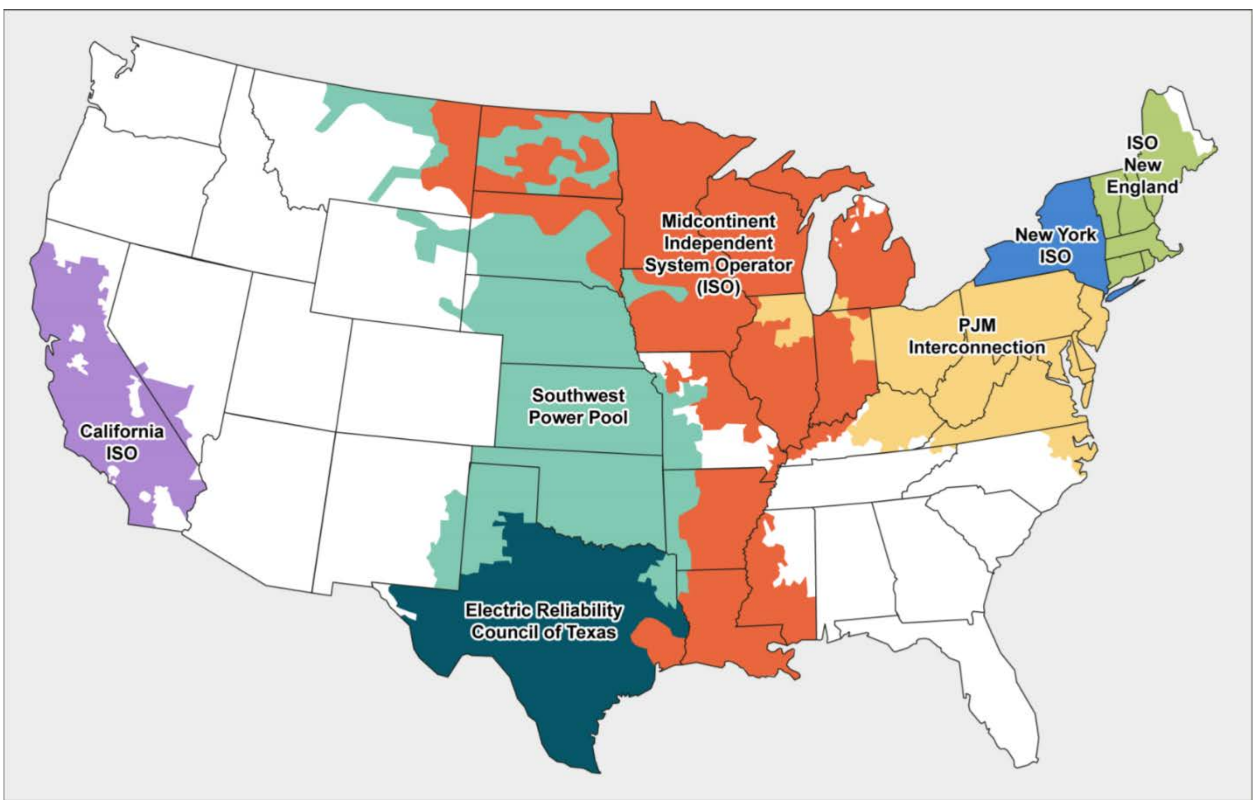

Figure 27. Map of RTOs within the contiguous United States [1].

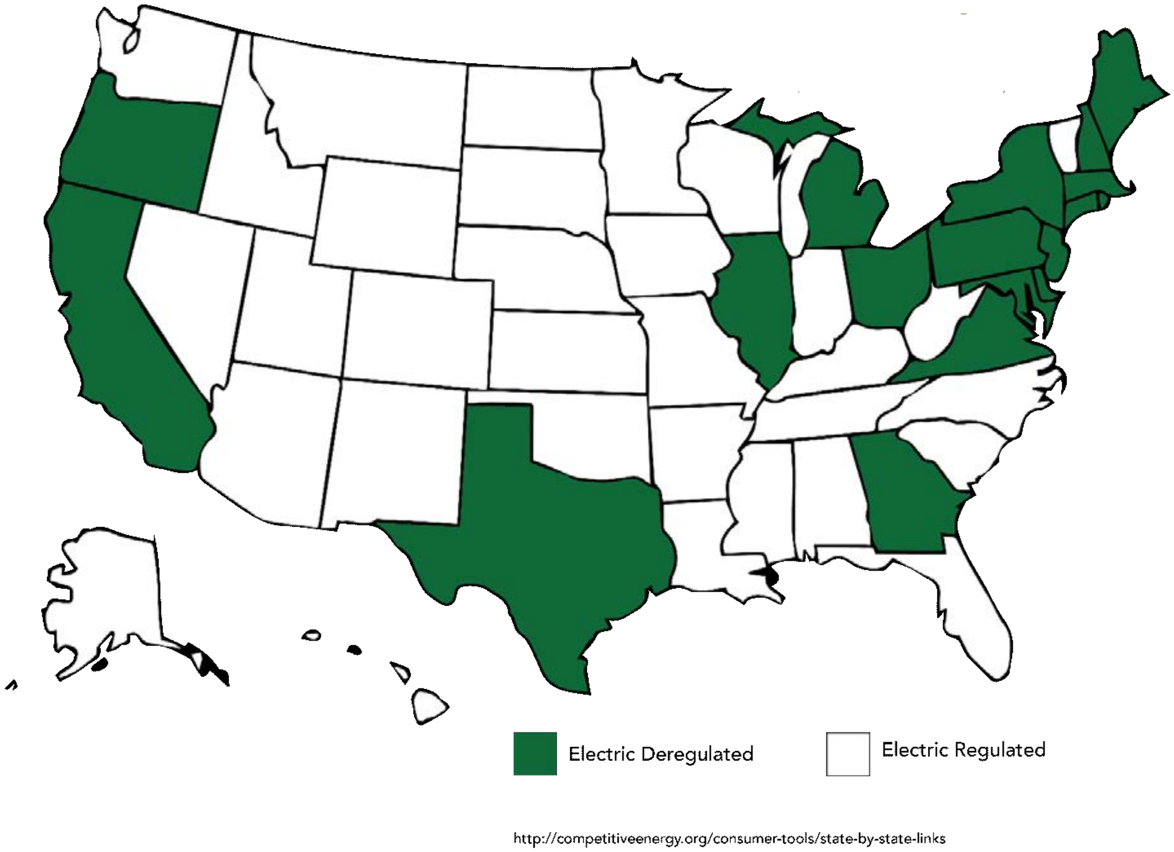

Figure 28. Regulated vs. deregulated markets [2].

For the analysis carried out in this report, the deregulated market was chosen. This is due to the market competition inherent in deregulated markets. In regulated markets, utilities can more effectively set pricing in such a manner as to protect viable assets such as a nuclear power. In a deregulated market, utilities are at the mercy of the market price set by the competition. Therefore, if the nuclear power plant is consistently unprofitable, the utility will consistently take a loss. Since this analysis seeks to provide nuclear plants under near-term duress with alternative economic pathways to success while still maintaining electricity generating capabilities, the deregulated market structure was chosen.

To properly determine market rules by which to run the techno-economic assessment, a particular RTO market had to be chosen. By overlaying Figure 27 and Figure 28 alongside maps of nuclear and hydrogen markets in the United States, it became clear that the PJM interconnection was the RTO of choice. It encompasses 33 of the 98 nuclear units in the United States, is mainly a deregulated market, and fits solidly in an expanding hydrogen market [3].

5.1 PJM Market

In the PJM interconnect there are several markets a utility can monetize: the capacity market (now called the Reliability Pricing Model or RPM), the day-ahead and real-time energy market, and the ancillary services market. The capacity market is designed to incentivize utilities to build and maintain their plants. The day-ahead market, also called the energy market, is the bulk of the daily profits received by utilities. Finally, the ancillary services market is designed to provide grid stabilization during moments when supply and demand of electricity are mismatched, either via frequency issues or unplanned utility outages. Generators can compete in each of these markets so long as they are able to meet certain requirements for operation. The ability of a coupled nuclear-hydrogen facility to participate in each of these markets is laid out in the following sections.

5.1.1 Capacity Market

The capacity market is the first market generators bid into and is designed as a grid reliability market. The PJM interconnect incentivizes utilities three years ahead to maintain the generation capacity by offering a capacity payment to generators simply for existing. This market ensures PJM has generating capacity, resiliency, and flexibility three years in advance. Additionally, it offers a modicum of security to generators for their continued operation.

In 2015, PJM modified the RPM capacity market for the 2018/2019 delivery year. A new product, termed capacity performance, was introduced. Capacity performance required additional characteristics compared to previously cleared capacity. Capacity performance resources that clear in the capacity market must be able to "provide up to their installed capacity value for at least 16 hours per day for three consecutive days throughout the entire year. Demand response resources that provide this product would have to be capable of the same requirements over the entire delivery year." The rules also dictate certain minimum flexibility requirements, such as startup time, minimum down times, and notification times. The entirety of the rules is beyond the scope this report but can be found in "PJM Manual 18: PJM Capacity Market." [4]

For a hydrogen plant coupled to a nuclear reactor, the product would be deemed a load management product. In the PJM market, particular rules apply to such assets as outlined under Section 4.3 in PJM Manual 18 [4]. The limitation of note is the notification period for demand response lead time as outlined in Section 4.3.1 of the rules. The notification period limitations are outlined as described in Table 10.

Table 10. Load management response notification period per PJM Manual 18 Subsection 4.3.1 [4].

Notification Period (Lead Times)	Description
Under 30 minutes (standard)	Curtailment level must be fully implemented within 30 minutes of a notification.
Under 60 minutes	Curtailment that requires longer than 30 minutes but less than 60 to be fully implemented.
Under 120 minutes	Curtailment that takes more than 1 hour but less than 2 hours to be fully implemented

The regulations classify that products requiring longer than two hours to respond cannot compete in the capacity market. As mentioned in previous sections, approximately 3-10% of the energy provided to the HTSE plant is in the form of thermal energy, with the rest coming from the electrical input. Of the electrical input into the system, 75–90% is used in the electrolysis process, with the remaining electrical input being utilized as electrical topping heat. Studies have shown that the electrolysis piece of the equation can be cycled on and off on the order of minutes [5] and, therefore, can be considered in the capacity performance market. However, as discussed in Chapter 2, to combat thermal gradients in the fuel cells, the electrical topping heat cannot be ramped as quickly and falls outside the two-hour window to be considered for the capacity performance market.

The capacity the generator is able to submit to the capacity markets within a PJM regional transmission organization is called unforced capacity (UCAP); it must be less than or equal to the installed (nameplate) capacity, adjusted by the equivalent forced outage rate demand (EFORd) [4,6]. The EFORd is a measure of the probability that a unit will not be available due to forced outages or forced de-ratings when there is a demand on the unit to generate [4]. Therefore, *UCAP = Installed Capacity * (1 – EFORd)*. The capacity market clearing price for the PJM region between 2018 and 2022 is summarized in Table 11. Due to the variability in the clearing price, an average of the four years will be used for this analysis. Additionally, the average EFORd for nuclear generators between 2013 and 2017 for nuclear generators in the PJM region was utilized [7].

Table 11. Capacity market clearing prices.

Capacity Commit Period Start Date [Delivery Year]	Capacity Market Clearing Price ($/MWe-day) [PJM]	EFORd (%) [7]
6/1/2018 [2018/2019]	164.77	1.395
6/1/2019 [2019/2020]	100.00	1.395
6/1/2020 [2020/2021]	76.53	1.395
6/1/2021 [2021/2022]	140.00	1.395

The capacity payment the nuclear facility can receive from the capacity market is assumed to be reduced by an amount equal to the HTSE hot standby mode requirements plus the average amount of hydrogen the nuclear plant must produce in the hydrogen market due to an under-filled/undersized hydrogen storage tank, as shown in equations 14 and 15.

$$Capacity_{reduction}\,\% = \left(Hot\ Standby * \frac{HTSE_{cap}}{HTSE_{max}} + \ (1 - Hot\ Standby) * Flexible * \frac{H_{2demand}}{H_{2max}}\right) * 100\% \tag{14}$$

$$Flexible = 1 - \min\left(1.0, \frac{Average\ storage\ level}{H_2\ market\ demand}\right) \tag{15}$$

Where $HTSE_{cap}$ is the size of the installed HTSE and $HTSE_{max}$ is the maximum possible HTSE upon which the nuclear plant is fully dedicated to hydrogen production. Additionally, $H_{2demand}$ is the contractual obligation of the power plant and H_{2max} is the maximum contract the power plant could take on. If the average storage level when called upon is above the market demand, then capacity is reduced only by the amount needed to maintain an HTSE of the installed capacity in hot standby mode. However, if the average storage level is less than the market demand, then the capacity payment is reduced by the hot standby amount plus a portion of the flexible energy, since, on average, it must be utilized to produce hydrogen even when it is desired to sell it instead.

5.1.2 Day-Ahead Energy Market

The bulk of the sales and revenue for utilities comes through the day-ahead locational marginal price market and is the primary market in which generators compete. This market is bid on a day-ahead schedule where the 24th hour is bid on 24 hours ahead of time. The bidding structure works in the following way. Each individual generator submits their own bid to the system operator to meet the expected customer demand for the following day [8]. After receiving the bids, the system operator selects them from lowest to highest as expressed in Figure 29. Once all generation needs are met, the market price is set to the bid price of the last selected generator, which is referred to as the clearing price or Locational Marginal Price (LMP) for a specific node. Generators that are not selected are notified.

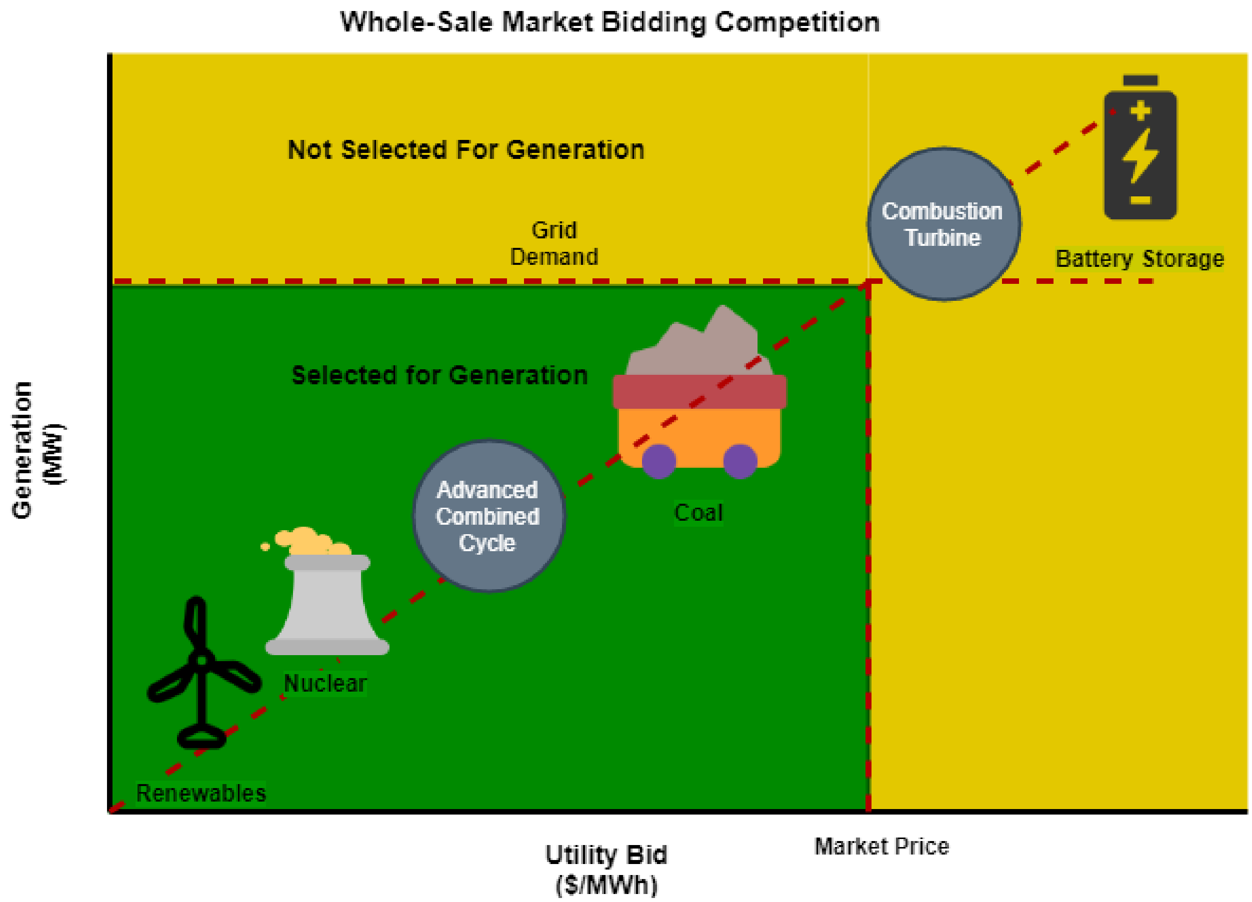

Figure 29. Example representation of generation bidding competition in PJM market; the market price for this hour is the price at which the last unit of coal was bid. Combustion turbines and battery storage were not selected for this hour.

In the aforementioned bidding structure, there is a risk on any given hour that a particular unit is not dispatched in the case its bid is too high. For generators with very slow ramp times due to physical limitations of the systems, or those that have extremely low short run variable costs (such as nuclear plants), the risk of not earning for an hour can far outweigh the potential of taking a minor loss during an hour. Therefore, nuclear utilities often choose to bid a price of zero to ensure they are always selected for generation, regardless of generation cost [8]. By doing this, they ensure they are selected for dispatch but are also more likely to generate at a loss during times of low demand. Figure 30 shows an example LMP seen in the PJM markets from May 2018 to May 2019. Also depicted in the figure is the average cost to operate a nuclear power plant of $33.50/MWe as reported by NEI in a 2018 study [9]. At all points below the cost to generate line, the nuclear utility is losing money. However, generation tends to directly surround these times making it unprofitable to go down in power or bid the true marginal cost of electricity.

Through the addition of an HTSE unit, where electricity can be fluctuated via the switchyard after the turbine, there is the opportunity for the nuclear facility to reduce hours of negative revenue by selling to the hydrogen market and only bidding into the electricity market when it is profitable to do so.

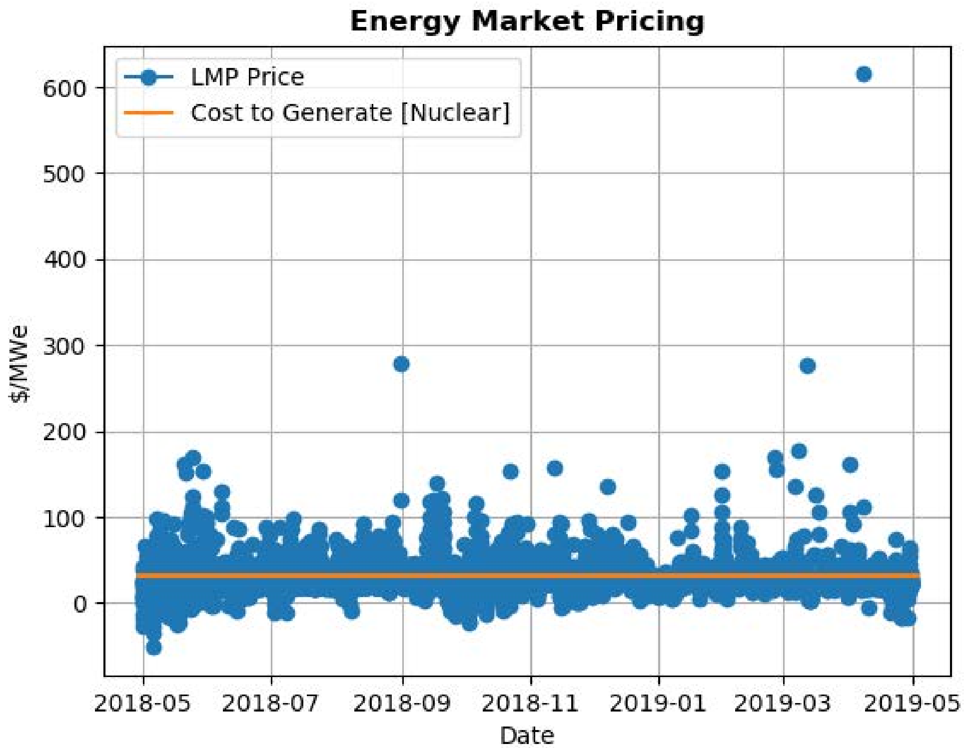

Figure 30. PJM LMPs from May 2018 to May 2019 (average cost to generate $33.50/MWe).

For a given plant, the market can be considered a "price-maker," and thus the utility "price taker" can choose to sell to the market or not based on their own operating costs. Under this assumption it is possible to disassociate the coupled nuclear power plant and HTSE unit from market response.

5.1.3 Ancillary Services Market:

In the PJM interconnect, there are three ancillary service markets: regulation, synchronized reserves, and primary reserves. Table 12 summarizes the basic requirements for each of the markets.

Table 12. Summary of ancillary services offered by PJM [10].

Product	**Description**
Regulation	- Must be able to immediately increase or decrease their output in response to automated signals within five minutes to maintain system frequency
Synchronized Reserves	- Synchronized to the grid frequency - Must respond within 10 minutes
Primary Reserves	- Must respond within 10 minutes - Includes synchronized reserves

Regulation reserves must be able to increase or decrease their output in response to automated control signals within five minutes in order to maintain frequency regulation on the grid. A more comprehensive description of the regulation market can be found in a recent report completed by Argonne and EPRI [10, 11]. Regulation resources must be able to sustain full output for 40 minutes. There is no separate regulation product for the PJM MAD sub-zone, only a single product for the entire PJM RTO. The regulation requirement is equal to 700 MW during peak periods (0500–2359 hours) and 525 MW during off-peak periods (0000–0459 hours). The regulation reserve market is shallow when compared to the overall size of the grid.

Synchronized reserves must be synchronized to the grid and be able to convert their capacity into generation within 10 minutes of receiving a signal from the system operator. Primary reserves represent the combined quantity of available synchronized and non-synchronized reserves (also available within 10 minutes). [10, 11]

Historically, nuclear power plants are unable to participate in the ancillary services market due to ramp rate restrictions in the plant. However, if the nuclear power plant is integrated with an HTSE unit and operating in multiple markets, there is potential for the plant to operate in ancillary service markets. As mentioned previously, 75–90% of the total power supplied to the HTSE unit is supplied in the form of electrical energy for electrolysis. This fraction of energy is grid synchronized, readily available, and can be oscillated back forth almost immediately from a physical perspective [5].

For this report it was decided that ancillary service markets would not be considered for three main reasons.

1. Ancillary service market size is not well characterized; it anecdotally has been characterized as fairly limited in size.
2. Market feedback is not modeled in this report, meaning price feedback that would naturally occur in a capitalist market is not modeled.
3. Market rules for operating generators in this mode are not well characterized and would require more insight into the PJM-specific operation.

5.1.4 Market Opportunities

Of the capacity, day-ahead real-time energy, and ancillary service markets, it has been determined that the coupled nuclear-HTSE facility has the potential to operate in all three. However, due to uncertainty in the ancillary services market, only the capacity and real-time energy markets will be modeled in this report. It should be noted that this restriction on the model makes the result inherently conservative as the participation in additional markets would increase overall profitability of the system

5.2 Market Construction

To properly model the PJM marketplace, expertise at the National Renewable Energy Laboratory (NREL) was utilized. Part of NREL's workscope was to develop a toolset for large-scale capacity expansion and economic dispatch that can project reasonable electricity pricing in a region under a given set of assumptions. As part of this work, NREL used its Regional Energy Deployment Systems (ReEDS) model for projecting capacity additions to the grid in four-year intervals from 2026 to 2042. NREL then translated the resulting five generator fleets (i.e., 2026, 2030, 2034, 2038, and 2042) into the commercial-grade PLEXOS production cost modeling software to simulate hourly energy and operating reserve prices for the target location. The year 2026 was chosen, as the start year as this appears to be the nearest-term prediction for which a plant of this size and magnitude could optimistically become operational.

ReEDS is a capacity expansion model that simulates the expansion and operation of the North American generation and transmission system given projections of load, fuel prices, technology costs and performance, and policies/regulations. It has a high spatial and temporal resolution including 205 balancing areas, 454 renewable resource regions, and 17 modeled time slices. The 17 time slices include four distinct time periods (morning, afternoon, evening, and night) in each of the seasons (summer, fall, winter, and spring) as well as one time slice modeling the peak generation period during the summer season [12]. ReEDS optimizes the expansion of all types of traditional generation while accurately representing the spatial and temporal availability of renewable generation technologies within its 205 balancing areas and 454 renewable resource regions. The ReEDS model was used to determine the quantity and location of all new generation additions in this study.

Several input assumptions were required within the ReEDS model in order to capture predicted changes for fuel prices, load growth, and renewable energy expansion. NREL's 2018 Standard Scenarios provided a set of input assumption options from which to select for the final modeled scenario [13]. The 2018 Standard Scenarios contain 42 forward-looking scenarios that capture a range of possible power system futures from 2010 to 2050 modeled with ReEDS; these futures include sensitivities to factors such as demand growth, fuel prices, technology/finance costs, fleet retirement, transmission expansion, and policy considerations. In addition to the 42 scenarios, a "mid-case" scenario serves as a reference case using 2018 policies and economic projections from the Energy Information Administration (EIA), International Energy Agency (IEA), and Bloomberg New Energy Finance (BNEF). Through several rounds of conversations with the CRADA partners, a combination of these sensitivities was chosen and used to model the future scenario used in this effort. The chosen sensitivities are as follows:

- Low natural gas prices
- Low renewable energy technology costs
- Low demand growth
- Nuclear plant lifetime of 80 years.

The CRADA team decided to model low natural gas prices due to the high likelihood of continued extraction and processing of large amounts of natural gas within the U.S., which could result in low prices well into the future. Low renewable energy technology costs were also chosen based on the assumption that the use and development of wind and solar resources will continue to grow within the U.S. to meet policy-based renewable energy targets and emission limits. Because the location surrounding the modeled nuclear plant is experiencing negative load growth, a low demand growth was chosen. As this study is focused on the potential of nuclear hydrogen production, an 80-year nuclear lifetime was selected instead of the 60-year lifetime default in ReEDS. This prevents the closure of nuclear generation in the later modeled years. Other than the four sensitivities listed above, all other inputs are from the 2018 NREL Standard Scenarios mid-case scenario.

Following the ReEDS modeling, the generator buildout results from ReEDS for the five study years (2026, 2030, 2034, 2038, and 2042) were converted into a PLEXOS database using a custom ReEDS-to-PLEXOS nodal model conversion tool in order to perform production cost modeling at an hourly resolution. The generator build-out that is passed from ReEDS to PLEXOS is added to an existing PLEXOS nodal database, which is an evolution of a database used in previous NREL studies, such as the Eastern Renewable Generation Integration Study (ERGIS) [14]. Here, "nodal" refers to the PLEXOS database with representation of individual transmission buses (referred to here as nodes) with explicit inter-nodal transmission flows; this is in contrast to the coarser, aggregated "zones" that only capture inter-zonal transmission lines. Each node has an energy price, which corresponds to an LMP. Figure 31 depicts the steps in the ReEDS-to-PLEXOS nodal model conversion.

The ReEDS outputs that were transferred to PLEXOS include:

- Load and renewable energy generation profiles: The underlying raw hourly load and renewable energy profiles that are used in an aggregated form within ReEDS for estimating renewable energy curtailment and capacity values are also passed to PLEXOS at the same or finer resolution. The load profiles vary by region in PLEXOS and match the load growth over time from ReEDS. The renewable energy technologies are represented for each renewable technology and resource class at the more spatially resolved nodal level in PLEXOS.
- Generator buildout and retirements: The nodal ReEDS-to-PLEXOS converter passes new generator additions and retirements to PLEXOS. The converter does this by identifying capacity additions and retirements in the ReEDS results compared to the underlying PLEXOS nodal database.

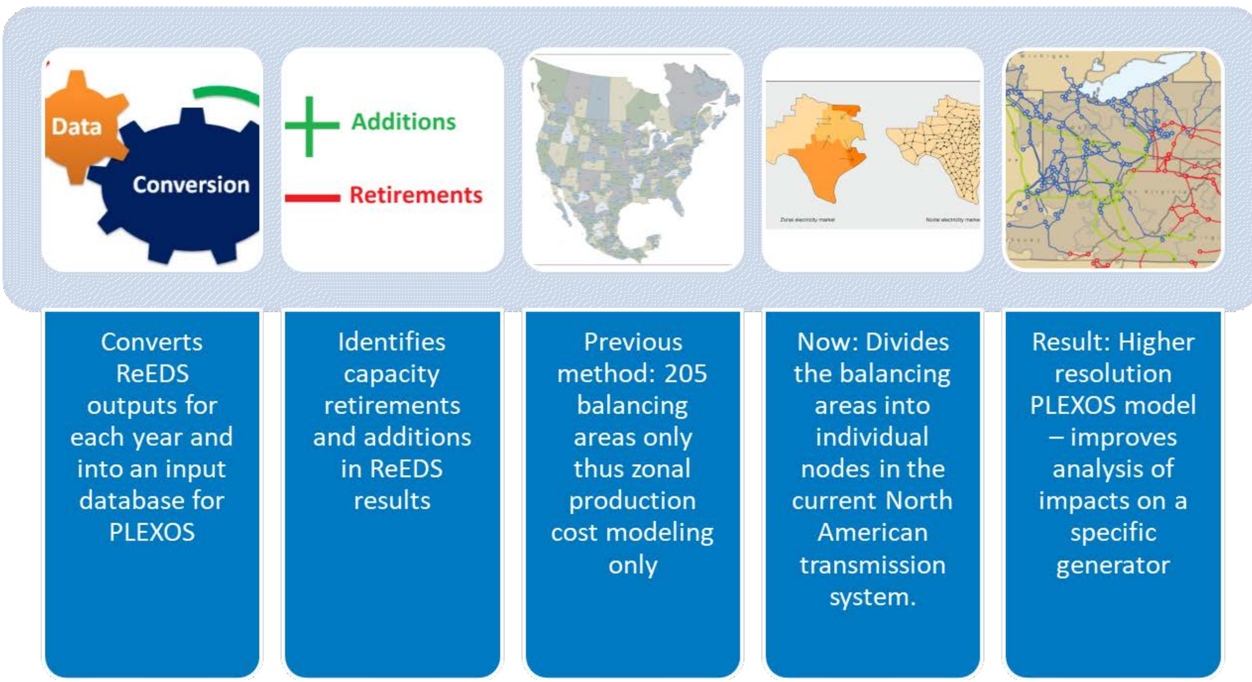

Figure 31. ReEDS-to-PLEXOS Nodal Model conversion steps.

Additional generator properties, which are required by PLEXOS but do not exist in ReEDS, were also added to the PLEXOS database during the conversion. These values were taken from the WECC TEPPC database [15] and include:

- Min up/down time
- Forced outage rates
- Start costs
- Minimum generation level
- Max ramp rates

Gas prices were not passed between ReEDS and PLEXOS due to limited knowledge of delivery and distribution costs of gas. Gas prices were kept constant in PLEXOS across the five study years. This is reflective of the low natural gas price projections from the NREL 2018 Standard Scenarios.

A major advantage of the nodal ReEDS-to-PLEXOS converter is that it provides the highest available spatial resolution for operational analysis. The nodal ReEDS-to-PLEXOS converter divides the ReEDS balancing areas into their individual nodes present in the current North American transmission system, which contains over 100,000 transmission nodes. This high spatial resolution was critical due to the analysis of a specific nuclear generation station located at a node within the ComEd region of PJM; nodal prices are necessary to capture the impacts of transmission constraints on that specific location.

One limitation of the current versions of the nodal ReEDS-to-PLEXOS converter is that transmission upgrades are not passed from ReEDS to PLEXOS. Since ReEDS is a zonal model, all transmission flows and upgrades are at a zonal resolution and, therefore, cannot be translated to a nodal model without some form of manual adjustment. These manual adjustments are detailed in Appendix A.

Following the nodal ReEDS-to-PLEXOS conversion, NREL undertook its final role of performing hourly operational modeling at nodal resolution for each of the four-year intervals from 2026 to 2042. This was undertaken using the commercial-grade production cost modeling software, PLEXOS [16]. PLEXOS optimizes the unit commitment and dispatch of generators to minimize the overall production cost while observing generator operating constraints (minimum generation, ramping rate limits, etc.) and various system constraints such as generator reserve requirements and transmission flow limits.

The PJM region is the focus region for this study, but since it is highly interconnected to the surrounding regions, the entire Eastern Interconnection (EI) was modeled. To reduce computational requirements, only the PJM and immediate regions were modeled at the nodal resolution, while the remaining regions of the EI at a zonal resolution. This allowed for accurate transmission flows and LMPs in the vicinity of the nuclear plant while reducing total simulation runtime. The final spatial treatment for the PLEXOS model can be seen in Figure 32.

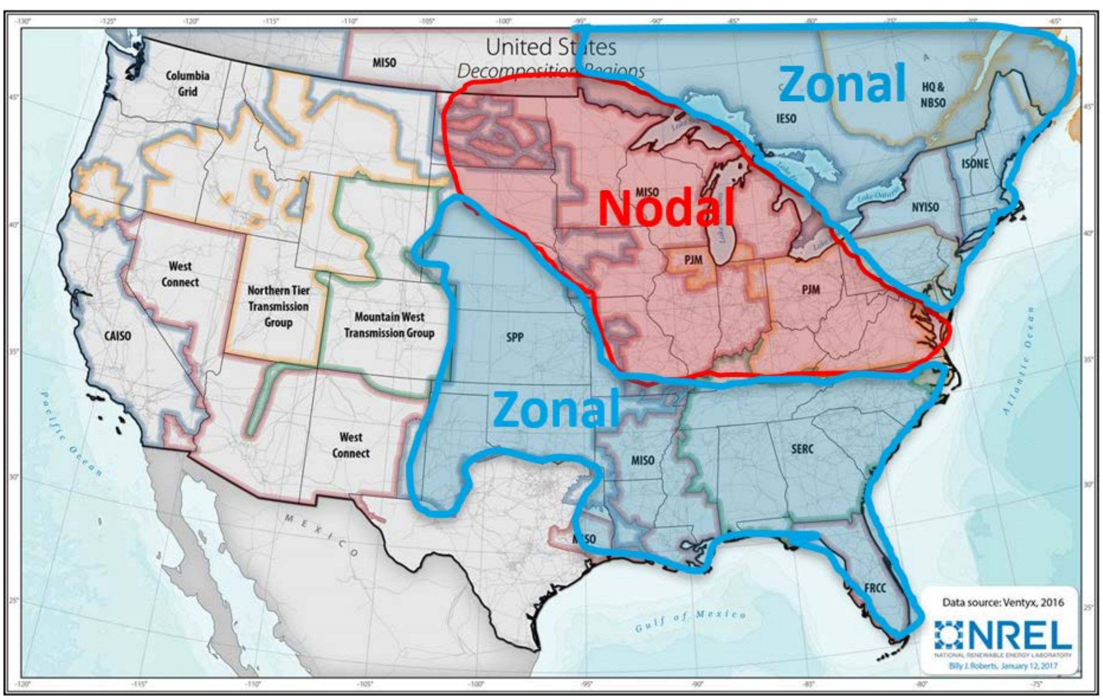

Figure 32. Approximation of spatial treatment in PLEXOS runs.

The final PLEXOS models for the years 2026, 2030, 2034, 2038 and 2042 were individually run at an hourly timestep resolution for a 24-hour period, with an additional 24-hour "lookahead" window at four-hour resolution. The lookahead allows PLEXOS to "see," but not keep, the operational outcomes over a longer temporal extent; this is particularly useful for generator startup decisions. To reduce overall computation time, each of the yearly runs were divided into 12 parallel monthly runs with no overlap and then seamed back together to obtain a full solution year. On average, each monthly run required about five days of runtime on the HPC. Additional details on reserve markets, workflow, and penalty functions modeled are available in Appendix A.

The resulting output, shown in Figure 33, provided hourly locational marginal prices for each of the modeled nodes within the system. In a close-up of a four-day period, as illustrated in Figure 34, the daily diurnal trend in electricity pricing between the hours of 3:00 p.m. and 7:00 p.m. can be seen. This corresponds to the diurnal usage of consumers during the late afternoon and early evening hours associated with activities such as dinner and housing cooling loads.

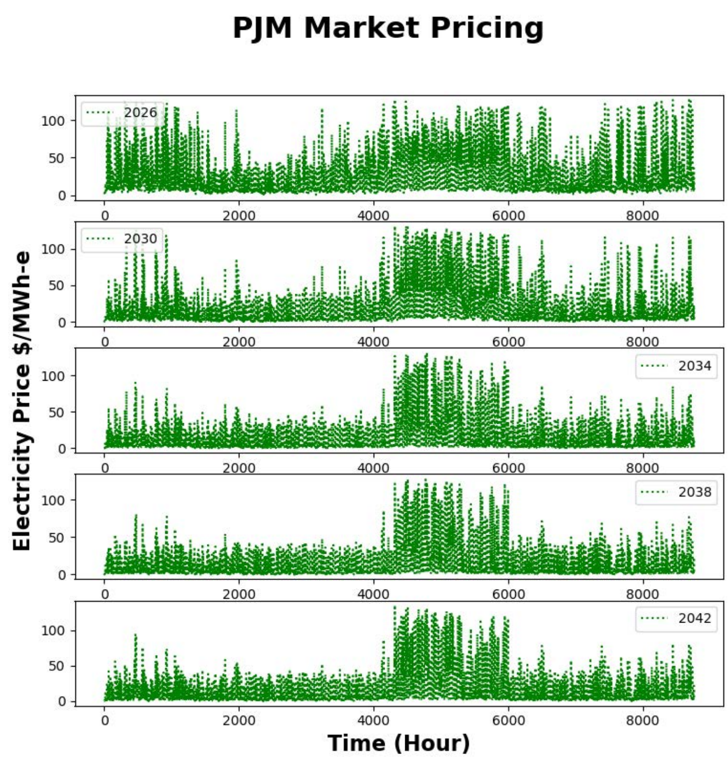

Figure 33. Locational marginal pricing in the PJM market due in years 2026, 2030, 2034, 2038, and 2042.

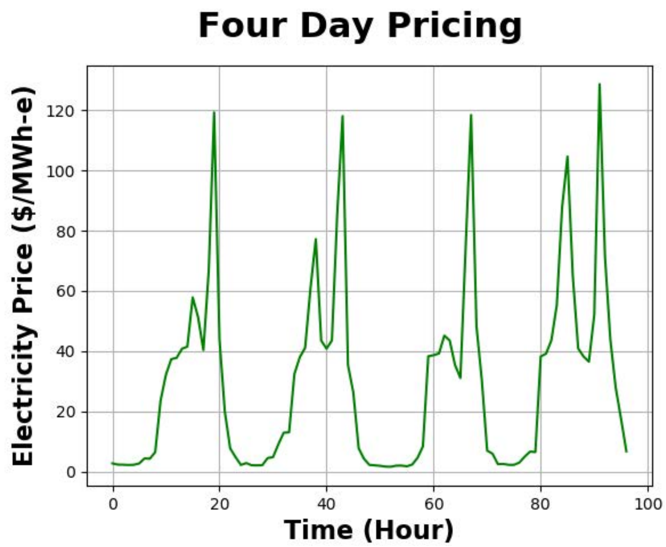

Figure 34. Four-day snapshot during one of the summer months of 2042.

5.3 References

[1] Electricity Markets. *Report to Congressional Committees*. United States Government Accountability Office. December 2017. GAO-18-131

[2] Regulated and Deregulated Markets. Customers First Renewables. Accessed 5 July 2019. https://www.customerfirstrenewables.com/resources/regulated-deregulated-energy-markets/

[3] DiSavino, Scott. *Higher PJM auction prices won't save some U.S. nuclear plants.* Reuters. May 24, 2018. Accessed 5 July, 2019. https://www.reuters.com/article/us-exelon-nuclear-pjm/higher-pjm-auction-prices-wont-save-some-u-s-nuclear-plants-idUSKCN1IP2P8

[4] PJM, *PJM Manual 18*, https://www.pjm.com/-/media/documents/manuals/m18.ashx, 2019 [accessed 5 July 2019].

[5] Petipas Floriane et al. Transient Operation of a solid oxide electrolysis cell. *International Journal of Hydrogen Energy*. Vol 38. 2013. Pages 2957-2964.

[6] PJM, "Capacity Market (RPRM)," https://www.pjm.com/markets-and-operations/rpm.aspx; 2019 [accessed 5 July 2019].

[7] PJM 2013 - 2017 Average EFORd and Weighted Average EFORd and XEFORd by Fuel Type. https://www.pjm.com/-/media/planning/res-adeq/res-reports/2013-2017-pjm-generating-unit-class-average-values.ashx?la=en [accessed 5 July 5, 2019]

[8] Cain Collin, Lesser Jonathan. A Common Sense Guide to Wholesale Electric Markets. *Bates White Economic Consulting*. April 2007

[9] Nuclear Costs in Context. October 2018. Nuclear Energy Institute (NEI). https://www.nei.org/CorporateSite/media/filefolder/resources/reports-and-briefs/nuclear-costs-context-201810.pdf [accessed 8 July 2019].

[10] Zhou Zia, Levin Todd, and Conzelmann Guenter. "Survey of U.S. Ancillary Services Markets". *Energy Systems Division*. Argonne National Laboratory. January 2016. ANL/ESD-16/1

[11] Ela E. Wholesale Electricity Market Design Initiatives in the United States: Survey and Research Needs. 2016 Technical Update. Electric Power Research Institute (EPRI).

[12] Stuart Cohen et al. “Regional Energy Deployment System (ReEDS) Model Documentation: Version 2018.” NREL/TP-6A20-72023. Golden, CO: National Renewable Energy Laboratory. 2018. https://www.nrel.gov/docs/fy19osti/72023.pdf

[13] Wesley Cole, Will Frazier, Paul Donohoo-Vallett, Trieu Mai, and Paritosh Das. 2018. “2018 Standard Scenarios Report: A U.S. Electricity Sector Outlook” NREL/TP-6A20-71913. Golden, CO: National Renewable Energy Laboratory. https://www.nrel.gov/docs/fy19osti/71913.pdf

[14] Aaron Bloow et al. “Eastern Renewable Generation Integration Study”. Golden, CO: National Renewable Energy Laboratory. 2016. NREL/TP-6A20-64472. https://www.nrel.gov/docs/fy16osti/64472.pdf

[15] https://www.wecc.org/SystemAdequacyPlanning/Pages/Datasets.aspx

[16] PLEXOS Integrated Energy Model version 7.400 R02 x64 Edition [computer software] https://energyexemplar.com/

6. Technoeconomic Analysis Framework

In order to stochastically perform technoeconomic analyses for grid-energy systems, the work in this document makes use of the stochastic framework RAVEN (Risk Analysis Virtual ENvironment) [2] through its resource dispatch plugin HERON (Heuristic Energy Resource Optimization Network). HERON offers templates to easily construct RAVEN inputs common to many grid-energy technoeconomic analyses and provides models for arbitrary resource dispatch. HERON has been developed under work in the DOE Light Water Reactor Sustainability (LWRS) program. Its functionalities were leveraged for the analysis performed here.

6.1 Stochastic Technoeconomic Analysis

Performing technoeconomic analysis for a grid-energy system with several components can be a complex, nonlinear process. Because peaks and valleys in energy demand and supply often drive the economics of a grid-energy system, it is often necessary to consider how the grid behaves at a fine time resolution, often hourly or less, lest the driving outliers be smoothed out in aggregation. This requires a computationally intensive analysis of grid behavior at many time steps, often with inertial terms such as unit production ramp rates and energy storage spanning adjacent steps.

Furthermore, due to the unpredictable behavior of natural phenomena such as wind speeds and solar availability, as well as the noisy behavior of electrical grid demand, any technoeconomic analysis performed at a high resolution must be considered stochastically or risk representing only a small portion of the possible solution space. In order to understand the behavior of a grid-energy system, the potential range of outcomes must be considered together as a response space rather than considering only one possible series of stochastic measurements.

HERON, through creating RAVEN inputs and providing dispatch optimization models, answers the needs of high-fidelity grid dispatch simulation as well as stochastic grid performance. Signal processing and synthetic history production in RAVEN makes it possible to simulate many alternate scenarios for a given grid-energy system, allowing a stochastic evaluation of a particular portfolio and a better understanding of the range of possible solutions.

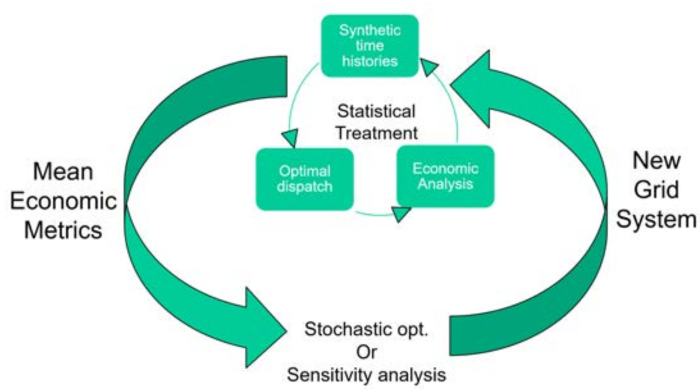

Figure 35. Stochastic technoeconomic analysis workflow in HERON.

Figure 35 shows the typical workflow of a stochastic technoeconomic analysis using HERON. The general structure is a two-loop optimization system. The outer loop either sweeps or optimizes the sizing of units within a grid-energy portfolio with respect to the average economic metrics of the portfolio. The average economic metrics are calculated via the inner loop. The inner loop optimizes the dispatch of fixed-capacity units within the portfolio for each hour of the project's life to maximize the economic metrics of the system. The inner loop is run many times per outer loop. At the beginning of each inner loop, a new stochastic sampling of the synthetic time histories is performed, which serves as a boundary condition for the dispatching of the units in the portfolio. Statistics about the NPV captured across all the inner runs for a particular portfolio sizing are returned as the result of the combined inner loop. The outer loop then uses these statistical, stochastic metrics to produce a new portfolio mix to consider.

HERON operates either in "sweep" mode or "optimization" mode, depending on the desired result. In sweep mode, a combination of desired portfolio mixes is predetermined, and statistical measures are collected for each mix in the process described above. This yields a topology of economic metrics as a function of the portfolio mixes. Alternatively, optimization mode uses feedback from each set of inner runs to drive a stochastic gradient descent search for the most desirable economic metrics. In this mode, a single optimal portfolio mix is returned, based on the search parameters of the optimization algorithm selected. The terms "sweep" and "optimization" refer to the performance of the outer loop; the inner loops always optimize the dispatch of the portfolio hourly throughout the project's life.

For clarity, we describe this process as it relates to the work documented here. The process starts in the outer cycle by selecting a tentative grid-energy system portfolio, including the capacity of the hydrogen production facility, hydrogen storage facilities, and size of the hydrogen market, as well as buy and sell thresholds for the hydrogen storage. These five factors make up the outer cycle sweep/optimization variables. With these capacities selected, the workflow moves to the inner cycle. At the start of each inner cycle, the stochastic electrical price is sampled, establishing synthetic time series as boundary conditions for a unique scenario solve; the process for synthetic history generation is described below. The workflow then dispatches the units in the grid-energy system at each time step in the synthetic time series spanning the project life, optimizing to find the most economical dispatch of the grid components. An economic metric, such as net present value (NPV), is then calculated for the full grid dispatch and returned as a single stochastic metric. This economic metric serves as the goal function of the outer cycle if optimization is performed. The inner cycle is repeated many times to achieve a statistically converged value of the economic metric. Statistics are then collected on the many samples of the economic metrics and used to inform further exploration of the sizing and existence of the grid-energy system portfolio in the outer cycle. This outer-inner cycle continues until sufficient data have been collected to represent the behavior of the system.

The features of HERON and RAVEN used in this hierarchal cycle analysis are discussed in the following sections.

6.2 Stochastic Time Series

One of the main strengths of HERON's approach to grid-energy system technoeconomic analysis is a robust approach to stochastic consideration. Because the weather, load, and market conditions that drive optimal resource utilization in a grid-energy system are often unpredictable, they can be treated as stochastic systems and comprehended through a sampling approach. Producing synthetic time series with fundamentally consistent behavior while still retaining statistical independence is the main focus of RAVEN signal analysis methodologies. The initial Fourier plus ARMA (Auto-Regressive Moving Average) methodology was introduced in 2016 [3] and has been expanded since with many improvements. The algorithms for seasonal detrending through Fourier analysis and residual noise capture through ARMA fitting have been discussed in the works cited and are only described briefly here. Several recent features of particular interest to this analysis are also discussed.

6.2.1 Fourier and ARMA

In traditional RAVEN synthetic history generation, a surrogate model is trained by first detrending periodic data with Fourier analysis, then fitting an ARMA (auto-regressive moving average) on the residual data. The Fourier periods for detrending are selected as part of the analysis inputs with intent to remove consistent periodic signals. The ARMA is trained on the detrended signal, with the intent of capturing deviations from the consistent periodic signal [3].

Consideration has also been made for signals that are correlated. For example, when air temperature and global horizontal irradiance (two weather signals for solar power production) are low in the summer, the residential demand for electrical cooling is often also low. To preserve this correlation, the ARMA is further expanded as the VARMA (vector auto-regressive moving average) [4]. The VARMA algorithm retains the correlation between changes in the coupled signals via an expanded covariance treatment including time-lag terms.

6.2.2 Periodic Peak Identification

In this work, the combination of generation and demand effects have been summarized using the ReEDS/PLEXOS system. The results are reconstructed hourly energy prices every four years. These energy prices tend to be strongly peaked with consistent periods; for example, there is frequently a spike in energy prices during the evening as renewable energy generation from solar and wind declines and residential demand increases. The peaks in the data obtained from ReEDS/PLEXOS are sharply peaked, often only lasting a handful of hours but reaching energy prices orders of magnitude higher than the median daily energy price. At cursory glance, this seems to align with expected price behaviors in other grid systems.

This sharply peaked periodic behavior is not captured well by traditional Fourier analysis. As the width of a peak shrinks with respect to its period, the number of Fourier terms required to accurately capture the peak grow quickly, making it quite difficult to accurately capture these periodic peaks throughout the signal. As part of the work for the DOE-NE Systems Analysis and Integration campaign, an algorithm has been added to RAVEN's signal processing module to identify and characterize peaks then remove them from the Fourier and ARMA analysis, stochastically recreating the peaks on each synthetic history generation.

To identify the periodic peaks, windows are identified where a peak is periodically found. The height, location within the window, and probability of occurring are stored as fundamental properties of individual peak windows. To reconstruct the peaks, for each type of peak, in each corresponding periodic window, the location and height of the peak are stochastically sampled to create a representative peak. The probability of occurring is used to assure the peaks appear consistently with the original signal.

By way of example, the periodic peak algorithm has previously been applied to publicly-available historical Houston day-ahead electricity markets, as shown in Figure 36. The search window was between 5 PM and 9 PM daily, as shown by the yellow bands. The peaks identified and characterized are indicated by the red cross marks.

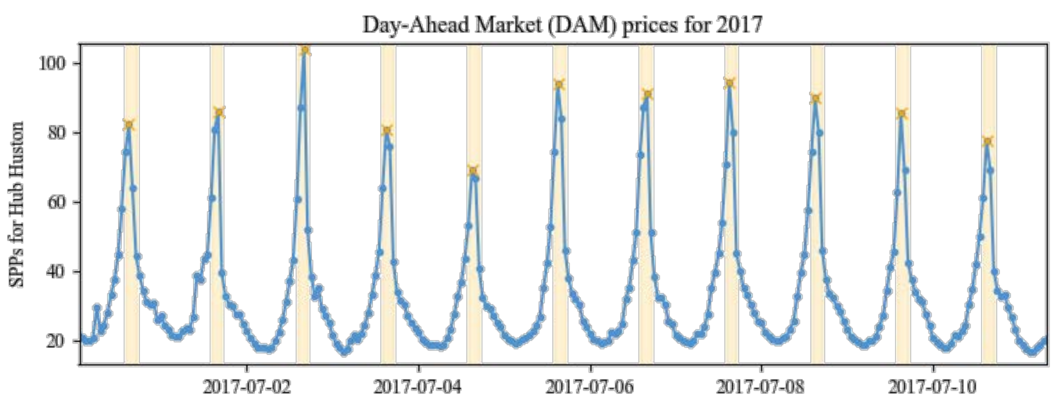

Figure 36. Period peak picking algorithm demonstration.

6.2.3 Interpolated Surrogates

The ReEDS/PLEXOS methodology results in hourly data for a year, with every four years in the sixteen-year analysis provided. In order to properly stochastically determine the economic impact of a particular grid portfolio, the intervening years need to be interpolated. To support this, and as part of this work, the synthetic history generation algorithms in RAVEN were expanded to include interpolation capabilities between statepoints of existing data.

Rather than interpolate between sampled years for the electricity price in each hour, instead the surrogate models themselves are interpolated. By interpolating the fundamental properties of the Fourier, ARMA, and peaks between two years, a new surrogate representing a continuous shift from one year to another is constructed and used to produce synthetic data for that year. This approach yields interpolated years that are independent statistically and unique in value, more representative of traditional yearly values.

6.3 Workflow Generation

To run the two-cycle technoeconomic analysis discussed in Section 6.1, HERON uses an XML input containing grid unit and economic drivers to prepare two RAVEN input files. The first or "outer" RAVEN input is used to either sweep or optimize the energy grid portfolio unit capacities, adjusting the capacities of the hydrogen electrolysis, storage, and market. The second or "inner" RAVEN input generates many synthetic price histories of electricity prices and for each one performs dispatch optimization and economic analysis. The outer input runs the inner input via RAVEN's self-driving interface. This interface allows parallelization in both the outer and inner level, simultaneously running different portfolio cases as well as individual synthetic histories for each portfolio. The combined workflows were run on Idaho National Laboratory's FALCON supercomputer, running portfolios and synthetic scenarios simultaneously in approximately 2 hours per workflow for a full-gradient optimization using 60 parallel processors, equating to roughly 120 CPU hours per workflow. This included 46 iterative steps to obtain an optimal solution, each of which ran 6 inner cycles with 10 stochastic samples per inner cycle.

One advantage of using HERON to prepare RAVEN inputs is reduction in complexity. Due to the information transfer between the outer and inner RAVEN runs, it can be challenging to maintain and update the RAVEN inputs even for an experienced user as the workflows are developed. Using HERON, however, only one simplified input needs to be maintained as the grid system simulation is developed, tested, and analyzed.

6.4 HERON Dispatch Optimization

In addition to input generation, HERON provides a generic dispatcher that uses generic physics-based resource optimization algorithms to solve dispatching problems [7]. After initial trials, it was determined that the genericity of this strategy resulted in slower performance than necessary (as much as several seconds per time step). As a result, a case-specific dispatcher was employed, leveraging HERON's option to provide a custom algorithm for dispatching. This custom dispatcher solved each hour sequentially by considering the LMP versus the hydrogen storage buy and sell thresholds. This results in three possible behaviors:

- If the LMP in an hour is less than the storage buy threshold, the HTSE produces all the hydrogen required by the hydrogen market, then produces as much hydrogen during the hour as the hydrogen storage can contain. This is because the opportunity cost of selling electricity at the grid is sufficiently low.
- If the LMP in an hour is between the hydrogen storage buy and sell thresholds, the HTSE produces all the hydrogen required by the hydrogen market but does not produce any excess for the storage; instead, the remaining electricity is sold at the grid.
- If the LMP in an hour is greater than the hydrogen storage sell threshold, the market is satisfied as much as possible by the hydrogen in storage before dispatching the HTSE, freeing up as much electricity as possible to sell at the grid.

The resulting algorithm is several orders of magnitude faster than the generic dispatcher, trading genericity for speed. For a typical 20-year project life, this specific dispatcher needs several tenths of a second to solve the system.

An illustration of the results of the specific dispatcher is shown in Figure 37. The top two axes show the dispatch of electricity and hydrogen respectively for each component in the grid system, and the bottom shows the hydrogen storage level and the electrical grid prices superimposed. All values given are positive except in the case of the hydrogen storage, where a negative value indicates storing up hydrogen during the hour, while a positive value indicates providing hydrogen during the hour. The sizing of each unit has been modified from the analysis cases to demonstrate dispatch performance more clearly.

Two horizontal dotted lines have been added to the bottom axes to show the changing behavior of the storage. When the electricity price is below the bottom dotted line, the storage will greedily attempt to store as much hydrogen as is available. When the electricity price is above the top dotted line, it will attempt to provide hydrogen to the system. These interactions assure that the HTSE can be brought to low production levels when the price of electricity is high, so more electricity can be sold at the grid.

For example, consider the first several hours shown. Throughout these hours, the electricity produced by the balance of plant (BOP, blue dots) and the hydrogen consumed by the market (H_2_market1, purple hashes) are fixed. Initially, the price of electricity is below the fill level, so the HTSE ramps up to produce more hydrogen than demanded by the market; the remainder is absorbed by the storage (H_2_storage, red triangles). The storage level rises during these hours. Starting at hour 6 until hour 18 the electricity price is above the fill level but below the use level, so the storage maintains its level and the HTSE (HTSE, green circles) produces the hydrogen needed for the hydrogen market. In hour 41, the price of electricity spikes, causing the storage to release its reserve and mitigate the HTSE's production so that more electricity can be sold to the grid (Electric_Grid, orange stars). Note that during hour 41, the HTSE production drops significantly and the storage "production" increases dramatically, while simultaneously the electricity provided to the grid increases proportionately. Throughout the hours shown, the hydrogen storage never reaches its capacity, as the price of electricity is only low enough to encourage storage during a few hours before noon of each day. As a result, when the price of electricity spikes, the storage almost always completely empties, as it does not contain enough hydrogen to meet the demands of the hydrogen market during that hour. In the hours shown, following each spike in price, electricity spikes drop sufficiently low to allow for some hydrogen storage before electricity prices spike again, and the storage empties.

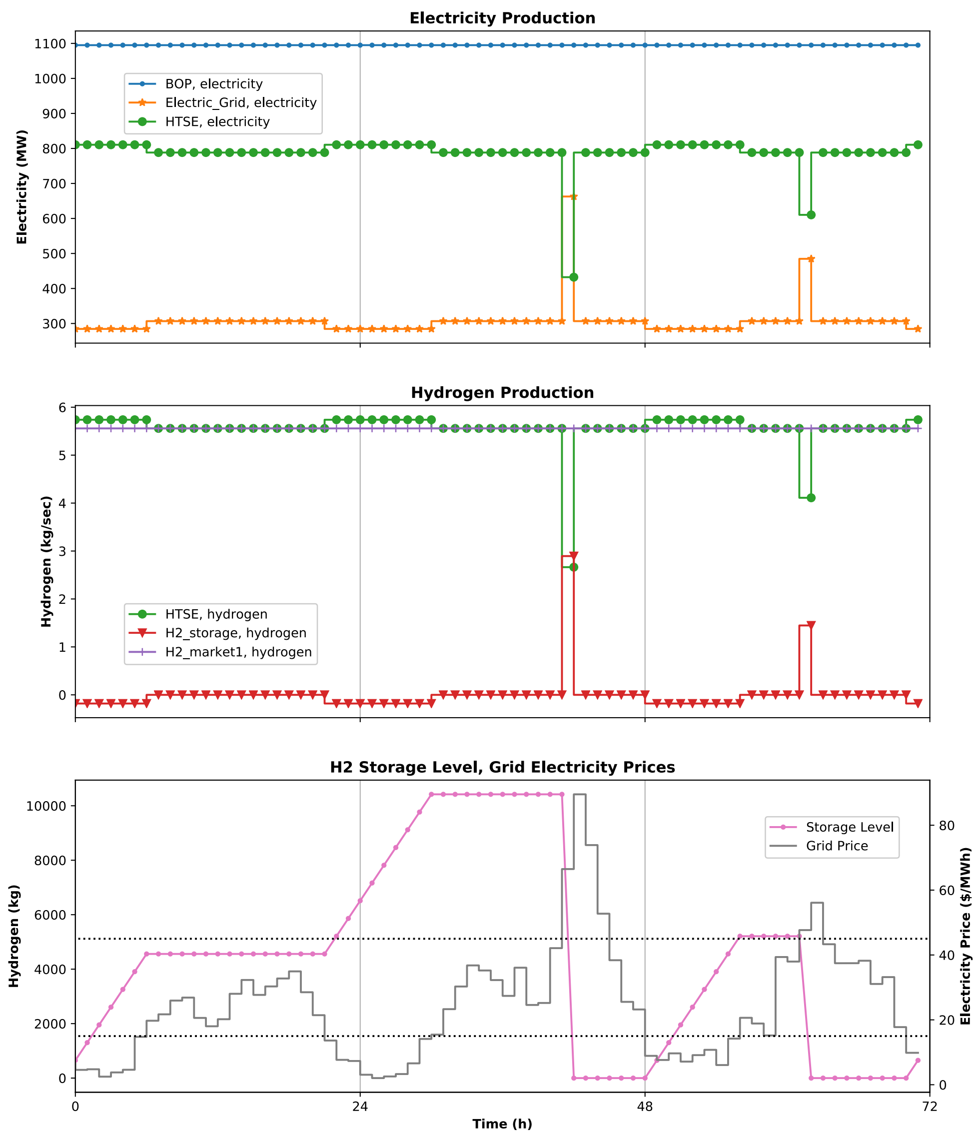

Figure 37. Example HERON dispatch. Top: electricity dispatch. Middle: hydrogen dispatch. Bottom: hydrogen storage level and electricity price.

6.5 References

[1] C. Rabiti, A. S. Epiney, P. Talbot, J. S. Kim, S. Bragg-Sitton, A. Alfonsi, A. Yigitoglu, S. Greenwood, S. M. Cetiner, F. Ganda, G. Maronati, "Status Report on Modeling and Simulation Capabilities for Nuclear-Renewable Hybrid Energy Systems," Idaho National Laboratory, September 2017, INL/EXT-17-43441.

[2] C. Rabiti, A. Alfonsi, J. Cogliati, D. Mandelli, R. Kinoshita, S. Sen, C. Wang, J. Chen, "RAVEN User Manual," INL/EXT-15-34123, Printed March 2017.

[3] J. Chen, C. Rabiti, "Synthetic wind speed scenarios generation for probabilistic analysis of hybrid energy systems", Energy 120, 2017, p. 507-517.

[4] P. W. Talbot, C. Rabiti, A. Alfonsi, C. Krome, M. R. Kunz, A. S. Epiney, C. Wang, D. Mandelli, "Correlated Synthetic Time Series Generation for Energy System Simulations using Fourier and ARMA Signal Processing," NURER 2018, Sept 30 – Oct 3, 2018, Jeju, Korea.

[5] Stauff, N., Maronati, G., Ponciroli, R., Ganda, F., Kim, T., Taiwo, T., Cuadra, A, Todosow, M., Talbot, P., Rabiti, C., and Kim, S. Tue. "Daily Market Analysis Capability and Results". Argonne National Laboratory, April 2019, ANL\NSE-19/5152100.

[6] Nicolas E. Stauff, R. Ponciroli, T. K. Kim, T. A. Taiwo, "Economic Impact of Flexible Nuclear Operation Estimated with EDGAR Optimization Code," NURER 2018, Sept 30 – Oct 3, 2018, Jeju, Korea.

[7] P. W. Talbot, J. Richards, P. Burli, A. Epiney, J. Zhou, C. Rabiti, "Status Report on Modeling and Simulation Capabilities for Integrated Energy System Technoeconomic Dispatch in Regulated Markets," Idaho National Laboratory, pending September 2019.

7. Case Study

This section can be broken down into two main subsections: Assumptions/Case Setup and Results. To understand the results of the simulations a detailed synoptic view on the model input space, overall driving assumptions, component control logic, and economic input parameters was conducted. Once the case is setup a results subsection provides the culmination of all aspects of the report into a series of seventeen-year, differential cash flow analyses to conclude whether the inclusion of a hydrogen production facility would be beneficial to a nuclear power plant operating in the PJM marketplace. This subsection will provide details of individual simulation results but will leave main system conclusions until the final conclusions chapter.

7.1 Scenario Selection and Assumptions

HERON requires the formulation of a well constrained problem that clearly identifies the resources utilized and the components capable of utilizing each resource. For the analysis considered there are six components: the nuclear power plant, turbine, electricity market, high-temperature steam electrolysis plant, hydrogen storage, and the hydrogen market. Component resources are outlined in Table 13, with overall system interaction depicted in Figure 38.

Table 13. Resource utilization in terms of HERON workflow.

Component	*Consumes*	*Produces*	*Assumption*
Nuclear Power Plant	--	Steam	Constant Steam Flow
Turbine	Steam	Electricity	Sells Electricity to either HTSE or Electric Grid
HTSE	Steam, Electricity	Hydrogen	Operates between hot-standby mode and full hydrogen production
Hydrogen Storage	Hydrogen	Hydrogen	Buys from HTSE during low electricity pricing; sells to hydrogen market during high electricity pricing
Hydrogen Market	Hydrogen	--	Fixed Market Demand
Electricity Market	Electricity	--	Infinite Sink of Electricity

Inherent in each component are assumptions about capacity and flexibility. The two end-users of the system are the electricity market and hydrogen market. The hydrogen market is assumed to not be an infinite/free market but rather consists of defined customers in the agricultural and petrochemical industries that typically consist of companies signing single or multiyear fulfillment requirements. Therefore, the hydrogen market is modeled as a fixed market based on contractual agreements made in the outer capacity expansion loop of HERON. During the seventeen-year simulation hydrogen demand must be met throughout.

Conversely, the electricity market in the PJM interconnect is massive compared to the electrical output of a singular nuclear facility. In addition, it operates under free-market rules, meaning no yearly contractual obligations are required from a given energy producer. Instead obligations are bid in on the day-ahead real time energy market. As such, the electricity market is modeled as an infinite sink that will pay a set price per MWh-e provided based on the overall hourly LMP price of the PJM market regardless of actual nuclear production rates.

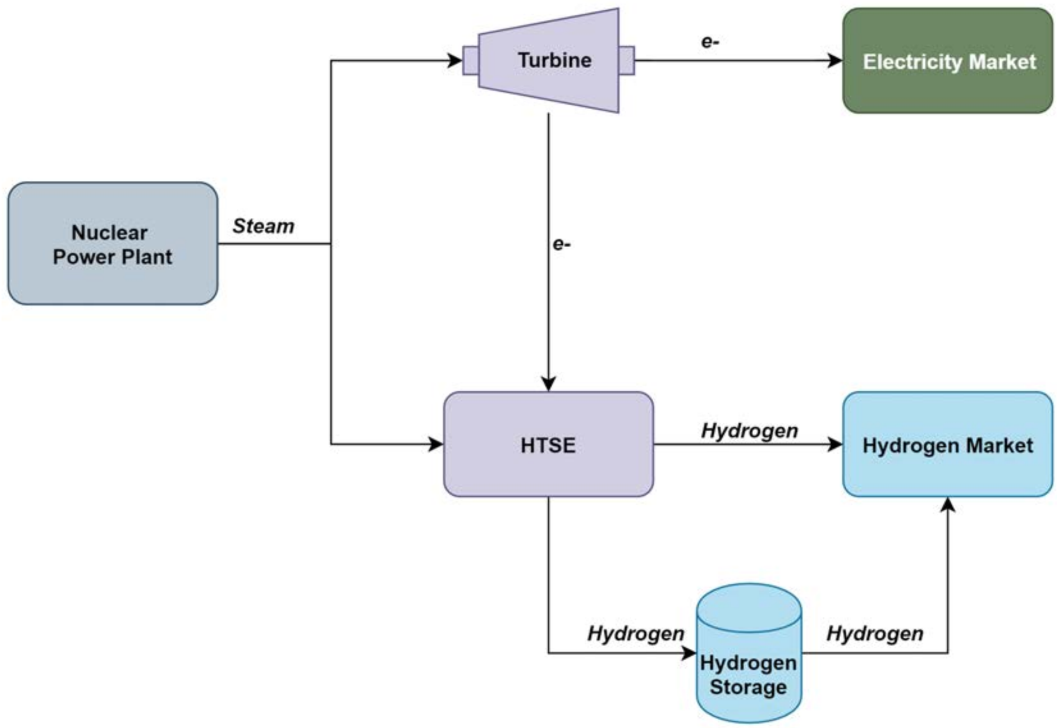

Figure 38. Case setup: The nuclear power plant creates steam that can be used to drive the HTSE for hydrogen production via a combination of electrical production and steam production. Alternately, the steam can make electricity for the electricity market.

The overall system producer is the nuclear power plant. It is assumed in this analysis that the nuclear power plant never load follows, but instead either produces hydrogen via the HTSE or it produces electricity for PJM market. Load following was not considered as ramps rates consistent with typical United States PWR operation are slow compared to market pricing fluctuations and overall system profitability would suffer. Additionally, increased thermal stresses in the power plant would increase overall system wear and tear.

The turbine utilizes steam to produce electricity that will then be sent either to the HTSE for hydrogen production or to the electric grid. The HTSE can operate the fuel stacks flexibly between hot standby mode and full operation. Further details on this range will be discussed in subsequent sections.

To allow flexibility between the two markets described above hydrogen storage is required. Hydrogen storage operates on the 24-hour day ahead real time energy market price and is described in further detail later in the section. A synopsis of all these assumptions are set forth in Table 13.

7.1.1 Fuel Cell Design Selection

Two HTSE designs have been discussed thus far in the report. One from Dominion Engineering. The other based on a preliminary design with Fuel Cell Energy. The Dominion engineering design was the basis of the Modelica models developed at INL between 2015 and 2017. This design runs the stacks at higher pressure to increase steam utilization rates. The Fuel Cell Energy Design utilizes low pressure SOEC stacks which allows the system to utilize less topping heat. This benefit decreases the capacity payment restraint as mentioned in the market analysis chapter. For comparison sake the Dominion engineering design requires approximately 26% electrical topping heat, where the FCE design requires just 10%. This differential allows the nuclear plant to maintain a higher capacity payment from the PJM market per current market rules. To keep the capacity payments for the nuclear power plant as high as possible the Fuel Cell Energy design was selected and will serve as the basis of simulations moving forward.

7.1.2 Surrogate Model Development

High-fidelity models (i.e., Modelica or ASPEN/HYSYS) may provide an accurate reflection of reality but require significant computational power. To minimize computational needs surrogate models were constructed to mimic the behavior of the high-fidelity models as closely as possible while maintaining computational efficiency. For components utilized in this system two surrogate models were required. One for the HTSE and one for the turbine. Initial surrogate development will focus on the HTSE.

As outlined previously only the electrolysis portion of the energy input in the HTSE can be cycled. In the FCE design this amount is about 87% of total nominal power input into the system. The other 13% of nominal power input is required at all times to maintain the system in a hot-standby mode and is broken down as follows:

1. Electrical Input = ~10% Nominal HTSE power: Utilized for topping heat, pumps, and compression cycle (e.g. For a HTSE sized to occupy a full 1100 MWe nuclear plant, ~109 MWe will always be provided to maintain the HTSE in hot-standby mode.))

2. Steam Input = ~3% Nominal HTSE power (Assuming 33% thermal-electric conversion ratio): Utilized to preheat feedstocks for the HTSE modules. (e.g. for an HTSE sized to occupy a full 1100 MWe nuclear plant, 108.7 MWt or an effective 35.93 MWe, will always be provided in the form of steam to maintain hot-standby mode.)

To estimate hydrogen production in the HTSE as a function of the electrolysis input a linear regressor of the form proposed in Eq. 16 is chosen.

$$H_2 = a + b * \dot{W}_{electrolysis} \tag{16}$$

Where a and b are model fitting parameters.

Several simulations were run in ASPEN/HYSYS to estimate parameters for the Fuel Cell Energy Design. Regression results for Eq. 16 is plotted in Figure 39. The estimated model-fitting parameters and R^2 values is listed in Table 14. The quality of the surrogate models compared to the ASPEN model outputs indicate excellent model fits.

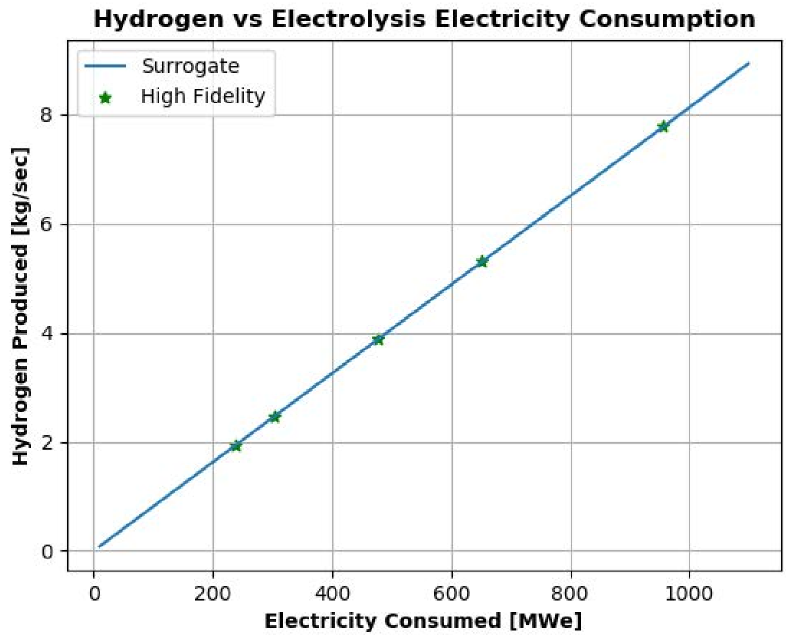

Figure 39. Hydrogen production vs. electrolysis electricity consumption.

Table 14. Model parameter estimates for Equations 14 and 15.

	Parameter	Parameter	Goodness of Fit
Equation 1	a	b	R^2
$\boldsymbol{H_2 = a + b * \dot{W}_{electrolysis}}$	-0.00008690	0.00813085	0.999999998
$\boldsymbol{\dot{W}_{Turb} = a + b * \dot{m}_{steam}}$	-114.9956	0.676318	0.999970070

The total effective electrical demand of the HTSE on the nuclear plant is the combination of electrical topping electricity, electricity used in the electrolyzers, and the lost turbine output incurred by sending steam to the HTSE plant. The topping electricity and preheating steam are constant and a function of HTSE capacity.

Similar to the HTSE a linear regressor of the form proposed in Eq. 17 was utilized to estimate electricity production in the Turbine as a function of steam input.

$$\dot{W}_{Turb} = a + b * \dot{m}_{steam} \tag{17}$$

To estimate parameters for the Turbine several simulations in Modelica were run. Regression results for Eq. 17 are plotted in Figure 40. The estimated model-fitting parameters and R^2 values is listed in Table 14. The quality of the surrogate models compared to the Modelica model outputs indicate excellent model fits.

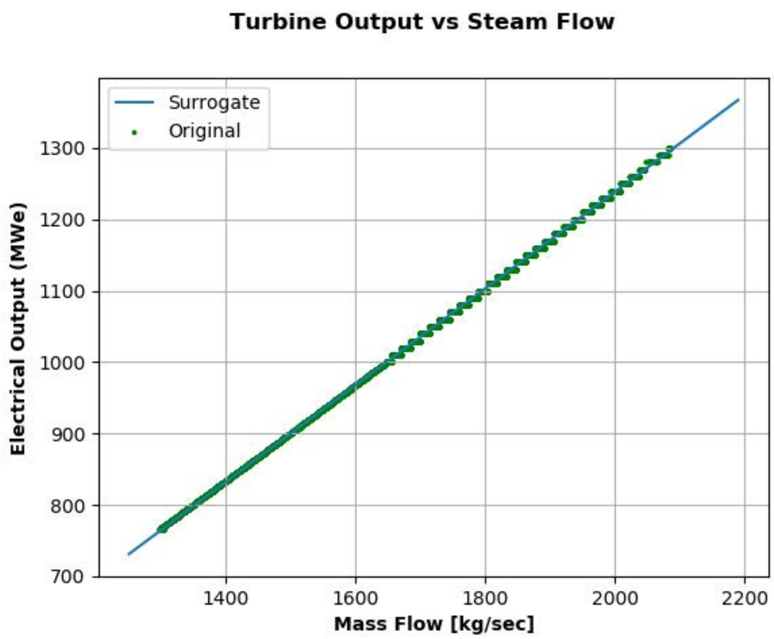

Figure 40. Turbine electricity production vs. steam input.

Through the creation of surrogate models, substantial computational resources can be saved while still maintaining acceptable model fidelity.

7.1.3 Hydrogen Storage Control Logic

For a nuclear power plant to properly accommodate inclusion into multiple markets, flexibility is key. If both markets were considered to be infinite market sinks, then an economic driver purely on relative cost could be made. Unfortunately, hydrogen markets operate under contractual agreements that require a set amount of hydrogen be delivered constantly. To accommodate the desire to operate flexibly and be able to monetize electricity pricing peaks appropriately, reserves of hydrogen in the form of hydrogen storage is required. Additionally, it is important to have excess hydrogen stored during times of peak pricing. Thus, requiring a hydrogen storage control strategy that operates on electricity pricing.

The idealistic control strategy for the hydrogen storage unit is to charge during periods of low electricity pricing and discharge during periods of high electricity pricing. To motivate the system to charge and discharge a storage cost as detailed in Table 15 was developed.

Table 15. Operating modes for hybrid co-generation facility.

Mode	*Nuclear Plant Preferred Operation*	*Electricity Price [$/MWh-e]*
1	Provide H_2 to the market via the HTSE and produce excess hydrogen to store	<15.0
2	Provide H_2 to the market via the HTSE and sell the rest to the electricity market	15.0 – 45.0
3	Provide electricity to the market and the storage unit provides H_2 to the market	>45.0

When considering to buy hydrogen from the HTSE, the storage will bid in a cost equivalent to an average price (~$15/MWh-e) of electricity, meaning the H_2 storage tank will only buy hydrogen if the electricity price is sufficiently low. Otherwise, it is better for the HTSE to ramp down and for the nuclear power plant to sell electricity to the grid. It should be noted that these set-points are not optimized to be the ideal set-points but instead are meant to show the motivational points of storage and how one could be operated to enhance flexibility of the overall system to increase profitability. Individual owner/operators of these facilities would set forth their own proprietary control strategies based upon regional market rules and contractual agreements with hydrogen end-users. For simulations in this analysis it is assumed that the hydrogen storage is completely empty at the beginning of each 17-year run and that initial motivations will begin to fill the storage tank.

By introducing hydrogen storage into the system the nuclear power plant can now operate in three distinct modes based on economic drivers as outlined in

Table 15. If electricity pricing is low, the storage tanks begin to fill, if electricity pricing is average the storage tanks do not operate, and if electricity pricing is high, discharge the storage tanks to free the nuclear plant to capitalize on electricity pricing. Economic optimization studies between tank sizing and storage motivators will be run in later sections. However, an optimization on overall pricing frequency of different markets and the inclusion of policy motivators to fully capitalize on storage capabilities is beyond the scope of this report. Through the inclusion of hydrogen storage, the nuclear facility can operate freely in between multiple markets.

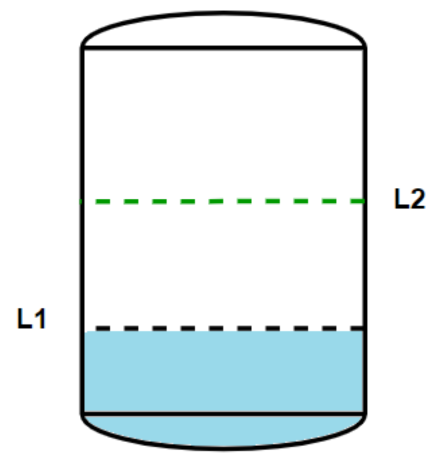

Figure 41. Hydrogen tank with level control.

Capabilities to operate the storage tanks in a multi-level approach as shown in Figure 41 have been considered. However, for the purposes of this report a single buy low, sell high approach was taken. In additional a sliding scale-seasonal buying and selling price, where summer buying and selling prices are different than winter buying and selling prices, could be used.

7.1.4 Electricity Market

The exact prediction of market pricing is impossible to do; however, storage sizing, operation, and system profitability is entirely dependent the time-specific nature of the electricity pricing. Therefore, running simulations utilizing the same hourly pricing data isn't ideal. This is because a single set of pricing data cannot adequately capture all pricing scenarios. Such simulations could lead to improperly sized storage units, overbid hydrogen contracts, or improper buying and selling motivators on the storage system.

To properly simulate different scenarios of the same year that are statistically the same but stochastically different a multi-year ARMA training was completed on the data provided by NREL of the PJM market as outlined in Chapter 5. By doing this the same year can be simulated repeatedly while giving different pricing values during different days for the system to adhere to. This is because the runs are statistically the same, yet no two runs have the same values. The reverence for the ARMAs created can be determined on three main things: 1. overall spot checking of the data vs the initial data and 2. Price Duration Curves and 3. Speed of Simulation.

Price duration curves depicted in Figure 42 show that for each year of simulated and real data the number of price spikes and dips are approximately the same. The melding of these curves between years creates the price duration curves for the interpolated years.

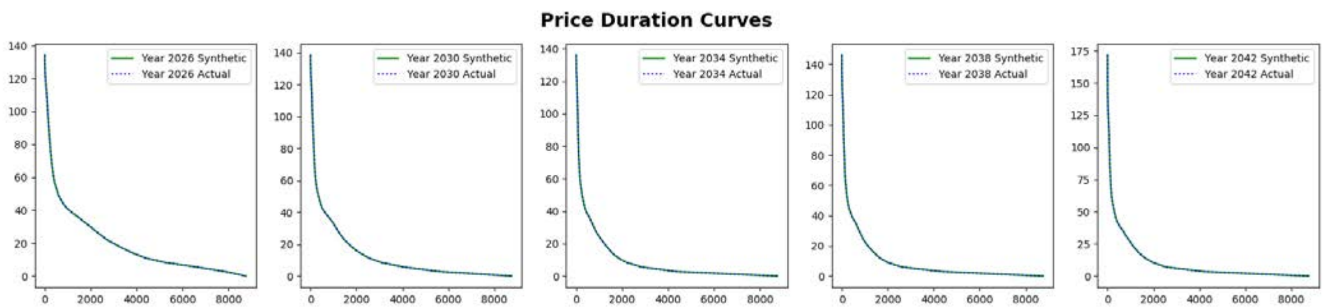

Figure 42. Price duration curve comparisons of synthetic data vs. NREL data.

A single seventeen-year realization of the system is shown in Figure 43. It should be noted the stochastic nature of the ARMA realization algorithm means the original data and the synthetic data will not line up. Instead the two pieces of data are statistically the same. This behavior is illustrated in Figure 43 on years 2026,2030,2034,2038, and 2042. Summer months (middle) tend to have significantly more “peak” pricing than the winter months as time progresses. Additionally, it can be seen that interpolated synthetic histories tend to be a blending of the two years that bound it. Both in terms of overall statistics and time placement of pricing peaks.

For a four-day realization of the ARMA it can be seen that the original data has pricing spikes associated with the hours of 3pm to 7pm that corresponds to when people are coming home from work, air conditioner units are cooling homes, and heavy hitters such as stoves and ovens are operating for dinner. By utilizing peak picking tools within the ARMA recreation of such peaks is possible as displayed in Figure 44. Notice the peaks still demonstrate stochastic behavior in terms of overall magnitude, yet they remain in a periodic fashion as would be consistent with typical diurnal pricing curves.

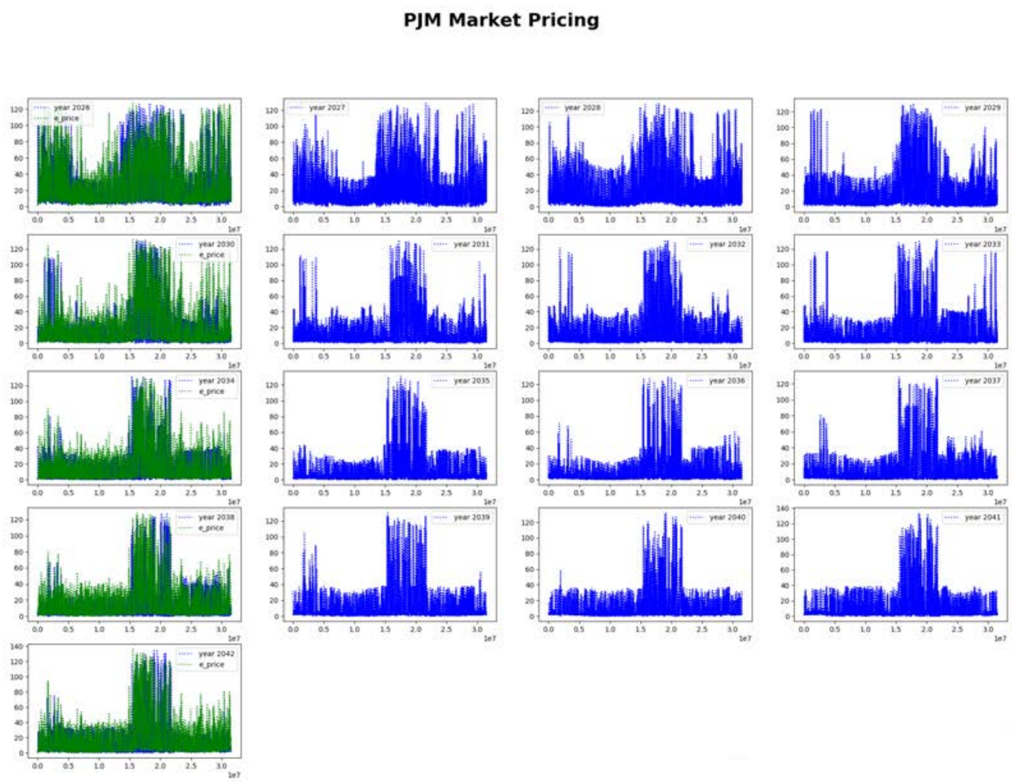

Figure 43. A single seventeen-year realization of the ARMAs. n_clusters =10, with a three-day window.

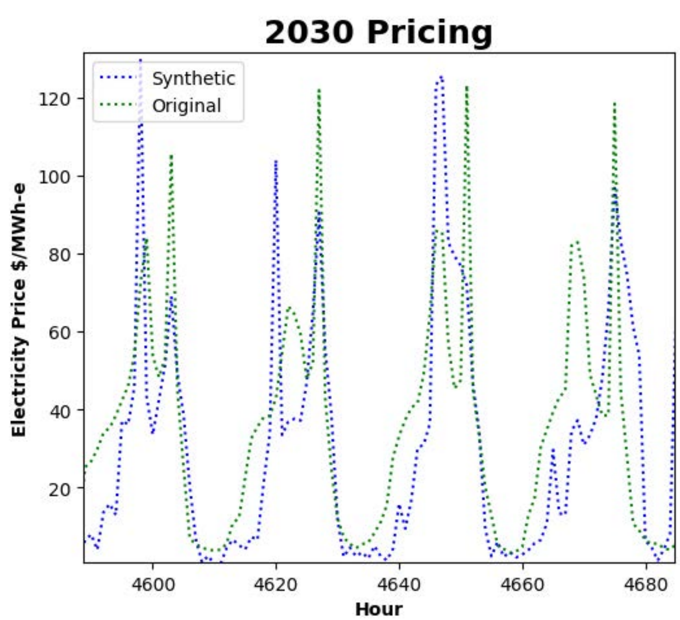

Figure 44. Four-day realization of 2030 pricing illustrating peak pricing recreation.

By deconstructing the PJM markets provided by NREL via the ARMA trainer the system can now be evaluated and sampled many times with each simulation being unique. This will increase the applicability of the simulations and conclusions as distinctive seventeen-year simulations can be run.

7.1.5 Cash Flow Analysis

To compare the investment options of deploying a hydrogen generation facility for hydrogen co-generation at a nuclear facility or maintaining a business as usual approach a differential, discounted cash flow analysis was performed utilizing the CASHFLOW plugin in RAVEN [1].

Differential net present value (NPV) is defined by Equation 18.

$$\Delta NPV = NPV_{cogen} - NPV_{ref} \tag{18}$$

A $\Delta NPV > 0$ suggests the case under consideration is more profitable than the reference case. It does not make a claim on total system profitability, but rather identifies a more economically advantaged scenario. An additional benefit of the differential cash flow scenario is its ability to ascertain meaningful results with a reduced number of cashflows. In differential cash flows only divergent cash flow streams are needed. For example, nuclear plant O&M costs are not present as they are the same in both configurations. A drawback of this approach is that in spite of differential cash flow calculation being positive, the overall investment could still be at a loss assuming a sufficiently negative starting point.

To calculate NPV_{cogen} and NPV_{ref} a discounted cash flow analysis was completed as shown in equation 19, where the cash flow for each year is calculated and then added together. This calculation gives the net present dollar value of future cash flows for the plant, when assuming some discount rate for the system.

$$NPV = \sum_{year=0}^{Lifetime} \frac{CF_{total,year}}{(1+r)^{year}} \tag{19}$$

Cash flows for each component are shown in equation 20. Where X is the economies of scale factor, $driver_{ref}$ is the reference amount for which economies of scale is valid. α_y is the initial cost of the component cash flow.

$$CF_y = \alpha_y \left(\frac{driver}{driver_{ref}}\right)^X \tag{20}$$

Each component in system has its own cash flow, CF_y, and it is the sum of all these cash flows that make up CF_{total}. Included within the cash flow module is tax, inflation, amortization schedules, etc. A detailed overview of the discounted cash flow analysis performed inside the module can be found in a 2014 study completed by INL [2]. Important to note is that since the cash flow analysis is performed in real terms the only effect of inflation is to depreciate the value of the CAPEX amortization.

7.2 Case Setup

Proper sizing of individual units will be dependent on a multitude of factors ranging from hydrogen market pricing, to electricity spikes inherent in an average year, to storage costs. As previously mentioned, this analysis focuses on the PJM market, with electricity pricing developed by NREL, and hydrogen market pricing developed by Argonne National Laboratory when assuming high, medium, and low natural gas prices in accordance with the 2018 AEO report. The results developed here will utilize ten stochastic histories per sample point alongside a sweep over component and market capacities.

To properly analyze different and unique market scenarios a multitude of cases were run as shown in Table 16. Sweeps of unit capacities were utilized thus creating a tensor of simulations to run. Based on four different HTSE capacities with five potential storage sizes, four H_2 market demands, and three different H_2 market prices this creates a system with 240 scenarios to run.

Each of these 240 scenarios utilized ten denoising's and then each one of the 240 scenarios require one of three discount rates. Putting all this together requires a total of 7,200 individual seventeen-year runs. An additional thirty runs are added to simulate the baseline case of just a nuclear power plant at different discount rates. To accommodate such a large number of simulations the supercomputer Falcon at Idaho National Laboratory was utilized.

The cash flow analysis run is a discounted cash flow analysis in present dollars with a sweep of a discount rates ranging from 8% to 12%. System calculations will analyze a corporate tax rate of 21% consistent with federal tax law as of the 2019 fiscal year [4]. All cash flow assessments in the analysis are differential cash flows between coupled nuclear-hydrogen cogeneration, and the business as usual model. Therefore the *business as usual* calculation was subtracted from the coupled nuclear-HTSE NPV to produce the differential NPV calculation. Standard Deviations of both scenarios were added together utilizing error propagation methodologies. Therefore, it is again noted that this analysis does not claim system **profitability**, but instead showcases the **differential** between business as usual and co-generation. Just because a system shows an increase in profitability over seventeen years does not mean the system is profitable overall, just whether or not the owner/operator is better off than they were before the decision in question.

Table 16. Simulation parameters for parametric study of nuclear-HTSE scenarios.

Parameter	*Value*
Nuclear Steam Flow	1921 kg/sec
HTSE Capacities	[2, 3.8, 5.6, 7.4] kg/sec
H_2 Storage Capacity	[0, 28800, 57600, 115200, 230400] kg
H_2 Market Demand	[1.8, 3.6, 5.4, 7.2] kg/sec
H_2 Market Price	[Low, Medium, High] via Chapter 4
Corporate Tax Rate	21% [3]
Discount Rates (WACC)	[8, 10, 12] %
Inflation Rate	2.188% [per 2000-2018 average][4]
Stochastic De-noising per sample	4
HTSE: Capital Cost (Includes-manifold addition)	545,263,737 for 7.4 kg/s H_2 [640tpd]
HTSE: O&M	70,752,705
Economies of Scale Factor for HTSE	0.955
HTSE Amortization Schedule	15 year MACRS
Number of Pipelines	6
Pipeline	$996,492/mile (compressor included)
Pipeline Amortization Schedule	15 year MACRS
Total Pipeline Length	19.4 miles / [kg/sec H_2 production]
Storage	$600/kg
Storage Amortization Schedule	5 year MACRS [5]

It should be noted that not all of 7,230 simulations will have a solution. Scenarios that require a hydrogen demand of more than what the HTSE can provide on its own are ill posed and therefore drop out.

7.3 Scenarios

A myriad of simulations were run to understand the combinatorial effects of component interactions when exposed to economic drivers. Results presented here will be sufficient to explain the trends of the system and to propose an ultimate solution. However, to mitigate redundancy full results will be detailed in Appendix B. Discussions will present system viability as a function of capacities, contractual agreements, hydrogen selling price, and company discount rates. All results plotted will utilize the same axes so as to allow readers to properly discern the impact of discount rates and hydrogen selling price on overall differential NPVs. It should be re-iterated that high, medium, and low hydrogen pricing is based on high, medium, and low natural gas pricing respectively as outlined in Chapter 4.

7.3.1 Coupled HTSE-Storage- Discount Rate (8%), High H_2 Selling Price

Results below present a sweep of 80 possible differential NPV solutions related to a simultaneous sweep of HTSE capacities, hydrogen storage sizes, and fixed hydrogen market contractual agreements with a discount rate of 8% and high hydrogen prices. The particular hydrogen contract price points are depicted in Figure 45 and correspond to hydrogen contracts of [1.8, 3.6, 5.4, 7.2] kg/sec respectively. Of the 80 possible scenarios, 30 had no solution since the HTSE was not sized to meet market contractual demand as was expected. For each of the 50 scenarios that were well-posed, a stochastic history of ten simulations was run. Following this the baseline "business as usual case as run over seventeen years with a total NPV of 847 million. As mentioned before this solution was subtracted from the 30 scenarios to give the differential NPV values illustrated Figure 46 and Table 17. Axes show the capacity of each component either as a rate (HTSE and H_2 market) or as total (storage).

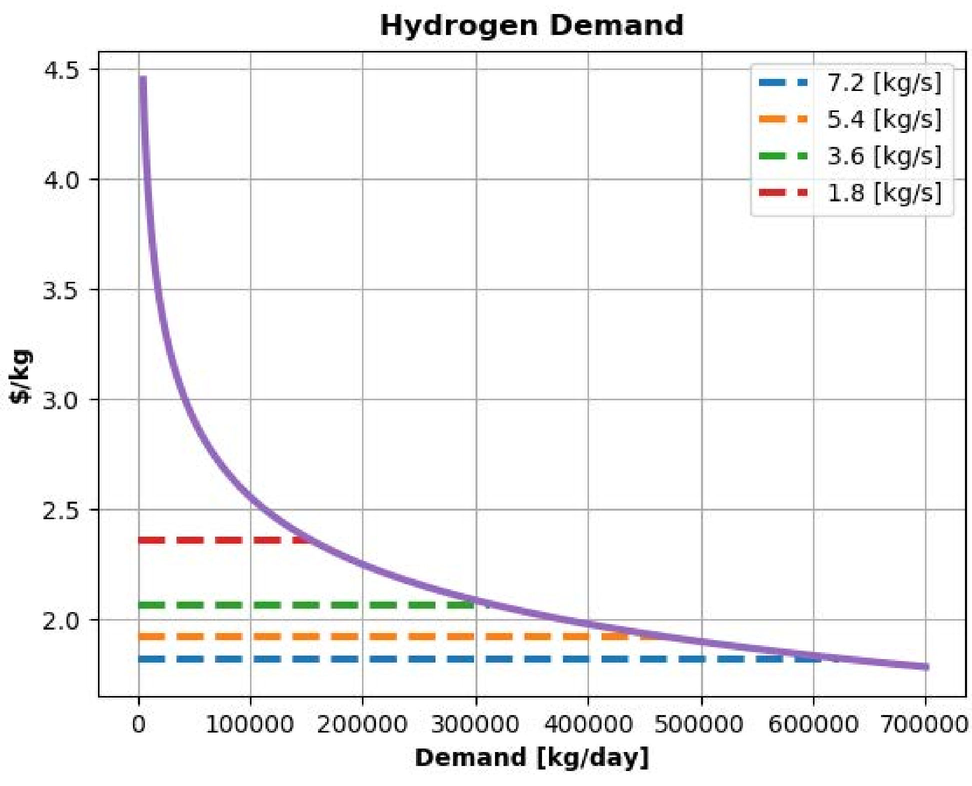

Figure 45. High hydrogen pricing with sweep values on hydrogen market contractual obligations realized.

Illustrated in Figure 46 are the possible combinations of HTSE size, storage size, and hydrogen market price. Results illustrate it is beneficial to have contractual agreements in the hydrogen market that are similar in size to the constructed HTSE unit. If this is not the case large negative NPVs are incurred as depicted in Figure 46. Additionally it can be seen through investigation of both Figure 46 and Table 17 that profitability increases as storage size increases. This is for two reasons:

1. The nuclear plant is able to appropriate electricity to the grid during times of high electricity pricing as storage fulfills the hydrogen market demand.
2. The capacity payment penalty incurred by the nuclear facility decreases since the storage unit can be fully utilized.

However, there comes a point that storage capacity is too large for the system and profitability decreases due to hydrogen storage cost. Results here suggest a profitability increase from building additional storage up to 115,200 kg (Large enough to allow up over four consecutive hour of discharge, assuming the largest contractual agreement). Yet, suggest a profitability decrease with a storage size of 230,400 kg.

Further, scenarios analyzed advocate that increased HTSE production rates and contract sizes increase profitability for the system. This can be attested to two main factors. One, is the economies of scale of HTSE units such that the $n^{th}+1$ unit of installed hydrogen production cost less than the n^{th}. The other factor being that hydrogen pricing is higher on average than is electricity pricing, even with the inclusion of additional pipeline to transport the hydrogen. Moreover, in the results presented it is assumed the nuclear plant can maintain participation in the electricity market and therefore continues to receive capacity payments on the sliding scale scheme set presented in equations 14 and 15.

The sliding scale scheme becomes particularly noticeable at low storage capacities. At low storage capacities the effect of missing out on capacity payments is noted. During these times not only is the nuclear facility unable to capitalize on high electricity pricing via flexible operations, but a steady source of income, in the form of capacity payments, has been lost.

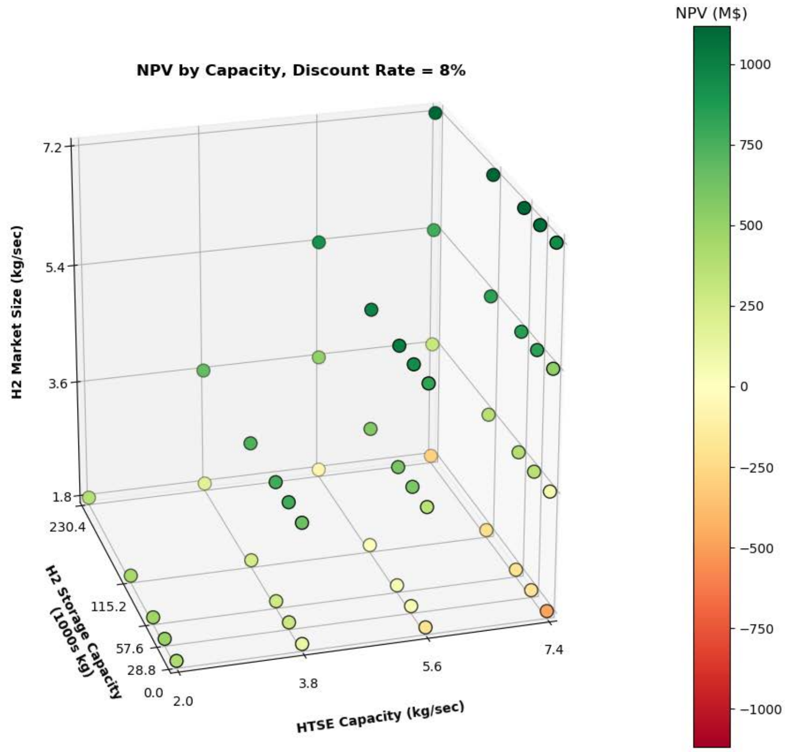

Figure 46. Differential NPV over seventeen years of a co-generating nuclear station in PJM market assuming high hydrogen selling prices. Discount rate = 8%, corporate tax rate = 21%, yearly inflation = 2.188%.

Table 17. Differential NPV over seventeen-year lifetime between electricity-only production and production of hydrogen at a fixed rate at high hydrogen market price predictions.

H_2 market (kg/sec)	Storage (kg)	HTSE (kg/sec)	ΔNPV (2019$)	σ (2019$)
1.8	57600	7.4	-1.84E+08	1.92E+06
1.8	0	3.8	1.08E+08	1.92E+06
1.8	28800	3.8	2.72E+08	1.92E+06
1.8	28800	7.4	-1.76E+08	1.92E+06
1.8	57600	2	4.66E+08	1.94E+06
1.8	57600	3.8	2.65E+08	1.94E+06
1.8	28800	2	4.82E+08	1.92E+06
1.8	57600	5.6	3.94E+07	1.92E+06
1.8	28800	5.6	4.67E+07	1.95E+06
1.8	0	5.6	-1.84E+08	1.93E+06

1.8	0	2	4.06E+08	1.92E+06
1.8	0	7.4	-4.74E+08	1.92E+06
1.8	115200	3.8	2.32E+08	1.93E+06
1.8	115200	2	4.33E+08	1.94E+06
1.8	115200	5.6	6.73E+06	1.94E+06
1.8	115200	7.4	-2.16E+08	1.96E+06
1.8	230400	2	3.66E+08	2.01E+06
1.8	230400	7.4	-2.86E+08	1.92E+06
3.6	0	5.6	3.47E+08	2.08E+06
1.8	230400	3.8	1.64E+08	2.00E+06
1.8	230400	5.6	-6.24E+07	1.99E+06
3.6	0	3.8	6.39E+08	2.04E+06
3.6	0	7.4	5.71E+07	1.92E+06
3.6	28800	7.4	3.65E+08	1.94E+06
3.6	28800	3.8	7.77E+08	1.94E+06
3.6	57600	3.8	7.71E+08	1.98E+06
3.6	57600	5.6	5.96E+08	2.22E+06
3.6	115200	3.8	7.39E+08	1.92E+06
3.6	28800	5.6	5.87E+08	2.15E+06
3.6	57600	7.4	3.77E+08	2.05E+06
3.6	115200	5.6	5.73E+08	2.09E+06
3.6	115200	7.4	3.62E+08	1.92E+06
3.6	230400	3.8	6.73E+08	2.05E+06
3.6	230400	5.6	5.08E+08	2.01E+06
3.6	230400	7.4	2.97E+08	2.01E+06
5.4	0	7.4	5.23E+08	2.97E+06
5.4	0	5.6	8.20E+08	2.06E+06
5.4	28800	5.6	9.45E+08	2.79E+06
5.4	57600	5.6	1.01E+09	2.06E+06
5.4	28800	7.4	8.34E+08	2.25E+06
5.4	57600	7.4	8.51E+08	2.33E+06
5.4	115200	5.6	9.83E+08	2.10E+06
5.4	230400	5.6	9.17E+08	2.57E+06
5.4	115200	7.4	8.36E+08	1.92E+06
5.4	230400	7.4	7.76E+08	2.02E+06
7.2	0	7.4	9.50E+08	4.02E+06
7.2	28800	7.4	1.08E+09	2.99E+06
7.2	115200	7.4	1.19E+09	2.04E+06
7.2	57600	7.4	1.13E+09	2.72E+06
7.2	230400	7.4	1.12E+09	2.17E+06

Figure 47 displays a three day dispatch window for the of the most profitable scenarios HTSE size = 7.4 kg/sec, H_2 contractual agreement = 7.2 kg/sec, and a hydrogen storage = 115,200 kg. The top two axes show the dispatch of electricity and hydrogen respectively for each component in the grid system, and the bottom shows the hydrogen storage level and the electrical grid prices superimposed.

As outlined earlier in the chapter the storage tank will receive hydrogen if the electricity price for the hour is below \$15/MWh-e. During these moments of low electricity pricing the hydrogen tank begins to fill and during times of high pricing >45/MWh-e the storage tank will discharge to the hydrogen market. Discharging the storage tank during peak pricing allows the nuclear power plant to provide power to the electric market and capitalize on high electricity prices.

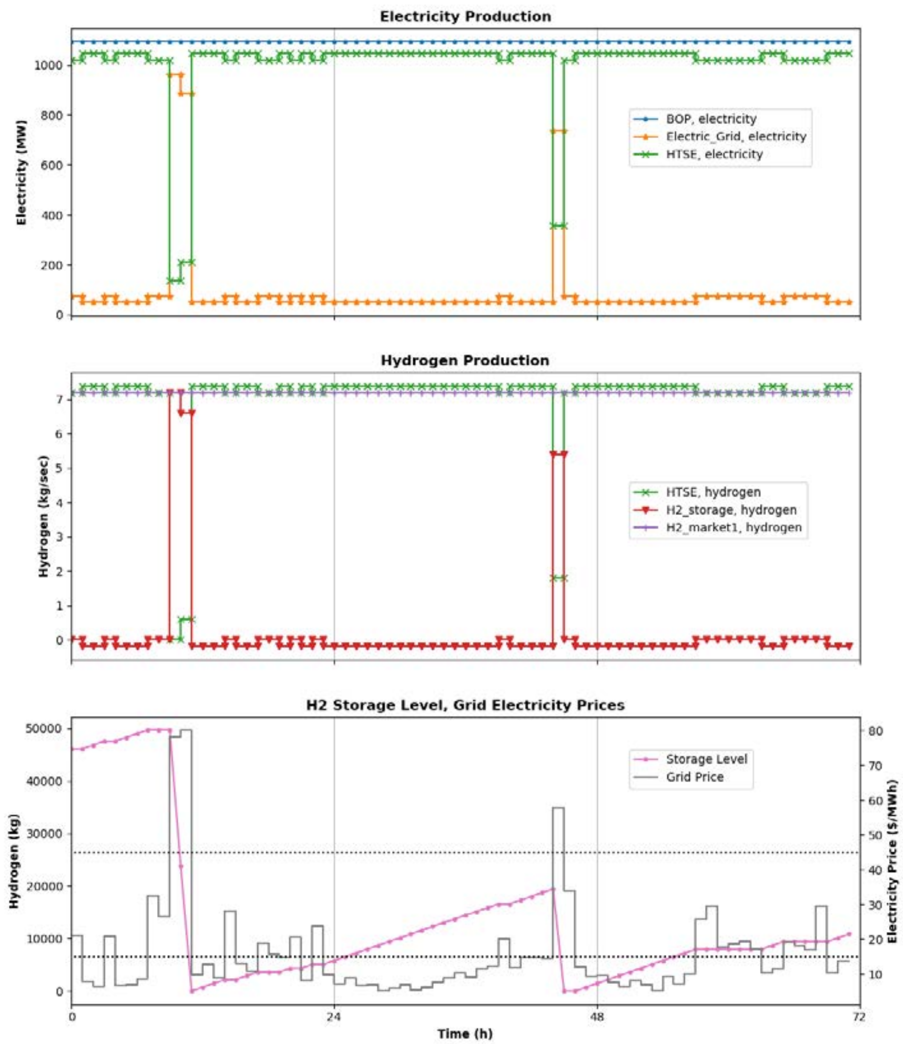

Figure 47. Top: electricity dispatch. Middle: hydrogen dispatch. Bottom: hydrogen storage level. (HTSE size = 7.4 kg/sec, H_2 contractual agreement = 7.2 kg/sec, and a hydrogen storage = 115,200 kg.)[2]

All aspects of this control are illustrated. Initially the hydrogen storage tanks about 40% full and continue to fill or hold position as the electric selling price remains <\$45/MWh-e. Then at hour nine electricity pricing rises to \$77/MWh and remains at these levels for two consecutive hours. Throughout the first hour the storage tank is able to completely accommodate the hydrogen market, allowing the nuclear facility to shift electrical production to the grid. Then during the second hour the hydrogen storage tanks

[2] Note: Hour zero corresponds to noon.

are able to accommodate a majority of the hydrogen market, with the HTSE providing the rest. This allows the nuclear plant to capitalize on high electricity pricing throughout the peak pricing moments. Such an operational strategy maximizes profits for the nuclear reactor and guarantees both market entities are satisfied.

Following this consecutive spike, electricity pricing drops and the storage unit is able to begin filling periodically for the next day until it is called upon again. This time the storage unit is not completely filled but is able to provide approximately three quarters of the hydrogen needed during this hour, but is unable to help in the following hour. This represents a missed opportunity cost that can only be captured with a dynamic charge/discharge strategy. It is noted that the buying and selling strategy presented here does not represent the ideal control methodology and it important to note that proprietary company decisions would place this set-point elsewhere in accordance with the company's personal market pricing projections, seasonal projections, and specific contractual obligations.

7.3.2 Coupled HTSE-Storage- Discount Rate (8%), Medium H_2 Selling Price

As in previous runs Figure 49 illustrates the potential combinations of HTSE size, storage size, and hydrogen market price. Similar to before results advocate HTSE sizing similar to contractual hydrogen agreements to avoid large negative NPV's. As before storage size increases profitability initially before dropping overall profits as storage costs begin to outweigh benefits.

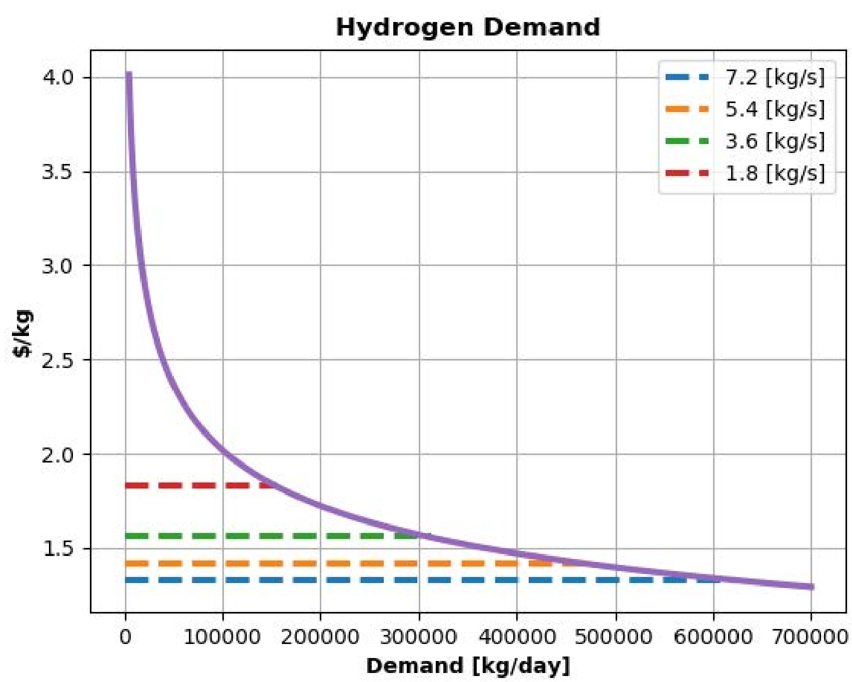

Figure 48. Medium hydrogen pricing with sweep values on hydrogen market contractual obligations realized.

As with the results presented in the high H_2 pricing case the most profitable scenario in the capacity sweep assuming medium hydrogen pricing is to build an HTSE = 7.4 kg/sec, H_2 market demand = 7.2 kg/sec with a storage capacity of 115,200 kg. However, the differential between an HTSE of size 7.4 kg/sec, market demand of 7.2 kg/sec, and storage of 115,200 kg vs an HTSE of size 5.6 kg, market demand of 5.4 kg/sec, and storage of 57,600 kg is only a few million dollars and falls within standard deviation error. The reason is these are so close is because hydrogen market sales are not large enough to fully overcome the capital cost expense associated with HTSE and pipeline construction over the seventeen-year period analyzed. Instead results begin to advocate for building a smaller HTSE that will increase hydrogen pricing per kg sold as demonstrated in Figure 48 to a point overall system profitability will increase.

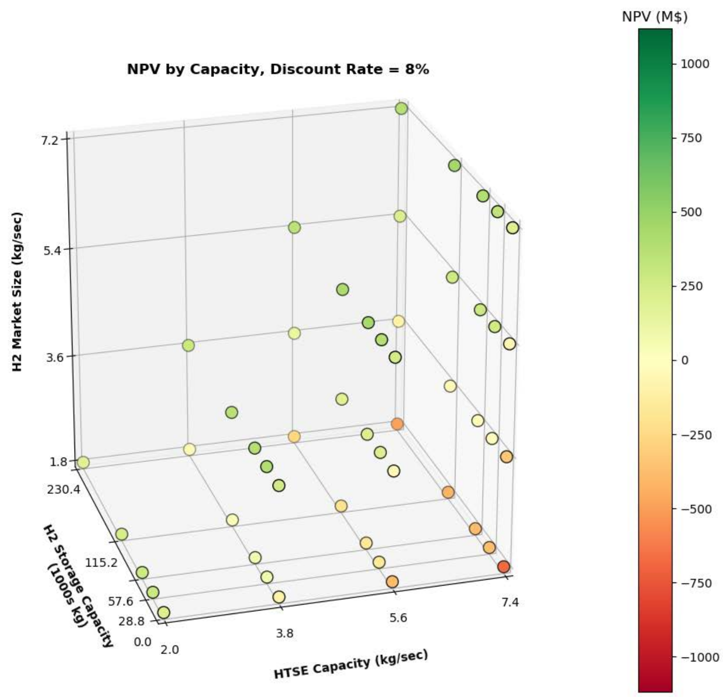

Figure 49. Differential NPV over seventeen years of a co-generating nuclear station in PJM market assuming medium hydrogen market selling prices. Discount rate = 8%, corporate tax rate = 21%, yearly inflation = 2.188%.

Table 18. Differential NPV over seventeen-year lifetime between electricity-only production and production of hydrogen at a fixed rate at medium hydrogen market price predictions.

H_2 market (kg/sec)	Storage (kg)	HTSE (kg/sec)	ΔNPV (2019$)	σ (2019$)
1.8	0	3.8	-9.09E+07	1.92E+06
1.8	0	5.6	-3.84E+08	1.92E+06
1.8	0	2	2.06E+08	1.92E+06
1.8	0	7.4	-6.73E+08	1.92E+06
1.8	28800	3.8	7.27E+07	1.93E+06
1.8	28800	2	2.82E+08	1.94E+06
1.8	57600	7.4	-3.83E+08	1.93E+06
1.8	28800	5.6	-1.53E+08	2.00E+06

1.8	57600	3.8	6.51E+07	1.94E+06
1.8	57600	5.6	-1.60E+08	1.94E+06
1.8	28800	7.4	-3.75E+08	1.99E+06
1.8	57600	2	2.66E+08	1.96E+06
1.8	230400	2	1.66E+08	2.00E+06
1.8	230400	3.8	-3.57E+07	1.95E+06
1.8	115200	7.4	-4.16E+08	1.92E+06
1.8	115200	2	2.34E+08	1.97E+06
1.8	115200	5.6	-1.93E+08	1.93E+06
1.8	115200	3.8	3.27E+07	1.93E+06
3.6	0	5.6	-4.23E+07	1.92E+06
3.6	0	7.4	-3.32E+08	1.92E+06
1.8	230400	5.6	-2.62E+08	1.92E+06
1.8	230400	7.4	-4.85E+08	1.92E+06
3.6	0	3.8	2.50E+08	1.92E+06
3.6	28800	3.8	3.88E+08	2.68E+06
3.6	28800	5.6	1.98E+08	2.01E+06
3.6	28800	7.4	-2.36E+07	1.94E+06
3.6	57600	3.8	3.82E+08	2.01E+06
3.6	57600	5.6	2.06E+08	2.03E+06
3.6	57600	7.4	-1.28E+07	2.11E+06
3.6	115200	5.6	1.83E+08	2.12E+06
3.6	115200	7.4	-2.78E+07	2.01E+06
3.6	115200	3.8	3.50E+08	1.94E+06
3.6	230400	5.6	1.19E+08	2.06E+06
3.6	230400	3.8	2.84E+08	2.03E+06
3.6	230400	7.4	-9.28E+07	2.17E+06
5.4	0	5.6	2.41E+08	1.92E+06
5.4	0	7.4	-4.89E+07	1.92E+06
5.4	28800	7.4	2.62E+08	1.98E+06
5.4	28800	5.6	3.73E+08	2.28E+06
5.4	57600	5.6	4.35E+08	4.88E+06
5.4	57600	7.4	2.78E+08	2.10E+06
5.4	115200	7.4	2.64E+08	2.03E+06
5.4	115200	5.6	4.11E+08	2.02E+06
5.4	230400	5.6	3.45E+08	2.14E+06
5.4	230400	7.4	2.04E+08	2.63E+06
7.2	0	7.4	2.00E+08	1.92E+06
7.2	28800	7.2	3.30E+08	2.75E+06
7.2	57600	7.4	3.79E+08	3.75E+06
7.2	115200	7.4	4.39E+08	1.97E+06
7.2	230400	7.4	3.74E+08	2.18E+06

7.3.3 Coupled HTSE-Storage- Discount Rate (8%), Low H_2 Selling Price

As in previous runs Figure 49 illustrates the solutioned combinations of HTSE size, storage size, and hydrogen market price. Similar to before results advocate HTSE sizing similar to contractual hydrogen agreements to avoid large negative NPV's.

Discordant to previous cases, low hydrogen pricing suggests smaller HTSE and pipeline construction. Hydrogen sales are not large enough to overcome capital costs over the seventeen-year timeline. Therefore, to increase profitability smaller contracts with higher average hydrogen selling prices should be initiated. This is consistent with the assumptions presented in Chapter 4 that hydrogen users are willing to pay a price equivalent to building their own steam methane reforming plant for their personal business needs.

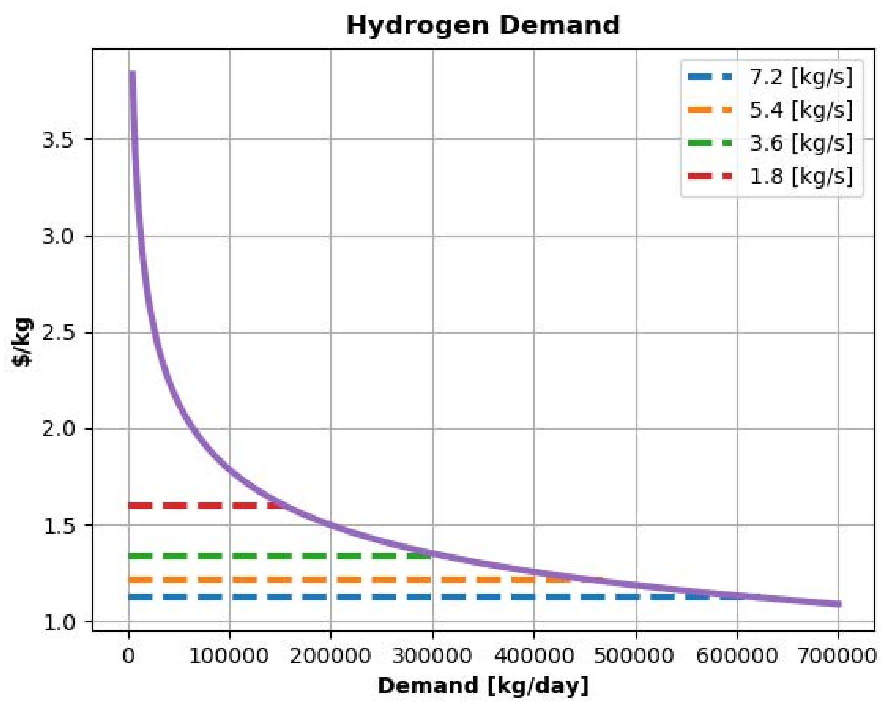

Figure 50. Low hydrogen pricing with sweep values on hydrogen market contractual obligations realized.

Low hydrogen pricing precludes the building of hydrogen storage due to the inability of the system to recoup capital expenses over the lifespan of the system. However, it should be noted that even with low projected hydrogen pricing, scenarios do still exist where system profitability is increased.

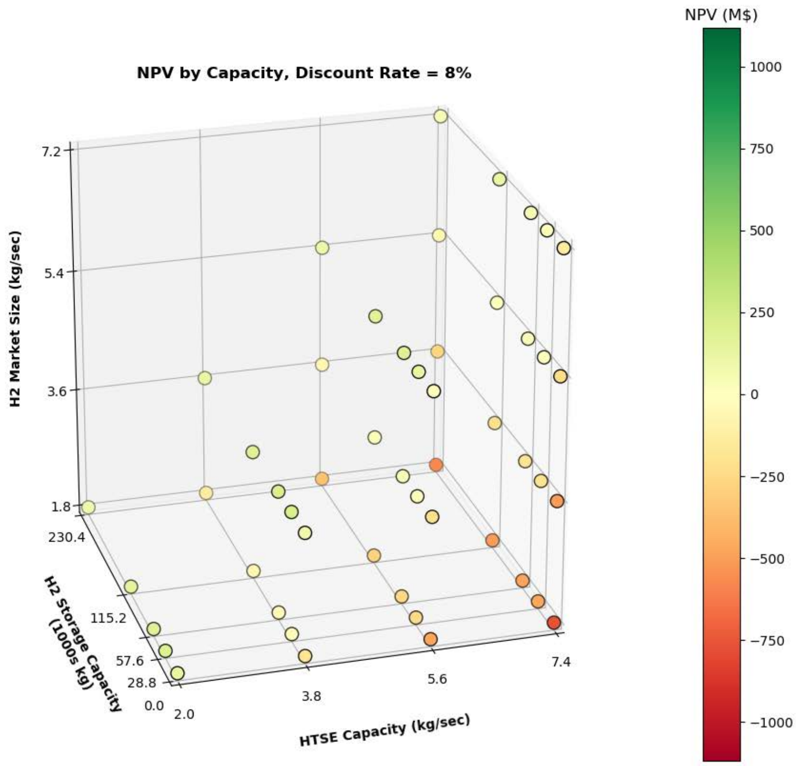

Figure 51. Differential NPV over seventeen years of a co-generating nuclear station in PJM market assuming low hydrogen market selling prices. Discount rate = 8%, corporate tax rate = 21%, yearly inflation = 2.188%.

Table 19. Differential NPV over seventeen-year lifetime between electricity-only production and production of hydrogen at a fixed rate where hydrogen selling price is deemed low based on current predictions.

H_2 market (kg/sec)	Storage (kg)	HTSE (kg/sec)	ΔNPV (2019$)	σ (2019$)
1.8	0	3.8	-1.82E+08	1.07E+06
1.8	0	2	1.15E+08	1.09E+06
1.8	0	7.4	-7.64E+08	1.05E+06
1.8	28800	2	1.91E+08	1.05E+06
1.8	0	5.6	-4.74E+08	1.05E+06
1.8	28800	3.8	-1.79E+07	1.05E+06
1.8	28800	5.6	-2.44E+08	1.09E+06
1.8	57600	5.6	-2.51E+08	1.08E+06

1.8	57600	2	1.76E+08	1.18E+06
1.8	28800	7.4	-4.67E+08	1.06E+06
1.8	57600	3.8	-2.58E+07	1.08E+06
1.8	57600	7.4	-4.74E+08	1.08E+06
1.8	230400	3.8	-1.27E+08	1.09E+06
1.8	115200	3.8	-5.80E+07	1.06E+06
1.8	115200	7.4	-5.07E+08	1.07E+06
1.8	115200	2	1.42E+08	1.05E+06
1.8	230400	2	7.53E+07	1.05E+06
1.8	115200	5.6	-2.84E+08	1.09E+06
1.8	230400	5.6	-3.53E+08	1.05E+06
3.6	0	7.4	-5.07E+08	1.06E+06
1.8	230400	7.4	-5.76E+08	1.05E+06
3.6	0	3.8	7.59E+07	1.05E+06
3.6	0	5.6	-2.17E+08	1.05E+06
3.6	28800	5.6	2.38E+07	1.86E+06
3.6	57600	3.8	2.08E+08	1.17E+06
3.6	28800	7.4	-1.98E+08	1.17E+06
3.6	28800	3.8	2.13E+08	1.12E+06
3.6	57600	5.6	3.20E+07	1.61E+06
3.6	57600	7.4	-1.87E+08	1.13E+06
3.6	115200	5.6	8.92E+06	1.35E+06
3.6	115200	7.4	-2.03E+08	1.31E+06
3.6	115200	3.8	1.75E+08	1.08E+06
3.6	230400	3.8	1.09E+08	1.45E+06
3.6	230400	5.6	-5.62E+07	1.27E+06
3.6	230400	7.4	-2.67E+08	1.05E+06
5.4	0	5.6	-1.29E+07	1.05E+06
5.4	0	7.4	-2.30E+08	1.08E+06
5.4	28800	7.4	7.67E+06	1.09E+06
5.4	28800	5.6	1.18E+08	1.46E+06
5.4	57600	5.6	1.82E+08	1.16E+06
5.4	57600	7.4	2.40E+07	3.51E+06
5.4	115200	5.6	1.57E+08	1.10E+06
5.4	115200	7.4	1.06E+07	1.20E+06
5.4	230400	5.6	9.12E+07	1.19E+06
5.4	230400	7.4	-4.92E+07	1.82E+06
7.2	0	7.4	-1.30E+08	1.05E+06
7.2	28800	7.4	-3.54E+06	3.37E+06
7.2	57600	7.4	5.10E+07	1.07E+06
7.2	115200	7.4	1.09E+08	1.09E+06
7.2	230400	7.4	4.37E+07	1.05E+06

7.3.4 Coupled HTSE-Storage- Discount Rate (10%), High H_2 Selling Price

Results presented show the effect of results based on the discount rate applied in the differential cash flow analysis. When compared to the results that included a discount rate of 8% the overall trends are the same however, absolute figures are reduced. To think about the meaning of the absolute figure the following explanation is applied. The differential NPV's expressed here are the differential dollars gained or lost after a guaranteed discount rate of 10% is achieved. All figures are in today's dollars. To reduce redundancy the full table of solutions swept can be found in Appendix B.

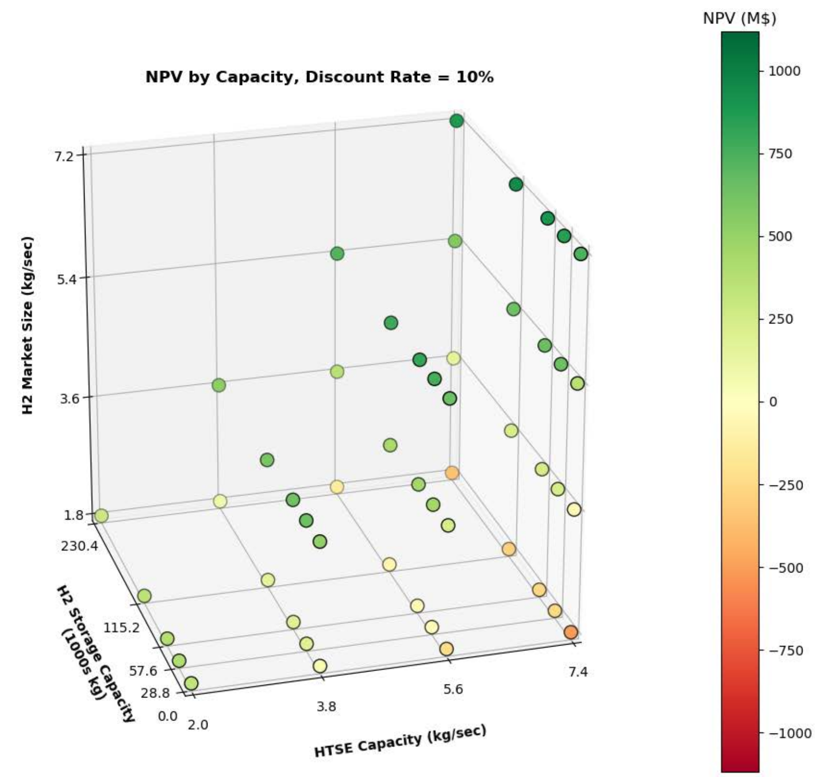

Figure 52. Differential NPV over seventeen years of a co-generating nuclear station in PJM market assuming high hydrogen selling prices. Discount rate = 10%, corporate tax rate = 21%, yearly inflation = 2.188%.

7.3.5 Coupled HTSE-Storage- Discount Rate (12%), High H_2 Selling Price

For completeness of discount rates applied in the analysis results are presented at a discount rate of 12%. Similar trends and explanation as expressed in section 7.3.4. The differential NPV's expressed here are the differential dollars gained or lost after a guaranteed discount rate of 12% is achieved. All figures are in today's dollars. A table of sweep values can be found in Appendix B.

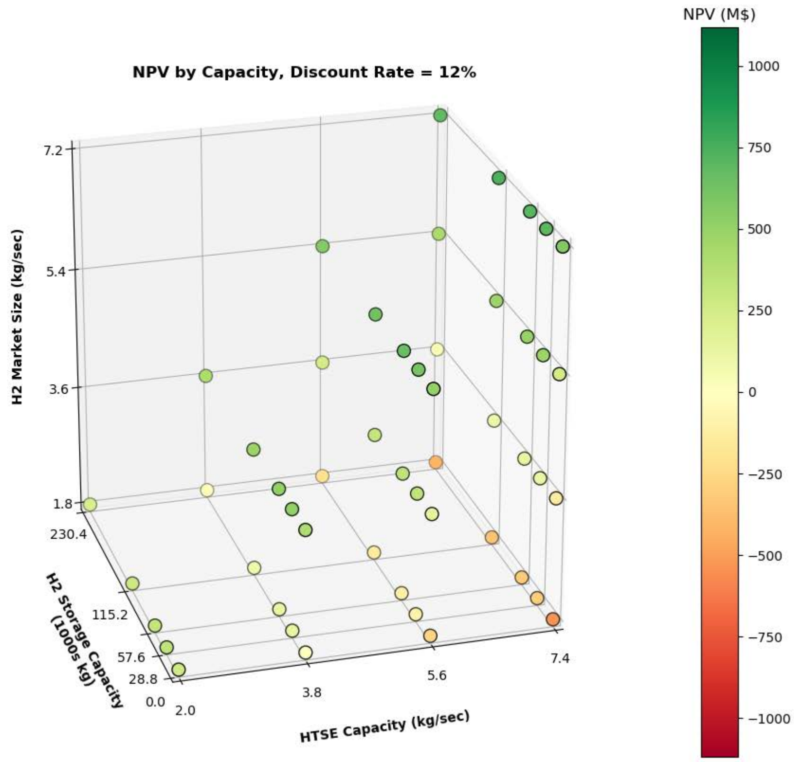

Figure 53. Differential NPV's over seventeen years of a co-generating nuclear station in PJM market assuming high hydrogen selling prices. Discount rate = 12%, corporate tax rate = 21%, yearly inflation = 2.188%.

7.4 Optimization Set

Now that overall systems trends have been determined a focused optimization about the best sweep point was completed to determine the optimal profit that can be utilized in this system. To do this the RAVEN optimizer computes an optimization sweep on five key variables: HTSE capacity, hydrogen market demand, storage requirements, buy price on the storage unit, and the sell price on the storage unit. Each point in the optimization space utilizes 20 stochastic de-noisings.

A five variable optimization is depicted in in Figure 54 with a target variable of ΔNPV. The initial starting point is near to the best possible sweep value and is able to explore the space about it to determine how much the ΔNPV can be improved and in what direction the variables need to be changed. All points with an [x] marked are sample points the optimizer tried and rejected. Points with a blue [o] on them are points the optimizer accepted as better than its current point and thus accepted that as the new optimal. The optimizer was able increase the NPV by about ten million dollars over the seventeen-year run. Throughout the run, there were 45 sampled points before the optimizer determined it was at the most optimal point it could find. Optimizer convergence criteria was set to a step size of 1e-7, with relative convergence criteria of 1e-8. These settings determine that if the step size taken by the optimizer is less than 1e-7 or relative step size is less than 1e-8 for three consecutive runs then it determines it has found the optimal solution. In the solution strategy set forth here the step size is shrunk after each failed point by 25% and re-evaluated to try and finds a new optimal path about it in the five dimensional space. Once a more optimal point is found the step size is increased by 50% and the walk continues.

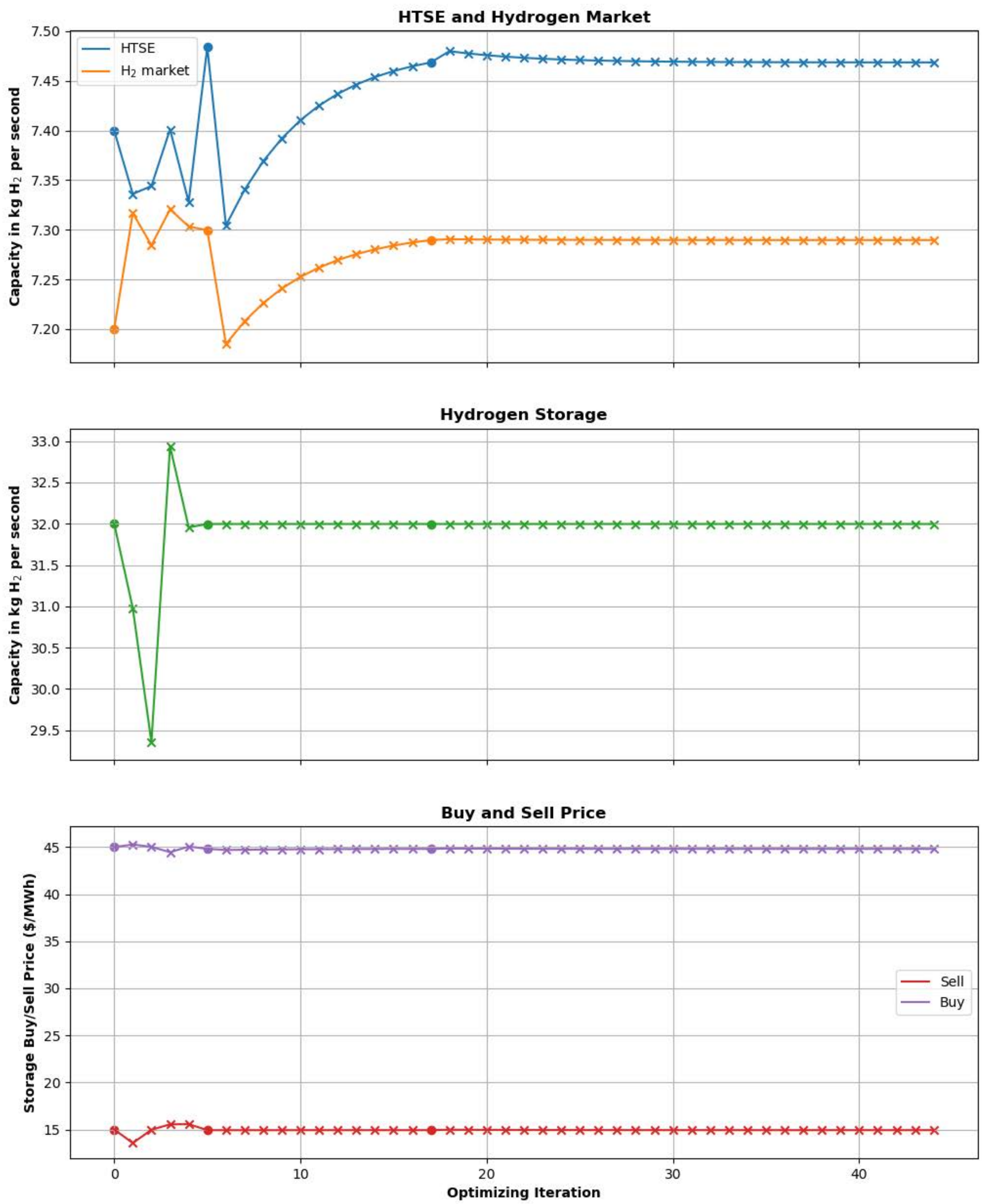

Figure 54. Optimization parameter walks.

From the initial seeded setpoint the optimization path determined the most optimal setpoint is a hydrogen market contract size of 7.29 kg/sec, hydrogen storage tank of 151,188 kg, and an HTSE size of 7.47 kg/sec. This configuration leads to an increase in profits over the seventeen-year lifespan in excess of ten million dollars as shown in Table 20. The initial point is accepted then for four consecutive attempts all points about it are less profitable. At point six there is an increase in the NPV of 9.5 million, making this the new optimal point. Then for the next ten attempts there is no increase in the NPV until at point 18 the optimal solution is found at an increase of 10 million dollars.

Table 20. Optimization points showing the increase in 2019$ of the optimization walk from Point 1.

Point	Increased ΔNPV	Accepted	Point	Increased ΔNPV	Accepted
1	0.000E+00	TRUE	**23**	9.998E+06	FALSE
2	-2.102E+08	FALSE	**24**	1.003E+07	FALSE
3	-1.330E+08	FALSE	**25**	9.850E+06	FALSE
4	-8.724E+07	FALSE	**26**	9.601E+06	FALSE
5	-1.950E+08	FALSE	**27**	9.462E+06	FALSE
6	9.548E+06	TRUE	**28**	9.875E+06	FALSE
7	-5.064E+07	FALSE	**29**	8.764E+06	FALSE
8	-2.048E+07	FALSE	**30**	8.892E+06	FALSE
9	-9.640E+06	FALSE	**31**	1.001E+07	FALSE
10	-3.430E+06	FALSE	**32**	9.742E+06	FALSE
11	3.188E+06	FALSE	**33**	9.778E+06	FALSE
12	6.611E+06	FALSE	**34**	9.752E+06	FALSE
13	7.562E+06	FALSE	**35**	9.883E+06	FALSE
14	8.236E+06	FALSE	**36**	9.729E+06	FALSE
15	1.587E+06	FALSE	**37**	9.966E+06	FALSE
16	6.015E+06	FALSE	**38**	9.574E+06	FALSE
17	9.094E+06	FALSE	**39**	9.647E+06	FALSE
18	1.004E+07	TRUE	**40**	9.707E+06	FALSE
19	9.954E+06	FALSE	**41**	8.215E+06	FALSE
20	9.588E+06	FALSE	**42**	9.825E+06	FALSE
21	9.917E+06	FALSE	**43**	9.607E+06	FALSE
22	9.816E+06	FALSE	**44**	9.249E+06	FALSE

7.5 References

[1] Rabiti C, Epiney A, Talbot P, Kim JS, Bragg-Sitton S, Alfonsi A, et al. “Status report on modelling and simulation capabilities for nuclear-renewable hybrid energy systems.” Idaho Falls (ID): Idaho national laboratory; 2017 Sep. Report No.: INL/EXT-17-43441. Contract No.: DE-AC07- ID14517.

[2] Rabiti C, Cherry R, Deason W, Sabharwall P, Bragg-Sitton S, Boardman R. “Framework for the Economic Analysis of Hybrid Systems Based on Exergy Assumption”. Idaho Falls (ID): Idaho National Laboratory, 2014 Aug. Report No.: INL/EXT-14-32934. Contract No.:DE-AC07-ID14517.

[3] Deloitte. “Corporate Tax Rates 2019*”. https://www2.deloitte.com/content/dam/Deloitte/global/Documents/Tax/dttl-tax-corporate-tax-rates.pdf. [Accessed August 2, 2019].

[4] CPI Inflation Calculator. http://www.in2013dollars.com/2000-dollars-in-2018. [Accessed August 2, 2019]

[5] Penev M, Rustagi N, Hunter C, Eichman J. “Energy Storage: Days of Service Sensitivity Analysis”. National Renewable Energy Laboratory. March 19, 2019. https://www.nrel.gov/docs/fy19osti/73520.pdf. [Accessed August 2, 2019].

8. CONCLUSIONS AND FUTURE WORK

This section provides a summary of the analysis performed and provides suggestions for possible future work scope in this arena. A determination is made as to whether the co-generation of hydrogen at a nuclear facility in the Midwest is a viable option based on boundary conditions and assumptions made in this work. Further, this section goes on to detail potential areas where research efforts can continue to spur industry expansion into additional energy markets.

8.1 Summary/Conclusions

An in-depth look at the possibility of retrofitting existing pressurized water reactors in the Midwest for the purposes of hydrogen co-generation via high-temperature steam electrolysis has been performed. To accommodate such an integration, a detailed discussion and analysis of HTSE process operation, requirements, and flexibility was conducted. As part of this, nuclear system control scheme modifications were proposed to allow dynamic operation of the HTSE, both thermally and electrically. High-fidelity Modelica simulations showcased the viability of such control schemes. However, due to limited knowledge of SOFC stack degradation due to thermal gradients, thermal cycling of the HTSE was decided against. Therefore, the control schemes proposed are only utilized to re-distribute steam at startup, and only the portion of electricity utilized in the electrolyzers will be cycled.

From the detailed analysis of the nuclear integration and the HTSE process design, a comprehensive cost estimation was conducted in the APEA and H2A models to elucidate capital and operational costs associated with the production, compression, and distribution of hydrogen from a nuclear facility. Alongside this costing analysis, market analyses were conducted by NREL and Argonne on the electric and hydrogen markets, respectively, in the PJM interconnect.

Utilizing the electricity data market projections in the PJM interconnect from NREL and hydrogen demand/pricing projections from Argonne, several seventeen-year, multiple-stochastic histories were run in HERON/RAVEN. Through investigation of the differential discounted cash flow analysis produced, results suggest positive motivations can be found at all of the included hydrogen market pricing projections.

The top result in the capacity sweep occurred with the following set points: high hydrogen prices, the largest possible HTSE unit in the sweep set, HTSE size = 7.4 kg/sec [640tpd], a contractual hydrogen market agreement of H_2 market = 7.2 kg/sec [622 tpd], and a medium storage size H_2 storage = 115,200 kg. The analysis suggested a discount rate of 8% the ΔNPV = 1.19E+09 over the seventeen-year span.

However, depending on component capacities, the analysis still showed benefits to the nuclear facility under all hydrogen market conditions and discount rates. The best of each is shown in Table 21.

Table 21. Maximum ΔNPV for each combination of hydrogen market prices and discount rates over a seventeen-year span.

Hydrogen Market Price	*Discount Rate [%]*	*HTSE size [kg/s]*	*Hydrogen Market Size [kg/s]*	*Storage Size [kg]*	*ΔNPV (2019$)*	*Deviation (2019$)*
Low	12	2.0	1.8	28800	9.83E+07	1.72E+06
Low	10	2.0	1.8	28800	1.41E+08	1.72E+06
Low	8	3.8	3.6	28800	2.13E+08	1.12E+06
Med	12	3.8	3.6	28800	2.09E+08	1.86E+06
Med	10	5.6	5.4	57600	3.07E+08	3.83E+06
Med	8	7.4	7.2	115200	4.39E+08	1.97E+06
High	12	7.4	7.2	115200	7.42E+08	1.17E+06
High	10	7.4	7.2	115200	9.45E+08	1.76E+06
High	8	7.4	7.2	115200	1.19E+09	2.04E+06

An optimization study on capacities and storage buy and sell prices was conducted on the maximum sweep point to explore the space to determine if additional profitability exists. It was concluded that by increasing the hydrogen market contract to 7.29 [kg/sec], the HTSE size to 7.47 [kg/sec], and the buy and sell prices to $14.83 and $44.92, respectively, overall system profitability could be increased by ten million dollars over the seventeen-year lifespan.

The results elucidate that by operating in multiple markets, a nuclear facility would be capable of dodging low electricity market pricing while maintaining the ability to capitalize on the high electricity market pricing.

It should be noted that results presented in this report are inherently conservative due to five key assumptions. First, considering the limited knowledge of stack degradation due to thermal gradients, the high-temperature steam electrolysis plant is not allowed to thermally cycle. This limitation decreases electricity generation capacity in the nuclear plant, reducing capacity payments and the maximum output to the electrical grid.

Second, this analysis considered the building of a separate hydrogen pipeline for use in the nuclear facility. Research is currently being conducted to determine if existing natural gas pipelines can accommodate direct hydrogen injection. If hydrogen can be integrated into existing natural gas pipelines, then a capital savings of ~$19,000,000 per kg/sec of installed HTSE capacity could be deducted from this analysis.

Third, the ancillary services market has been neglected in this analysis. Should the nuclear plant operate in the ancillary services market during periods when it is producing hydrogen, an additional substantial income stream could be considered, which would increase overall system profitability.

Fourth, zero carbon subsidies are introduced in these cash flow analysis, but instead are completed assuming raw numbers and electricity pricing.

Fifth, electric pricing is assumed to never go negative. Instead, it is assumed overall system curtailment will occur in such a manner that pricing remains at or above zero. This assumption inflates the "business as usual" scenario, thus decreasing the ΔNPV calculated. If negative pricing scenarios continue to occur as they do today, one would expect a further increase in ΔNPV.

8.2 FUTURE WORK

Results presented in this analysis incite several thrust vectors for additional research. In particular:

- Understanding if the nuclear plant can participate in the ancillary service market. If this is possible, overall system revenues will increase.
- Exploration of whether hydrogen can be pumped into existing natural gas pipelines. If this is possible, then capital savings of $19,000,000 per kg/sec of installed HTSE capacity would be possible.
- Increased fidelity on future electricity market pricing. Current results presented utilize linear programming methodologies for electricity market pricing predictions. Increased fidelity utilizing a combination of mixed integer and linear programming capabilities will increase predictive capabilities. This is a thrust vector currently underway at NREL.
- Increased fidelity on future hydrogen demand and natural gas pricing to better predict wholesale hydrogen pricing and demand.
- Increased control logic on the hydrogen storage unit's buying and selling prices to allow for profit maximization during electricity pricing peaks.
- Further research on thermal cycling capability of nuclear.
- Increased understanding of capital, operational, and legal costs associated with high-temperature steam electrolysis.

Through additional research of the topics mentioned above, an increased fidelity analysis could be run that would further illuminate the benefits of co-located hydrogen production at a nuclear facility.

APPENDIX A: Additional Market Construction

This section provides a continuation on the market construction process developed by NREL.

As mentioned in Chapter 5, transmission upgrades were not passed from ReEDS to PLEXOS with the nodal converter and therefore needed manual adjustments within PLEXOS. Starting from 2026, the model was run once to determine the transmission interface violations; these interfaces were then increased by 95% of their maximum violation in the 2026 and 2030 databases to obtain the "final" 2026 database and the initial 2030 database. The violations in the initial 2030 database were then used to create the "final" 2030 database and the initial 2034 database. This process continued until final results were obtained for each of the five years. A flow diagram showing this workflow can be seen in Figure 55.

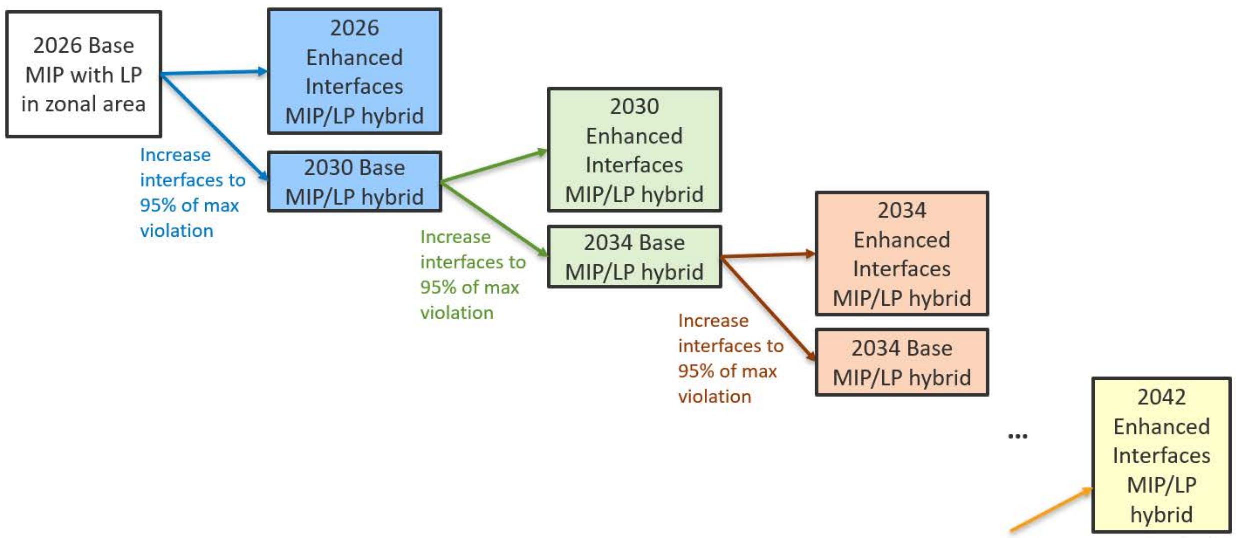

Figure 55. Workflow for increasing transmission capacity in PLEXOS.

The following products and associated violation penalties were included in the PLEXOS model.

- Energy (Value of Lost Load (VOLL) $10,000/MWh)
- Regulation Reserves (Regulation type, 5min response, $4100/MW)
- Spinning Reserves (Raise type, 10min response, $4000/MW)
- Flexibility Reserves (Raise type, 20min response, $3900/MW

Operating reserve products were also modeled in order to obtain hourly reserve prices for consideration in the techno-economic analysis. All reserve products are all mutually exclusive, meaning that spare capacity used to provide one reserve service cannot be used to provide reserve to any other service. The amount of reserve product to provide in each hour was calculated as follows at the PLEXOS "Region" level, where a region would represent an area such as PJM or MISO:

- Regulation = 1% load in region
- Spinning = 3% load in region
- Flex = 2% total variable generation (VG) in region

APPENDIX B: COMPLETE SERIES OF SIMULATIONS RUN

This section contains the complete results from the cases run in Chapter 7 of this report. The runs sampled that were not contained in the main body of the report are all combinations of the discount rates and hydrogen prices summarized here.

- Discount Rates = 10%, 12%
- Hydrogen Selling Prices = Low, Medium

8.2.1 Coupled HTSE-Storage- Discount Rate (10%), Medium H_2 Selling Price

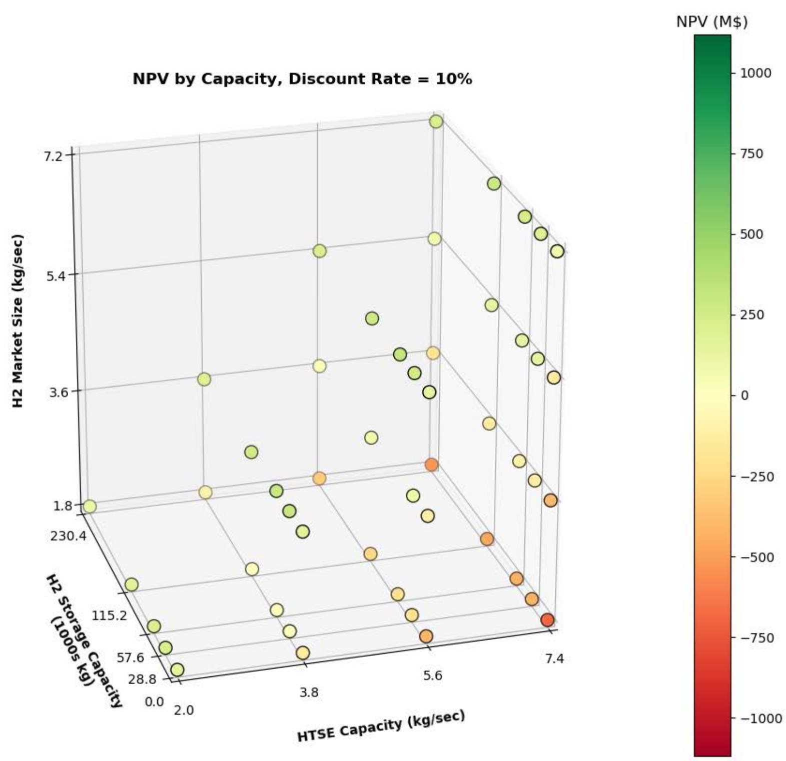

Figure 56. Differential NPVs over seventeen years of a co-generating nuclear station in PJM market assuming medium hydrogen selling prices. Discount rate = 10%, corporate tax rate = 21%, yearly inflation = 2.188%.

Table 22. Differential NPV over seventeen-year lifetime between electricity-only production and production of hydrogen at a fixed rate where hydrogen selling price is deemed medium based on current predictions.

H_2 market (kg/sec)	Storage (kg)	HTSE (kg/sec)	ΔNPV (2019$)	σ (2019$)
1.8	0	3.8	-1.28E+08	1.71E+06
1.8	0	2	1.56E+08	1.71E+06
1.8	28800	2	2.21E+08	1.72E+06
1.8	0	5.6	-4.07E+08	1.71E+06
1.8	28800	3.8	1.54E+07	1.78E+06
1.8	0	7.4	-6.84E+08	1.71E+06
1.8	57600	7.4	-4.30E+08	1.74E+06
1.8	28800	5.6	-2.05E+08	1.75E+06
1.8	57600	3.8	7.02E+06	1.81E+06
1.8	57600	5.6	-2.13E+08	1.72E+06
1.8	57600	2	2.05E+08	1.72E+06
1.8	28800	7.4	-4.22E+08	1.75E+06
1.8	115200	3.8	-2.51E+07	1.72E+06
1.8	115200	7.4	-4.63E+08	1.71E+06
1.8	230400	3.8	-9.40E+07	1.72E+06
1.8	115200	2	1.72E+08	1.74E+06
1.8	115200	5.6	-2.46E+08	1.72E+06
1.8	230400	2	1.05E+08	1.76E+06
3.6	0	3.8	1.70E+08	1.71E+06
1.8	230400	5.6	-3.15E+08	1.71E+06
3.6	0	5.6	-1.09E+08	1.71E+06
3.6	0	7.4	-3.86E+08	1.71E+06
1.8	230400	7.4	-5.32E+08	1.71E+06
3.6	28800	3.8	2.91E+08	1.83E+06
3.6	28800	5.6	1.03E+08	1.74E+06
3.6	28800	7.4	-1.14E+08	1.85E+06
3.6	57600	3.8	2.84E+08	1.80E+06
3.6	57600	7.4	-1.05E+08	1.87E+06
3.6	115200	5.6	8.45E+07	1.79E+06
3.6	115200	7.4	-1.23E+08	1.83E+06
3.6	115200	3.8	2.51E+08	1.77E+06
3.6	230400	3.8	1.84E+08	1.84E+06
3.6	230400	5.6	1.88E+07	1.98E+06
3.6	230400	7.4	-1.87E+08	1.76E+06
5.4	0	5.6	1.38E+08	1.71E+06
5.4	0	7.4	-1.39E+08	1.71E+06
5.4	28800	5.6	2.52E+08	1.79E+06
5.4	28800	7.4	1.34E+08	1.88E+06

5.4	57600	7.4	1.47E+08	1.84E+06
5.4	57600	5.6	3.07E+08	3.83E+06
5.4	115200	5.6	2.80E+08	1.75E+06
5.4	115200	7.4	1.31E+08	1.81E+06
5.4	230400	5.6	2.15E+08	1.74E+06
5.4	230400	7.4	7.19E+07	1.91E+06
7.2	0	7.4	7.80E+07	1.71E+06
7.2	28800	7.4	1.86E+08	2.33E+06
7.2	57600	7.4	2.35E+08	4.10E+06
7.2	115200	7.4	2.82E+08	1.81E+06
7.2	230400	7.4	2.16E+08	1.75E+06

8.2.2 Coupled HTSE-Storage- Discount Rate (10%), Low H_2 Selling Price

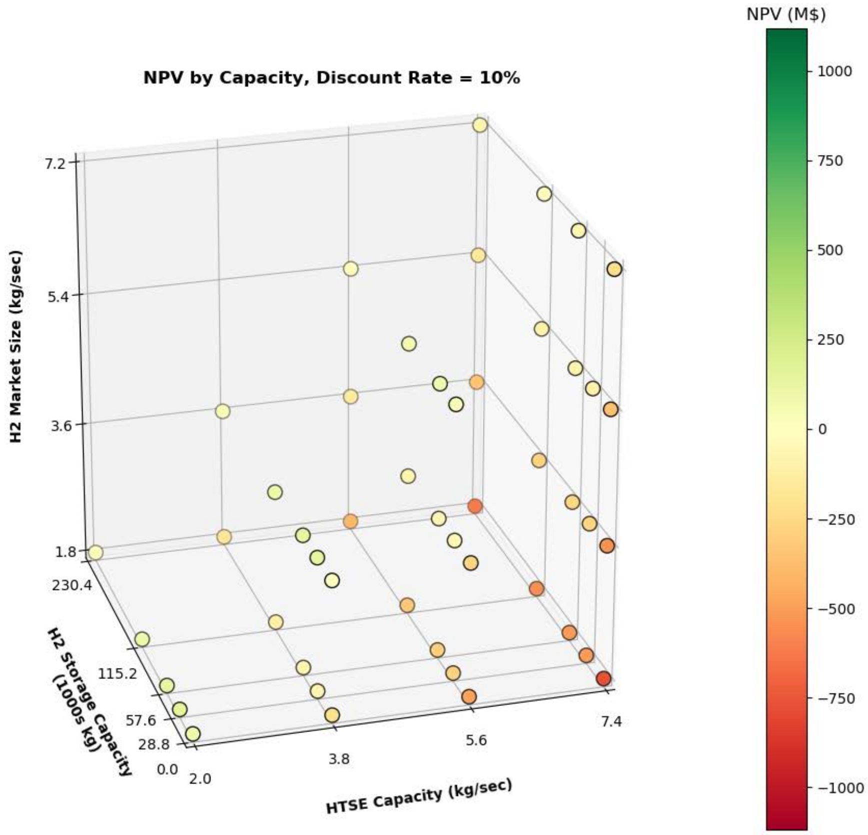

Figure 57. Differential NPVs over seventeen years of a co-generating nuclear station in PJM market assuming low hydrogen selling prices. Discount rate = 10%, corporate tax rate = 21%, yearly inflation = 2.188%.

Table 23. Differential NPV over seventeen-year lifetime between electricity-only production and production of hydrogen at a fixed rate where hydrogen selling price is deemed low based on current predictions.

H_2 market (kg/sec)	Storage (kg)	HTSE (kg/sec)	ΔNPV (2019$)	σ (2019$)
1.8	0	2	7.55E+07	1.71E+06
1.8	28800	3.8	-6.47E+07	1.71E+06
1.8	28800	2	1.41E+08	1.72E+06
1.8	0	5.6	-4.88E+08	1.71E+06
1.8	0	7.4	-7.64E+08	1.78E+06

1.8	0	3.8	-2.08E+08	1.71E+06
1.8	57600	3.8	-7.36E+07	1.74E+06
1.8	28800	7.4	-5.03E+08	1.75E+06
1.8	28800	5.6	-2.85E+08	1.81E+06
1.8	57600	2	1.25E+08	1.72E+06
1.8	57600	7.4	-5.11E+08	1.72E+06
1.8	57600	5.6	-2.93E+08	1.75E+06
1.8	115200	7.4	-5.44E+08	1.72E+06
1.8	230400	3.8	-1.74E+08	1.71E+06
1.8	230400	2	2.47E+07	1.72E+06
1.8	115200	3.8	-1.06E+08	1.74E+06
1.8	115200	2	9.17E+07	1.72E+06
1.8	115200	5.6	-3.26E+08	1.76E+06
1.8	230400	7.4	-6.13E+08	1.71E+06
3.6	0	7.4	-5.40E+08	1.71E+06
3.6	0	5.6	-2.63E+08	1.71E+06
1.8	230400	5.6	-3.95E+08	1.71E+06
3.6	0	3.8	1.61E+07	1.71E+06
3.6	28800	3.8	1.34E+08	1.83E+06
3.6	28800	7.4	-2.68E+08	1.74E+06
3.6	57600	3.8	1.29E+08	1.85E+06
3.6	28800	5.6	-5.18E+07	1.80E+06
3.6	57600	5.6	-4.57E+07	1.87E+06
3.6	57600	7.4	-2.60E+08	1.79E+06
3.6	115200	3.8	9.61E+07	1.83E+06
3.6	115200	7.4	-2.77E+08	1.77E+06
3.6	115200	5.6	-6.96E+07	1.84E+06
3.6	230400	3.8	3.03E+07	1.98E+06
3.6	230400	5.6	-1.35E+08	1.76E+06
3.6	230400	7.4	-3.41E+08	1.71E+06
5.4	28800	5.6	2.79E+07	1.71E+06
5.4	0	7.4	-3.63E+08	1.79E+06
5.4	28800	7.4	-8.98E+07	1.88E+06
5.4	57600	5.6	8.32E+07	1.84E+06
5.4	57600	7.4	-7.63E+07	3.83E+06
5.4	115200	5.6	5.62E+07	1.75E+06
5.4	115200	7.4	-9.29E+07	1.81E+06
5.4	230400	7.4	-1.54E+08	1.74E+06
5.4	230400	5.6	-1.01E+07	1.91E+06
7.2	0	7.4	-2.14E+08	1.71E+06
7.2	57600	7.4	-5.74E+07	2.33E+06
7.2	115200	7.4	-9.62E+06	4.10E+06
7.2	230400	7.4	-7.58E+07	1.81E+06

8.2.3 Coupled HTSE-Storage- Discount Rate (12%), Low H_2 Selling Price

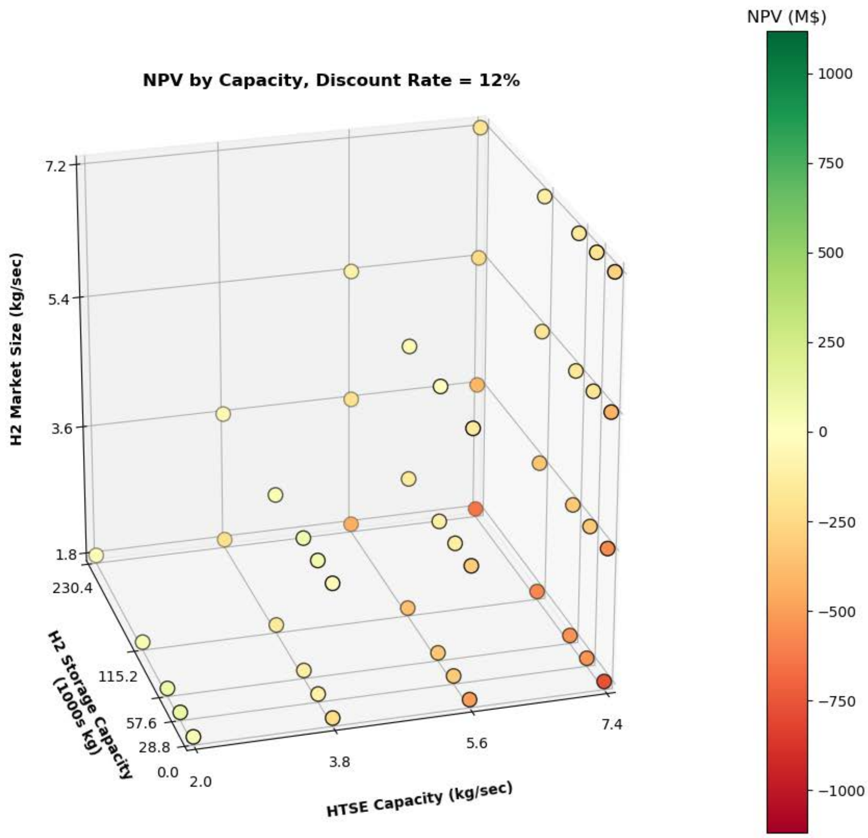

Figure 58. Differential NPVs over seventeen years of a co-generating nuclear station in PJM market assuming low hydrogen selling prices. Discount rate = 12%, corporate tax rate = 21%, yearly inflation = 2.188%.

Table 24. Differential NPV over seventeen-year lifetime between electricity-only production and production of hydrogen at a fixed rate where hydrogen selling price is deemed low based on current predictions.

H_2 market (kg/sec)	Storage (kg)	HTSE (kg/sec)	ΔNPV (2019$)	σ (2019$)
1.8	0	5.6	-5.00E+08	1.71E+06
1.8	0	2	4.19E+07	1.71E+06
1.8	28800	2	9.83E+07	1.72E+06
1.8	0	3.8	-2.31E+08	1.71E+06
1.8	0	7.4	-7.65E+08	1.78E+06
1.8	28800	3.8	-1.04E+08	1.71E+06
1.8	28800	5.6	-3.20E+08	1.74E+06
1.8	57600	2	8.23E+07	1.75E+06
1.8	28800	7.4	-5.33E+08	1.81E+06
1.8	57600	3.8	-1.14E+08	1.72E+06
1.8	57600	7.4	-5.42E+08	1.72E+06
1.8	57600	5.6	-3.29E+08	1.75E+06
1.8	115200	2	4.86E+07	1.72E+06
1.8	115200	3.8	-1.46E+08	1.73E+06
1.8	115200	5.6	-3.62E+08	1.72E+06
1.8	115200	7.4	-5.75E+08	1.74E+06
1.8	230400	2	-1.84E+07	1.72E+06
1.8	230400	3.8	-2.15E+08	1.76E+06
1.8	230400	5.6	-4.31E+08	1.77E+06
1.8	230400	7.4	-6.44E+08	1.71E+06
3.6	0	5.6	-3.02E+08	1.71E+06
3.6	0	3.8	-3.39E+07	1.71E+06
3.6	0	7.4	-5.68E+08	1.71E+06
3.6	28800	3.8	7.13E+07	1.83E+06
3.6	28800	5.6	-1.15E+08	1.74E+06
3.6	28800	7.4	-3.28E+08	1.85E+06
3.6	57600	5.6	-1.11E+08	1.80E+06
3.6	57600	3.8	6.28E+07	1.87E+06
3.6	57600	7.4	-3.21E+08	1.79E+06
3.6	115200	5.6	-1.37E+08	1.88E+06
3.6	115200	3.8	3.03E+07	1.77E+06
3.6	115200	7.4	-3.39E+08	1.84E+06
3.6	230400	3.8	-3.69E+07	1.98E+06
3.6	230400	7.4	-4.04E+08	1.76E+06
3.6	230400	5.6	-2.01E+08	1.75E+06
5.4	0	5.6	-1.48E+08	1.71E+06
5.4	0	7.4	-4.13E+08	1.79E+06

5.4	28800	7.4	-1.71E+08	1.88E+06
5.4	57600	5.6	-5.71E+05	1.84E+06
5.4	57600	7.4	-1.61E+08	3.83E+06
5.4	115200	7.4	-1.78E+08	1.75E+06
5.4	115200	5.6	-2.84E+07	1.81E+06
5.4	230400	5.6	-9.44E+07	1.74E+06
5.4	230400	7.4	-2.40E+08	1.91E+06
7.2	0	7.4	-2.83E+08	1.71E+06
7.2	28800	7.4	-1.88E+08	2.33E+06
7.2	57600	7.4	-1.48E+08	4.10E+06
7.2	115200	7.4	-1.09E+08	1.81E+06
7.2	230400	7.4	-1.75E+08	1.71E+06

8.2.4 Coupled HTSE-Storage- Discount Rate (12%), Medium H_2 Price

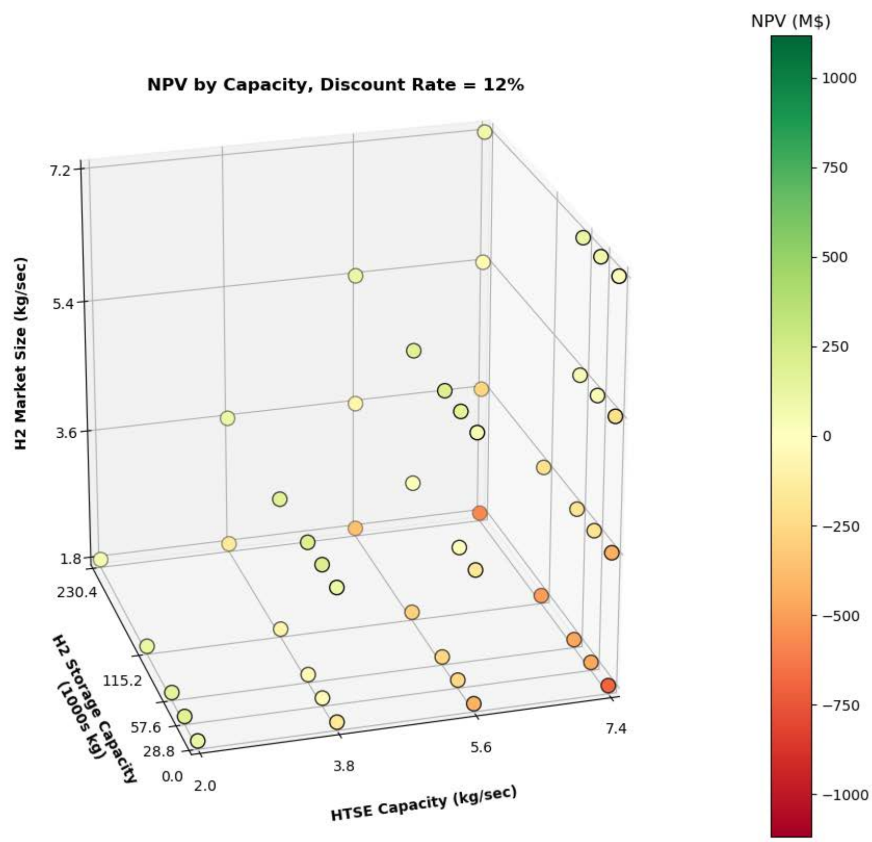

Figure 59. Differential NPVs over seventeen years of a co-generating nuclear station in PJM market assuming medium hydrogen selling prices. Discount rate = 12%, corporate tax rate = 21%, yearly inflation = 2.188%.

Table 25. Differential NPV over seventeen-year lifetime between electricity-only production and production of hydrogen at a fixed rate where hydrogen selling price is deemed medium based on current predictions.

H_2 market (kg/sec)	Storage (kg)	HTSE (kg/sec)	ΔNPV (2019$)	σ (2019$)
1.8	28800	2	1.70E+08	1.07E+06
1.8	28800	3.8	-3.28E+07	1.09E+06
1.8	0	5.6	-4.28E+08	1.05E+06

1.8	0	7.4	-6.94E+08	1.05E+06
1.8	0	3.8	-1.59E+08	1.05E+06
1.8	0	2	1.14E+08	1.05E+06
1.8	28800	5.6	-2.48E+08	1.09E+06
1.8	57600	3.8	-4.18E+07	1.08E+06
1.8	28800	7.4	-4.61E+08	1.18E+06
1.8	57600	5.6	-2.57E+08	1.06E+06
1.8	57600	2	1.54E+08	1.08E+06
1.8	57600	7.4	-4.70E+08	1.08E+06
1.8	115200	3.8	-7.43E+07	1.09E+06
1.8	115200	7.4	-5.03E+08	1.06E+06
1.8	230400	2	5.35E+07	1.07E+06
1.8	115200	5.6	-2.90E+08	1.05E+06
1.8	230400	3.8	-1.43E+08	1.05E+06
1.8	115200	2	1.21E+08	1.09E+06
3.6	0	5.6	-1.65E+08	1.05E+06
1.8	230400	5.6	-3.59E+08	1.06E+06
3.6	0	3.8	1.04E+08	1.05E+06
1.8	230400	7.4	-5.73E+08	1.05E+06
3.6	0	7.4	-4.31E+08	1.05E+06
3.6	28800	3.8	2.09E+08	1.86E+06
3.6	28800	5.6	2.26E+07	1.17E+06
3.6	28800	7.4	-1.90E+08	1.17E+06
3.6	57600	3.8	2.00E+08	1.12E+06
3.6	57600	7.4	-1.83E+08	1.61E+06
3.6	115200	3.8	1.68E+08	1.13E+06
3.6	115200	5.6	9.42E+05	1.35E+06
3.6	115200	7.4	-2.02E+08	1.31E+06
3.6	230400	3.8	1.01E+08	1.08E+06
3.6	230400	5.6	-6.43E+07	1.45E+06
3.6	230400	7.4	-2.67E+08	1.27E+06
5.4	0	5.6	5.22E+07	1.05E+06
5.4	0	7.4	-2.14E+08	1.05E+06
5.4	28800	7.4	2.90E+07	1.09E+06
5.4	28800	5.6	1.53E+08	1.46E+06
5.4	57600	7.4	4.04E+07	1.16E+06
5.4	57600	5.6	2.00E+08	3.51E+06
5.4	115200	5.6	1.72E+08	1.10E+06
5.4	230400	5.6	1.06E+08	1.20E+06
5.4	230400	7.4	-3.96E+07	1.19E+06
7.2	28800	7.4	7.31E+07	1.82E+06
7.2	0	7.4	-2.32E+07	1.05E+06
7.2	57600	7.4	1.10E+08	3.37E+06
7.2	230400	7.4	8.54E+07	1.37E+06

8.2.5 Coupled HTSE-Storage- Discount Rate (10%), High H_2 Selling Price

Table 26. Differential NPV over seventeen-year lifetime between electricity-only production and production of hydrogen at a fixed rate at high hydrogen market price predictions.

H_2 market (kg/sec)	Storage (kg)	HTSE (kg/sec)	ΔNPV (2019$)	σ (2019$)
1.8	0	5.6	-2.31E+08	1.71E+06
1.8	0	3.8	4.83E+07	1.71E+06
1.8	28800	3.8	1.92E+08	1.73E+06
1.8	0	7.4	-5.08E+08	1.71E+06
1.8	28800	2	3.98E+08	1.74E+06
1.8	0	2	3.32E+08	1.71E+06
1.8	28800	5.6	-2.85E+07	1.71E+06
1.8	28800	7.4	-2.46E+08	1.72E+06
1.8	57600	3.8	1.83E+08	1.73E+06
1.8	57600	5.6	-3.63E+07	1.74E+06
1.8	57600	2	3.82E+08	1.73E+06
1.8	57600	7.4	-2.54E+08	1.72E+06
1.8	115200	3.8	1.51E+08	1.73E+06
1.8	115200	5.6	-6.93E+07	1.71E+06
1.8	115200	2	3.48E+08	1.75E+06
1.8	115200	7.4	-2.87E+08	1.71E+06
1.8	230400	2	2.81E+08	1.72E+06
1.8	230400	3.8	8.23E+07	1.72E+06
1.8	230400	5.6	-1.38E+08	1.71E+06
1.8	230400	7.4	-3.56E+08	1.71E+06
3.6	0	3.8	5.14E+08	1.71E+06
3.6	0	5.6	2.35E+08	1.71E+06
3.6	0	7.4	-4.18E+07	1.71E+06
3.6	28800	3.8	6.34E+08	2.54E+06
3.6	28800	5.6	4.46E+08	1.76E+06
3.6	28800	7.4	2.30E+08	1.77E+06
3.6	57600	3.8	6.27E+08	1.73E+06
3.6	57600	5.6	4.52E+08	1.81E+06
3.6	57600	7.4	2.39E+08	2.01E+06
3.6	115200	3.8	5.95E+08	1.80E+06
3.6	115200	7.4	2.21E+08	1.82E+06
3.6	115200	5.6	4.28E+08	1.91E+06
3.6	230400	3.8	5.28E+08	1.84E+06
3.6	230400	5.6	3.63E+08	2.04E+06
3.6	230400	7.4	1.57E+08	1.84E+06
5.4	0	5.6	6.43E+08	1.71E+06

5.4	0	7.4	3.67E+08	1.71E+06
5.4	28800	5.6	7.59E+08	2.16E+06
5.4	28800	7.4	6.40E+08	1.92E+06
5.4	57600	5.6	8.13E+08	2.75E+06
5.4	57600	7.4	6.53E+08	2.11E+06
5.4	115200	7.4	6.37E+08	2.13E+06
5.4	115200	5.6	7.85E+08	1.78E+06
5.4	230400	5.6	7.20E+08	1.74E+06
5.4	230400	7.4	5.76E+08	2.03E+06
7.2	0	7.4	7.41E+08	1.71E+06
7.2	28800	7.4	8.49E+08	2.06E+06
7.2	57600	7.4	8.97E+08	3.14E+06
7.2	115200	7.4	9.45E+08	1.76E+06
7.2	230400	7.4	8.79E+08	1.82E+06

8.2.6 Coupled HTSE-Storage- Discount Rate (12%), High H_2 Selling Price

Table 27. Differential NPV over seventeen-year lifetime between electricity-only production and production of hydrogen at a fixed rate at high hydrogen market price predictions.

H_2 market (kg/sec)	Storage (kg)	HTSE (kg/sec)	ΔNPV (2019$)	σ (2019$)
1.8	0	7.4	-5.37E+08	1.05E+06
1.8	28800	2	3.27E+08	1.10E+06
1.8	0	5.6	-2.71E+08	1.05E+06
1.8	0	3.8	-2.31E+06	1.05E+06
1.8	28800	3.8	1.25E+08	1.13E+06
1.8	0	2	2.71E+08	1.05E+06
1.8	57600	2	3.11E+08	1.09E+06
1.8	57600	3.8	1.15E+08	1.10E+06
1.8	28800	7.4	-3.05E+08	1.14E+06
1.8	57600	5.6	-1.00E+08	1.06E+06
1.8	28800	5.6	-9.13E+07	1.07E+06
1.8	57600	7.4	-3.13E+08	1.08E+06
1.8	115200	2	2.77E+08	1.08E+06
1.8	115200	7.4	-3.46E+08	1.06E+06
1.8	115200	5.6	-1.33E+08	1.05E+06
1.8	230400	2	2.10E+08	1.08E+06
1.8	115200	3.8	8.28E+07	1.08E+06
1.8	230400	3.8	1.40E+07	1.07E+06
3.6	0	3.8	4.10E+08	1.05E+06
1.8	230400	7.4	-4.15E+08	1.05E+06

1.8	230400	5.6	-2.02E+08	1.06E+06
3.6	0	5.6	1.42E+08	1.05E+06
3.6	0	7.4	-1.24E+08	1.05E+06
3.6	28800	5.6	3.29E+08	1.20E+06
3.6	28800	7.4	1.17E+08	1.13E+06
3.6	28800	3.8	5.15E+08	2.24E+06
3.6	57600	3.8	5.07E+08	1.13E+06
3.6	57600	5.6	3.33E+08	1.23E+06
3.6	57600	7.4	1.23E+08	1.30E+06
3.6	115200	3.8	4.74E+08	1.20E+06
3.6	115200	5.6	3.08E+08	1.42E+06
3.6	230400	3.8	4.08E+08	1.07E+06
3.6	230400	5.6	2.42E+08	1.42E+06
3.6	230400	7.4	4.03E+07	1.13E+06
3.6	115200	7.4	1.05E+08	1.22E+06
5.4	0	5.6	5.03E+08	1.05E+06
5.4	0	7.4	2.37E+08	1.05E+06
5.4	28800	5.6	6.04E+08	1.56E+06
5.4	28800	7.4	4.79E+08	1.15E+06
5.4	57600	5.6	6.50E+08	2.82E+06
5.4	57600	7.4	4.90E+08	1.62E+06
5.4	115200	5.6	6.22E+08	1.24E+06
5.4	115200	7.4	4.72E+08	1.46E+06
5.4	230400	5.6	5.56E+08	1.18E+06
5.4	230400	7.4	4.11E+08	1.56E+06
7.2	0	7.4	5.68E+08	1.05E+06
7.2	28800	7.4	6.94E+08	2.36E+06
7.2	57600	7.4	7.02E+08	2.96E+06
7.2	115200	7.4	7.42E+08	1.17E+06
7.2	230400	7.4	6.76E+08	1.16E+06